

Field Testing Unvented Roofs with Asphalt Shingles in Cold and Hot-Humid Climates

Building America Report - 1409

June 2015 (rev)

Kohta Ueno and Joseph Lstiburek

Abstract:

In cold climates, a common practice of the weatherization industry is to retrofit compact roof/ceiling assemblies with blown-in dense-pack cellulose. However, this assembly has high moisture and durability risks (due to wintertime interior-sourced condensation) and violates building code. Developing methods to retrofit dense pack insulation into compact roof assemblies while controlling moisture risks would allow for widespread application of this lowcost technique without potentially compromising building durability.

In hot-humid climates, HVAC equipment is typically located in vented, unconditioned attics, with associated energy penalties; one method of moving the ductwork inside the conditioned space is to insulate at the roof deck. However, market penetration of this method has been slow, due to the expense of insulating at the roof line, typically using polyurethane spray foam. If roof assemblies with fibrous insulation could be developed that control moisture risks, this would likely reduce the first cost of unvented roofs, potentially increasing their adoption.

Field Testing Unvented Roofs with Asphalt Shingles in Cold and Hot-Humid Climates

K. Ueno, J.W. Lstiburek
Building Science Corporation

June 2015

NOTICE

This report was prepared as an account of work sponsored by an agency of the United States government. Neither the United States government nor any agency thereof, nor any of their employees, subcontractors, or affiliated partners makes any warranty, express or implied, or assumes any legal liability or responsibility for the accuracy, completeness, or usefulness of any information, apparatus, product, or process disclosed, or represents that its use would not infringe privately owned rights. Reference herein to any specific commercial product, process, or service by trade name, trademark, manufacturer, or otherwise does not necessarily constitute or imply its endorsement, recommendation, or favoring by the United States government or any agency thereof. The views and opinions of authors expressed herein do not necessarily state or reflect those of the United States government or any agency thereof.

Available electronically at <http://www.osti.gov/bridge>

Available for a processing fee to U.S. Department of Energy and its contractors, in paper, from:

U.S. Department of Energy
Office of Scientific and Technical Information
P.O. Box 62
Oak Ridge, TN 37831-0062
phone: 865.576.8401
fax: 865.576.5728
email: <mailto:reports@adonis.osti.gov>

Available for sale to the public, in paper, from:

U.S. Department of Commerce
National Technical Information Service
5285 Port Royal Road
Springfield, VA 22161
phone: 800.553.6847
fax: 703.605.6900
email: orders@ntis.fedworld.gov
online ordering: <http://www.ntis.gov/ordering.htm>

TO 5: 7.1.2 Field Testing Unvented Roofs with Asphalt Shingles in Cold and Hot-Humid Climates

Prepared for:

The National Renewable Energy Laboratory

On behalf of the U.S. Department of Energy's Building America Program

Office of Energy Efficiency and Renewable Energy

15013 Denver West Parkway

Golden, CO 80401

NREL Contract No. DE-AC36-08GO28308

Prepared by:

K. Ueno, J.W. Lstiburek

Building Science Corporation

3 Lan Drive, Suite 102

Westford, MA 01886

NREL Technical Monitor: Stacey Rothgeb

Prepared under Subcontract No. KNDJ-0-40337-00

June 2015

The work presented in this report does not represent performance of any product relative to regulated minimum efficiency requirements.

The laboratory and/or field sites used for this work are not certified rating test facilities. The conditions and methods under which products were characterized for this work differ from standard rating conditions, as described.

Because the methods and conditions differ, the reported results are not comparable to rated product performance and should only be used to estimate performance under the measured conditions.

Contents

List of Figures	vi
List of Tables	ix
Definitions.....	x
Executive Summary	xii
1 Introduction.....	1
1.1 Background.....	1
1.2 Experimental Approach	2
1.3 Relevance to Building America’s Goals.....	2
1.4 Cost-Effectiveness	3
1.5 Tradeoffs and Other Benefits.....	4
2 Background Literature and Field Experience.....	6
2.1 Unvented Roof Background Literature.....	6
2.2 Field Experience in Houston, TX and Jacksonville, FL (CZ 2A).....	8
2.3 Field Experience in Northern California (CZ 3C)	9
2.4 Salonvaara et al. (2013): Modeling Unvented Roofs in CZ 1-4	10
2.5 Boudreaux et al. (2013): Sealed Attic Monitored Performance (CZ 3A/4A)	12
2.6 Lstiburek (2014): Humidity Behavior of Unvented/Sealed Attics	12
2.7 Smegal and Straube (2014): Monitoring & Simulation of SPF Insulated Roofs.....	13
3 Cold Climate (Chicago) Experimental Setup	16
3.1 Overview.....	16
3.2 Experimental Roof Assemblies.....	17
3.2.1 Vented Compact Roof (Roof 1).....	18
3.2.2 Top Vent Cathedral-Cellulose (Roof 2).....	18
3.2.3 Top Vent Cathedralized-Cellulose (Roof 3).....	20
3.2.4 Top Vent Cathedralized-Fiberglass (Roof 4).....	21
3.2.5 Top Vent Cathedral-Fiberglass (Roof 5)	21
3.2.6 Diffusion Vent Cellulose (Roof 6).....	21
3.2.7 Unvented Cellulose (Roof 7)	22
3.3 Roof Bay Instrumentation	23
3.4 Interior Space Conditioning.....	26
3.5 Overview of Roof Installation	27
3.6 Roof Air Leakage Testing.....	29
4 Cold Climate (Chicago) Monitoring Results	34
4.1 Boundary Conditions	34
4.2 Sheathing Moisture Contents.....	35
4.3 Roof Ridge/Peak Sensor Packages	41
4.3.1 Rafter Framing Moisture Contents	42
4.3.2 Roof Peak/Ridge Relative Humidity	43
4.3.3 Roof Peak/Ridge Wafer Sensor	44
4.3.4 Roof “Doghouse” Sheathing Moisture Content.....	45
4.4 Ventilation Space Sensors.....	47
5 Cold Climate (Chicago) Disassembly.....	48
5.1 Ridge Exterior Conditions	48
5.2 Rafter Bay Peak Conditions.....	50
5.3 Conditions Away From Ridge	54
5.4 Interior Disassembly	56
6 Cold Climate (Chicago) Analysis	57
6.1 ASHRAE 160 Analysis.....	57
6.2 Ridge Average Temperature.....	59

6.3	Sheathing Temperatures and Ventilation Space Behavior.....	59
6.4	Conclusions for Cold Climate (Chicago) Test Roof.....	60
6.4.1	Boundary Conditions (Interior Humidification).....	60
6.4.2	Overview of Assemblies.....	60
6.4.3	Cellulose vs. Fiberglass Performance.....	62
6.4.4	Top Vent Assemblies.....	63
6.4.5	Air Leakage (Fiberglass Roofs).....	64
6.4.6	Interior Vapor Control.....	65
7	Hot-Humid Climate (Houston) Experimental Setup.....	66
7.1	Overview.....	66
7.2	Unvented Roof Assembly and Geometry.....	66
7.3	Diffusion Port Assembly.....	68
7.4	Roof Monitoring Setup.....	71
7.5	Inward Vapor Drive Experiment.....	74
7.6	Roof Air Leakage and Pressure Testing.....	75
8	Hot-Humid Climate (Houston) Monitoring Results.....	81
8.1	Boundary Conditions.....	81
8.2	Unvented Roof Measurements.....	85
8.3	Diffusion Vent Roof Measurements (Ridge).....	86
8.4	Diffusion Vent Roof Measurements (Hip).....	88
8.5	Inward Drive Experiment.....	89
9	Hot-Humid Climate (Houston) Analysis.....	92
9.1	Diffusion Vent and Unvented Roof Comparisons.....	92
9.2	ASHRAE 160 Analysis.....	94
10	Conclusions and Further Work.....	96
10.1	Cold Climate (Chicago).....	96
10.1.1	Experimental Results and Conclusions.....	96
10.1.2	Further Work.....	97
10.2	Hot-Humid Climate (Houston).....	98
10.2.1	Experimental Results and Conclusions.....	98
10.2.2	Further Work.....	99
	References.....	102
	Appendix A: Monitoring Equipment.....	106
	Appendix B: Chicago Attic Roof Ventilation Dewpoints.....	107
10.2.3	Roof 1 (Vented).....	107
10.2.4	Roofs 2 and 3 (Top Vent Cellulose).....	108
10.2.5	Roofs 4 and 5 (Top Vent Fiberglass).....	110
10.2.6	Ventilation Space Conclusions.....	111
	Appendix C: Chicago Sheathing T and Ventilation Space.....	112

List of Figures

Figure 1: Dense pack insulation of roof (L) and resulting moisture issues (R) Lstiburek (2010b)	1
Figure 2: Insulation material costs (no installation), in \$/sf-R value	4
Figure 3: Condensation on HVAC equipment located in vented attic (Zone 2A)	5
Figure 4: Unvented roof hybrid insulation options: rigid foam overclad (left) or spray foam (right)	6
Figure 5: Bottom-ventilated roof deck; right figure from Lstiburek (2011)	7
Figure 6: Top-ventilated dense-packed roof assembly (Schumacher & LePage 2012).....	8
Figure 7: Netted and blown cellulose roof insulation in Houston; moisture content at roof ridge....	8
Figure 8: Netted and blown cellulose roof insulation in Jacksonville; corrosion of ridge truss plate	9
Figure 9: Ridge sheathing degradation with dense pack cellulose in northern California	10
Figure 10: Dry sheathing lower at roof (L), and interior ridge conditions (R)	10
Figure 11: Air leakage communication from unvented attic to main space (L), and Houston-area roof underlayment study (R) (Lstiburek 2014).....	13
Figure 12: Test home with attached garage used for experimental roof	16
Figure 13: Chicago experimental roof test bays, showing materials	17
Figure 14: Ridge condition at Roof 1-Vented compact roof	18
Figure 15: Roof 1-Vented compact roof insulation, showing airspace/ventilation detail	18
Figure 16: Ridge condition at Roof 2- Top vent cathedral-cellulose (3, 4, and 5 similar)	19
Figure 17: Soffit condition at Roofs 2, 3, 4, and 5 - Top vent cathedral/cathedralized	19
Figure 18: Dropped sheathing and breather mesh at roof deck of Top vent roofs (2, 3, 4, 5)	19
Figure 19: Top vent roof (2, 3, 4, 5) ridge housewrap covering and cut openings	20
Figure 20: Top vent cellulose roofs (roofs 2 and 3)	20
Figure 21: Top vent fiberglass roofs (roofs 4 and 5).....	21
Figure 22: Ridge condition at Roof 6-Diffusion vent cellulose	22
Figure 23: Ridge condition at Roof 6-Diffusion vent cellulose	22
Figure 24: Diffusion vent (6) and unvented (7) ridge conditions	23
Figure 25: Instrumentation setup for Roof 2-Top vent cathedral-cellulose (3, 4, and 5 similar)	23
Figure 26: Instrumentation setup for Roof 7 – unvented cellulose	25
Figure 27: Experimental attic space heating (L), garage heating and relay box (right)	26
Figure 28: Schematic and photos of humidification setup; heated bucket and reservoir at right...	26
Figure 29: Completed test attic over garage (L), and disassembled “doghouse” detail (R)	27
Figure 30: Interior of experimental roof bays, showing air sealing, gaskets, and instrumentation.	27
Figure 31: West (front) face of experimental roof bays interior	28
Figure 32: East (rear) face of experimental roof bays interior	28
Figure 33: South (gable end) face of test attic	28
Figure 34: Infrared image of test roof (front) in winter conditions (26°F)	29
Figure 35: Infrared image of test roof (front) in mild conditions (47°F)	29
Figure 36: Air leakage at roof connection to main house (XPS sheathed wall)	30
Figure 37: Air leakage at ridge and instrumentation wire penetrations.....	30
Figure 38: Air leakage at gable end rake wall (connects to unvented cellulose Roof 7).....	31
Figure 39: Air leakage testing of attic space (left), and multipoint test results (right)	31
Figure 40: Testing pressure difference (ΔP) across ceiling gypsum board in test attic	32
Figure 41: Test attic interior, garage, and exterior temperatures, winter 2013-2014	34
Figure 42: Test attic interior relative humidity, winter 2013-2014	35
Figure 43: Test attic interior and exterior dewpoint temperature, winter 2013-2014	35
Figure 44: Roof 1 (vented) sheathing moisture contents	36
Figure 45: Roof 7 (unvented cellulose) sheathing moisture contents (unfiltered data).....	36
Figure 46: Roof 6 (diffusion vent cellulose) sheathing moisture contents (unfiltered data)	37
Figure 47: Roof 7 (unvented cellulose) sheathing moisture contents (filtered data)	37
Figure 48: Roof 6 (diffusion vent cellulose) sheathing moisture contents (filtered data).....	38
Figure 49: Roof 2 (top vent cellulose with gypsum board) sheathing moisture contents	38
Figure 50: Roof 3 (top vent cellulose, no gypsum board) sheathing moisture contents	39
Figure 51: Roof 5 (top vent fiberglass with gypsum board) sheathing moisture contents	39
Figure 52: Roof 4 (top vent fiberglass, no gypsum board) sheathing moisture contents	40

Figure 53: Top vent fiberglass, no GWB (4) water leak (L) and wet fiberglass batt (R).....	40
Figure 54: Top vent fiberglass, no GWB (4) wet sheathing (L) and wet batt (R)	41
Figure 55: Rafter framing moisture content, vented (1), diffusion vent (6), and unvented (7).....	42
Figure 56: Rafter framing moisture content, top vent cellulose (2, 3) and fiberglass (4, 5).....	42
Figure 57: Roof ridge peak RH, diffusion vent (6) and unvented (7)	43
Figure 58: Roof ridge peak RH, top vent cellulose (2, 3) and fiberglass (4, 5)	43
Figure 59: Roof ridge wafer sensor example, next to RH sensor	44
Figure 60: Roof ridge wafer sensor, vented (1), diffusion vent (6), and unvented (7)	44
Figure 61: Roof ridge wafer sensor, top vent cellulose (2, 3) and fiberglass (4, 5).....	45
Figure 62: Roof “doghouse” sheathing moisture content sensor.....	45
Figure 63: Roof “doghouse” sheathing moisture content measurements	46
Figure 64: Roof “doghouse” sheathing moisture content measurements with precipitation	46
Figure 65: Ridge conditions, before removal of breather mesh	48
Figure 66: Ridge conditions, after removal of breather mesh.....	48
Figure 67: Ridge conditions, after removal of breather mesh.....	49
Figure 68: Ridge sheathing conditions (“screwdriver test”) for Roofs 4 and 5	49
Figure 69: Ridge sheathing conditions, Roofs 1, 2, and 3.....	50
Figure 70: Ridge sheathing bottom (L) and top (R) conditions, Roof 3	50
Figure 71: Ridge sheathing top conditions, Roof 2 (L); cellulose conditions (R)	51
Figure 72: Ridge sheathing top (L) and bottom (R) conditions, Roof 4	51
Figure 73: Ridge sheathing bottom conditions, Roof 4	52
Figure 74: Ridge sheathing conditions, Roof 5	52
Figure 75: Fiberglass batt conditions at ridge, Roof 4.....	53
Figure 76: Fiberglass batt and framing conditions at ridge, Roof 4 (L) and Roof 5 (R)	53
Figure 77: Ridge sheathing top and bottom conditions, Roof 6	53
Figure 78: Ridge sheathing top and bottom; cellulose conditions, Roof 7	54
Figure 79: Sheathing away from ridge, west (front) face of roof	54
Figure 80: Sheathing away from ridge, east (rear) face of roof.....	55
Figure 81: Sheathing away from ridge, Roofs 4 and 5 (L), Roofs 6 and 7 (R).....	55
Figure 82: Sheathing away from ridge, Roofs 4 (left) and 5 (right).....	56
Figure 83: Staining of ceiling gypsum board at (L); mold on framing (R), Roof 5	56
Figure 84: ASHRAE 160 failures, vented (1), diffusion vent (6), and unvented (7).....	57
Figure 85: ASHRAE 160 failures, top vent cellulose (2, 3) and fiberglass (4, 5).....	58
Figure 86: 30-day running average temperatures at ridge (T/RH sensors) for all roofs.....	59
Figure 87: Top vent roofs, no interior GWB, East/front face; cellulose (L) and fiberglass (R)	62
Figure 88: Vapor permeance of plywood and OSB sheathing as a function of RH	64
Figure 89: Ridge condensation issues; Zone 3A pool with interior polyethylene vapor barrier	65
Figure 90: Front and side views of Houston-area test house	66
Figure 91: Rear quarter and overhead views of Houston-area test house	66
Figure 92: Interior of spray-applied fiberglass insulation in conditioned attic	67
Figure 93: Spray foam used for roof-to-wall air barrier connection	67
Figure 94: Air barrier/conditioned space line for unvented attic, front (L) and side (R).....	68
Figure 95: Diffusion vent design at roof ridge and hip	68
Figure 96: Open ridge (“diffusion port”) detail (L); permeable membrane applied over ridge (R)...	69
Figure 97: Hip “diffusion port” drilled hole detail (L); permeable membrane applied at hips	69
Figure 98: Venting detail at ridge (L) and hip (R), showing vent profile	70
Figure 99: Ridge monitoring “package” (sensors at ridge and hip peaks)	71
Figure 100: Houston roof plan, showing ridges, hips, and valleys, and measurement locations ...	72
Figure 101: Typical ridge monitoring package, with sensors highlighted.....	73
Figure 102: Ridge sheathing T/MCs and T/RH (L); ridge T/MC and wafer sensor (R).....	73
Figure 103: Interior attic temperature/RH sensor (L); exterior T/RH sensor under north soffit (R) .	74
Figure 104: Inward drive “box” before insulation (L); after insulation and clear plastic cover (R)..	74
Figure 105: Inward drive sensor package	75
Figure 106: Air leakage (blower door) testing (L); multipoint hatch open/closed results (R).....	76
Figure 107: Unsealed gas appliance exhaust/intake, with evidence of air leakage	77

Figure 108: Air leakage at roof-to-wall details at dormer/intersecting roofs (Location A)..... 78

Figure 109: Air leakage at front attic gable end (Location B)..... 78

Figure 110: Front and rear elevations, showing air barrier failure locations 78

Figure 111: Air leakage at roof-to-wall details at roof-wall intersection (Location C) 79

Figure 112: Air leakage at rear attic over master bedroom (Location D)..... 79

Figure 113: Air leakage at roof-to-wall connections, from interior space (first floor) 80

Figure 114: Air leakage at roof-to-wall connections, from interior space (second floor) 80

Figure 115: Houston exterior, attic, and main conditioned space temperatures 81

Figure 116: Heating degree days (L) and cooling degree days (R) for Houston (IAH airport)..... 81

Figure 117: Houston temperatures, summertime (July 2014) detail..... 82

Figure 118: Attic T/RH locations highlighted in plan (L) and front/rear elevations (R)..... 82

Figure 119: Houston temperatures, wintertime (January 2015) detail 83

Figure 120: Houston exterior, attic, and main conditioned space dewpoint temperatures 83

Figure 121: Houston dewpoint temperatures, summertime (July 2014) detail..... 84

Figure 122: Houston attic and main conditioned space relative humidity 84

Figure 123: Unvented roof (UV1) roof MC and RH measurements 85

Figure 124: Unvented roof (UV2) roof MC and RH measurements 85

Figure 125: Diffusion vent (DV1) roof MC and RH measurements..... 86

Figure 126: Diffusion vent (DV2) roof MC and RH measurements..... 87

Figure 127: Diffusion vent (DV3) roof MC and RH measurements..... 87

Figure 128: Diffusion vent (DV6) roof MC and RH measurements..... 87

Figure 129: Diffusion vent (DV1) roof MC and RH measurements, summer (July 2014) detail 88

Figure 130: Diffusion vent at hip (DV4) roof MC and RH measurements 88

Figure 131: Diffusion vent at hip (DV5) roof MC and RH measurements 89

Figure 132: Inward drive interior-side RH and wafer sensor, with outdoor T..... 89

Figure 133: Inward drive wafer sensor MC and sheathing MCs, with outdoor T 90

Figure 134: Inward drive wafer sensor MC and precipitation, with outdoor T 90

Figure 135: Inward drive interior-side RH, wafer MC and sheathing temperature 24 hour average 91

Figure 136: Inward drive interior-side RH, wafer MC and sheathing temperature 24 hour average
 (summertime detail) 91

Figure 137: Diffusion vent (DV1) and unvented (UV1) comparison (ridge RH and wafer MC)..... 92

Figure 138: DV1 and UV1 comparison (ridge RH and wafer), summertime detail..... 93

Figure 139: DV1 and UV1 comparison (ridge RH and wafer), summertime detail..... 93

Figure 140: Summertime dewpoint comparison: interior, attic, exterior, and UV1/DV1..... 94

Figure 141: Story and a half compact roof example (with insulation and ventilation chute) 98

Figure 142: Rudd and Henderson (2007) interior temperature data and Houston unvented data . 100

Figure 143: Rudd and Henderson (2007) interior RH data and Houston unvented data 100

Figure 144: Rudd and Henderson (2007) interior dewpoint data and Houston unvented data 100

Figure 145: Intake and exhaust dewpoints, w. interior & exterior (Roof 1-Vented) 107

Figure 146: Intake and exhaust dewpoints, w. interior & exterior (Roof 1-Vented)-Detail 107

Figure 147: Intake (L) and exhaust (R) T/RH sensors for “top vent” roofs..... 108

Figure 148: Intake and exhaust dewpoints, w. interior & exterior (Roof 2-Top Vent Cell.-GWB) ... 108

Figure 149: Intake and exhaust dewpoints, w. interior & exterior (Roof 2-Top Vent Cell.-GWB),
 detail 109

Figure 150: Intake and exhaust dewpoints, w. interior & exterior (Roof 3-Top Vent Cell.) 109

Figure 151: Intake and exhaust dewpoints, w. interior & exterior (Roof 3-Top Vent Cell.), detail.. 110

Figure 152: Intake and exhaust dewpoints, w. interior & exterior (Roof 5-Top Vent FG-GWB)..... 110

Figure 153: Intake and exhaust dewpoints, w. interior & exterior (Roof 4-Top Vent FG)..... 111

Figure 154: Wintertime sheathing temperatures for Roof 2 (top vent cellulose with gypsum board)112

Figure 155: Wintertime sheathing temperatures for Roof 7 (unvented cellulose) 112

Figure 156: Snow deposits and melting at front (west) orientation of test roof..... 113

Figure 157: Summertime sheathing temperatures for Roof 2 (top vent cellulose with gypsum
 board)..... 113

Figure 158: Summertime sheathing temperatures for Roof 7 (unvented cellulose)..... 113

Figure 159: Ridge and “doghouse” monitoring detail, unvented cellulose roof..... 114

Figure 160: Summertime sheathing temperatures for Roof 1 (vented fiberglass)..... 114

Unless otherwise noted, all figures were created by Building Science Corporation.

List of Tables

Table 1: Summary of simulation results (roof sheathing MCs) from Salonvaara et al. (2013), 11
Table 2: Test roof assemblies monitored in Smegal and Straube (2014) 13
Table 3: Description of Chicago experimental roof test bays 17
Table 4: Results of test attic air leakage testing..... 31
Table 5: Test attic air ΔP across gypsum board, with attic at 50 Pa 32
Table 6: Color code labels used for cold climate (Chicago) roof assemblies 41
Table 7: Number of hours roof ridge T/RH failing ASHRAE 160 criteria 58
Table 8: Third party air leakage and duct leakage test results 75
Table 9: Houston test house hatch open and closed air leakage measurements 76
Table 10: Houston test house hatch open and closed air leakage measurements 77
Table 11: Houston test house zone pressure diagnostic (ZPD) calculation results..... 77
Table 12: Hours and percent of monitored period failing ASHRAE 160 criteria 95
Table 13: Testing and monitoring equipment specifications 106

Unless otherwise noted, all tables were created by Building Science Corporation.

Definitions

ACH50	Air changes per hour at 50 Pa
ASHRAE	American Society of Heating, Refrigerating and Air-Conditioning Engineers, Inc.
ASTM	American Society for Testing and Materials
BA	Building America Program
BSC	Building Science Corporation
Btu	British thermal unit
ccSPF	Closed-cell Spray Polyurethane Foam
CDD	Cooling degree day
CFM50	Cubic feet per minute at 50 Pa
CZ	Climate Zone
DOE	U.S. Department of Energy
DV	Diffusion vent (roof)
EqLA	Equivalent leakage area
GWB	Gypsum wall board
HDD	Heating degree day
HVAC	Heating, ventilation, and air conditioning
ICC	International Code Council
IRC	International Residential Code for One- and Two-Family Dwellings
MC	Moisture content
NREL	National Renewable Energy Laboratory
ocSPF	Open-cell Spray Polyurethane Foam
ORNL	Oak Ridge National Laboratory
OSB	Oriented strand board

Pa	Pascal
RH	Relative humidity
SPF	Spray polyurethane foam
T	Temperature
UV	Unvented (roof)
W	Watt
WRB	Water-resistive barrier
XPS	Extruded polystyrene

Executive Summary

In cold climates, a common practice of the weatherization industry is to retrofit compact roof/ceiling assemblies with blown-in dense-pack cellulose. However, this assembly has high moisture and durability risks (due to wintertime interior-sourced condensation) and violates building code. Developing methods to retrofit dense pack insulation into compact roof assemblies while controlling moisture risks would allow for widespread application of this low-cost technique without potentially compromising building durability.

In hot-humid climates, HVAC equipment is typically located in vented, unconditioned attics, with associated energy penalties; one method of moving the ductwork inside the conditioned space is to insulate at the roof deck. However, market penetration of this method has been slow, due to the expense of insulating at the roof line, typically using polyurethane spray foam. If roof assemblies with fibrous insulation could be developed that control moisture risks, this would likely reduce the first cost of unvented roofs, potentially increasing their adoption.

To understand the long-term moisture performance of unvented roof assemblies with fibrous insulation, test roofs were built in two climates and monitored. A cold-climate test house was located in Bolingbrook, IL (Chicago area; Zone 5A), and hot-humid test house was located in Friendswood, TX (Houston area, Zone 2A). One test house was monitored at each site.

The Chicago-area test bed included seven parallel experimental rafter bays: the assemblies included a “control” vented compact (cathedral) roof, a dense-pack cellulose unvented roof, and an unvented roof with a “diffusion vent” (strip of vapor-permeable gypsum sheathing at the ridge to allow drying); the interior finish was gypsum board with latex paint. The other four bays were “top vent” roof assemblies, which have a polypropylene “breather mesh” between the roof sheathing and the asphalt shingles, thus allowing ventilation drying of the assembly from underneath the vapor-impermeable shingles. The four “top vent” roofs were two fiberglass batt and two dense-pack cellulose roofs, with either interior gypsum board, or open to the interior. Wintertime moisture-related failure was accelerated by providing interior humidification (72° F/50% RH; known to be an extreme interior loading). Data captured eight months, including a winter and following spring/early summer.

Under these conditions, all roofs except the vented cathedral assembly experienced wood moisture contents (MCs) and RH levels high enough to constitute failure. The unvented dense-pack cellulose roof experienced sheathing moisture MCs well above 40% at the ridge (i.e., risk of mold, rot, and decay). MCs lower in the roof were less severe (above 30%), but still in the dangerous range. In all assemblies, sheathing MCs were corroborated by rafter MC and roof peak RH. Other sensors indicated that liquid water condensation was occurring at the peak of all unvented test roofs. The diffusion vent roof had similar behavior to the unvented cellulose roof, but in the spring, ridge conditions dried much more rapidly in the diffusion vent roof. The “top vent” assemblies showed similar behavior to the unvented assemblies (high MCs). Roof assemblies with gypsum board has drier moisture levels than the assembly without gypsum board, which is consistent with the painted gypsum board providing some level of air leakage and vapor flow control. When the results were analyzed using ASHRAE Standard 160, all of the

unvented roof assemblies failed for significant portions of the spring, showing that moisture levels remained high into warmer weather, which would have allowed mold growth.

The roof was disassembled at the end of the experiment, to correlate measurements with actual assembly conditions. The unvented fiberglass batt roofs had wet sheathing and mold growth, although not structural failure. The cellulose roofs had only slight issues, such as rusted fasteners, staining and sheathing grain raise, despite the measured extreme moisture conditions. This difference was ascribed to cellulose's borate preservatives, its airflow retarding properties (especially compared to batts), and its ability to safely store moisture. The comparison of batt (installed with gaps) vs. loose fill insulation puts the fiberglass roof at a disadvantage.

The Houston-area roof is in a model house, which is unoccupied during the testing period. The test house was configured with an unvented/sealed attic, insulated at the roofline. Unlike the cold-climate roof, the entire roof was insulated with a single material (spray-applied/adhered fiberglass, left exposed). No intentional humidification or conditioning was provided in the unvented attic space; the space "floats" at conditions between interior setpoint and exterior conditions. Most of the roof ridges and hips were built with a "diffusion vent" detail, capped with a strip of a highly vapor permeable (550 perms) roof membrane. Some ridge sections were built as a conventional unvented roof, as a control comparison. Data have been collected from February 2014 through June 2015 (16 months), with ongoing data collection.

In the control unvented roofs, roof peak RHs reached high levels (90%+) in the first winter; as exterior conditions warmed, RHs quickly fell to 40-50%, as solar heating drove moisture out of the roof sheathing (inward). MC measurements were consistent with RH measurements: initial winter conditions were higher than recommended, but fell to safe levels in the summer. In the second winter (2014-2015), peak RHs rose again (60-80% typical), but not to the same levels as the first winter. This difference was due to lower interior RH levels in the second winter.

In contrast, the diffusion vent roofs had drier conditions at the roof peak in wintertime, but during the summer, RHs and MCs were higher than the unvented roof. However, these moisture levels were well within the safe range. The diffusion vent roof also showed strong diurnal variations of RH levels. Both of these behaviors are consistent with the roof rafter bay having a hygric/moisture connection to outside air, due to the vapor-open diffusion vent. The hip roofs treated with a diffusion vent showed behavior halfway between the unvented and diffusion vent roofs. This was attributed to the limited diffusion vent area (2 in. diameter drilled holes, rather than 3 in. strip) available in the hip geometry.

Overall, these results indicate that the diffusion vent roof has a greater amount of drying (and less wintertime moisture accumulation) than the unvented roof. However, the unvented roof did not have moisture contents high enough to truly constitute "failure."

1 Introduction

1.1 Background

In cold climates, a common practice of the weatherization industry is to retrofit compact roof/ceiling assemblies (e.g. cathedral ceilings) with blown-in dense-pack cellulose. Cold climate house plans often have conditioned space with compact sloped roof/ceiling assemblies above. This dense-pack retrofit minimizes the interior and exterior demolition required for retrofitting insulation, compared to (for example) spray foam retrofits.

However, a dense-packed compact roof assembly has high moisture and durability risks (due to wintertime interior-sourced condensation), as discussed by Lstiburek (2010b), and Schumacher and LePage (2012) (Figure 1).



Figure 1: Dense pack insulation of roof (L) and resulting moisture issues (R) Lstiburek (2010b)

In addition, this assembly does not meet building code: §R806.4 “Unvented attic assemblies,” of the International Residential Code/IRC (ICC 2009) has requirements for minimum quantities of air impermeable insulation on the exterior side of the assembly, to control condensing surface temperatures in winter.

Developing methods to retrofit dense pack insulation into compact roof assemblies while controlling moisture risks would allow for widespread application of this lower-cost technique without potentially compromising building durability.

In hot-humid climates, HVAC equipment (both ductwork and air handlers) are typically located in vented, unconditioned attics, with associated energy penalties due to duct leakage and conductive losses. One method of moving the ductwork inside the conditioned space (air barrier and thermal barrier) is to insulate at the roof deck, creating a “cathedralized” attic space (Rudd et al. 1997, Rudd and Lstiburek 1998, Lstiburek 2006). However, market penetration of this method has been slow despite its performance benefits, due to the expense of insulating at the roof line, typically using polyurethane spray foam (a more costly material than typical fibrous insulation materials). Previous experience of creating “cathedralized” attics in a hot-humid climate (DOE Climate Zone 2A) with asphalt roof shingles showed that moisture-related failures (condensation at the ridge) can occur (see §“Field Experience in Houston, TX and Jacksonville, FL”); this led to the requirements provided in §R806.4 of the IRC (ICC 2009). If roof assemblies could be developed that control moisture risks, this would likely reduce the first cost of unvented roofs, potentially increasing their adoption.

Both of these issues are, at their core, studies of the moisture-safe performance of unvented roof assemblies, with moisture vapor impermeable roofing materials (i.e., layers of asphalt shingles and underlayment) on the exterior. This research involved building and instrumenting a variety of unvented roof assemblies insulated with air permeable insulation (such as dense-pack cellulose) in cold and hot-humid climates, and to analyze their moisture performance over time. The goal was reasonable-cost, low moisture risk, and buildable assemblies that could be promoted in both the new construction and retrofit markets.

1.2 Experimental Approach

The experimental approach was to build unvented roof test assemblies in houses, and to install instrumentation to measure their long-term moisture performance (i.e., long-term monitoring). The cold-climate test house was located in Bolingbrook, IL (Chicago area; Zone 5A), provided by K. Hovnanian Homes. The hot-humid test house was located in Friendswood, TX (Houston area, Zone 2A), provided by David Weekley Homes. One test house was monitored at each site.

The Chicago-area test bed for the experimental roofs was the attic of an attached garage. Seven parallel rafter bays were used as experimental test bays; the assemblies included unvented dense-pack cellulose and fiberglass batt roofs, with one vented fiberglass roof as a control comparison. The attic space was heated and humidified for the experiment. Data were collected from October 2013 through June 2014, capturing a winter and a following spring/early summer. At the conclusion of the experiment, the assemblies were disassembled, to find any evidence of condensation, moisture accumulation, or moisture-related damage. The roof was then rebuilt, returning it to its original, non-experimental condition.

The Houston-area roof is in a model house, which is unoccupied during the testing period. The test house was configured with an unvented/sealed attic, insulated at the roofline. Unlike the cold-climate roof, the entire roof was insulated with a single material (spray-applied/adhered fiberglass, left exposed/no interior finish). No intentional humidification or conditioning was provided in the unvented attic space; the space “floats” at conditions between interior setpoint and exterior conditions. Most of the roof ridges and hips were built with a “diffusion vent” detail, capped with a strip of a highly vapor permeable roof membrane. Some ridge sections were built as a conventional unvented roof, as a control comparison. Data have been collected from February 2014 through June 2015 (16 months), with ongoing data collection.

Instrumentation was installed as per Straube et al. (2002), using a central data acquisition system per house. The roof assemblies were measured for temperatures, wood moisture contents (both sheathing and framing), and relative humidity. Interior and exterior temperature and relative humidity conditions were measured on-site; exterior data was supplemented by airport weather data (e.g., precipitation and wind). Instrumentation listing and specifications can be found in Appendix A.

1.3 Relevance to Building America’s Goals

Given the Building America goals of reducing home energy use by 30%-50% (compared to 2009 energy codes for new homes and pre-retrofit energy use for existing homes), the two cases described in the introduction will help achieve those goals in a more cost effective manner:

- In cold climates, retrofit insulation of roofs with dense-pack cellulose is a lower-cost and less intrusive technique than demolition and the use of spray foam insulation. However, it runs the risks of moisture and durability problems. Removing this obstacle will allow its adoption in cases where it would have been avoided in the past.
- In hot-humid climates, unvented roof assemblies can be used to bring ductwork and air handler units into the conditioned space, and improve airtightness. Doing so with materials that are lower cost than spray foam (the current solution) may increase its adoption.

NREL and the Standing Technical Committee on Enclosures presented top priorities for research in their document, “Building America Technical Innovations Leading to 50% Savings – A Critical Path” (NREL 2013b). Under the Enclosures section, Item E4 specifically addressed the issue of unvented dense-pack roof assemblies in cold climates:

By end of 2015, address common practices that use methods in violation existing codes, including those routinely performed by the weatherization industry such as dense packing unvented cathedral ceilings and low slope roofs.

Significance: Promoting methods that violate existing codes raise legal, moral and ethical issues.

Interim Steps: Change existing codes to allow alternative methods that currently do meet existing codes

Challenges: Field testing of alternative methods in various climate zones is necessary. Often failures and lessons learned are not disclosed due to litigation.

This work also falls under the category of “2.0 Risk Reduction and Minimization,” from the document FY 2014 Residential Energy System Research Needs (NREL 2013a).

1.4 Cost-Effectiveness

One of the goals of this research is to find moisture-safe methods to replace higher-cost spray polyurethane foam (SPF), or rigid board foam with lower cost fibrous fill insulation. The retrofit of an empty cavity (as per the cold-climate example of retrofit insulation of a cathedral ceiling) will clearly be a cost effective measure; this is compounded by the moderate air sealing effects of dense pack insulation (per Schumacher 2011).

The installed cost of closed cell spray foam (ccSPF) varies strongly based on contractor availability, the size of the installation, regional pricing, feedstock (crude oil) prices, and access (e.g. requirement for lifts or scaffolding; confined space installation). However, a typical installed price used for estimation purposes is roughly \$1/board foot (1 in. x 12 in. x 12 in.), although pricing variations range in practice anywhere from \$0.45 to \$1.40/board foot.

A comparison of insulation material costs is shown below in Figure 2, based on “big box” home center pricing gathered from 2007 through 2011. It is shown using the normalization metric of \$/sf·R value, which normalizes the area costs based on the R values.

It shows values for extruded polystyrene (XPS), polyisocyanurate, fiberglass, cellulose, spray foam, and mineral fiber. Note that closed cell spray foam is included in the graph with a caveat: there is no isolated “material cost” for ccSPF, since it is effectively manufactured and installed as a single step. An estimate was made using the \$1/board foot price and dividing by 2 (½ materials and ½ labor).

It is evident from the graph that ccSPF is at a comparable price to the rigid board foam plastic products (XPS and polyisocyanurate), which are both substantially more expensive than cavity fill fibrous insulation, such as fiberglass or cellulose.

Closed cell SPF, XPS, and polyisocyanurate are all premium products—with an associated cost penalty—because they are air impermeable insulation materials that are intrinsically moisture-tolerant. When designing enclosures, these premium materials should be used to take advantage of their properties. Assembly R value can be augmented (if desired) with lower cost fibrous insulation products, assuming that durability is not compromised by adding it to the design.

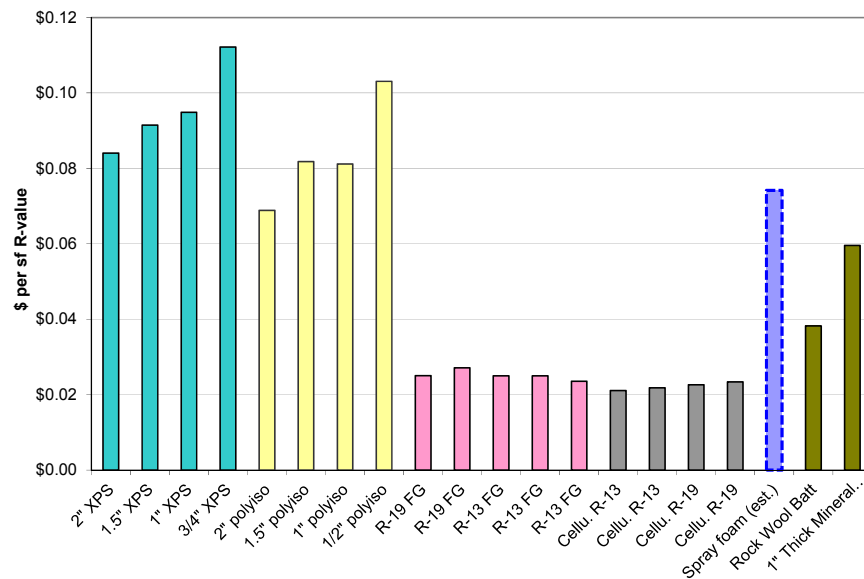


Figure 2: Insulation material costs (no installation), in \$/sf-R value

1.5 Tradeoffs and Other Benefits

The basic benefits of retrofit insulation of compact roof assemblies (including cathedral ceilings) include energy savings due to reduced heat flow and reduced air flow, and thermal comfort improvements for occupants (due to radiant surface temperature effects).

Benefits of unvented roof assemblies in hot humid climates include energy savings due to the elimination of duct conductive and air leakage losses; shifting the enclosure geometry to the roof line commonly improves building airtightness. In addition, bringing the ductwork and HVAC equipment within the conditioned space can reduce the risks of surface condensation on cold equipment surfaces, compared with high-dewpoint attic (essentially exterior) air.



Figure 3: Condensation on HVAC equipment located in vented attic (Zone 2A)

2 Background Literature and Field Experience

2.1 Unvented Roof Background Literature

Lstiburek (2010b) provides an overview of the use of dense-pack cellulose insulation, and shows examples of the problems that can occur in compact roof assembly applications. Schumacher and LePage provide a comprehensive analysis of the use of dense pack insulation in compact roof assemblies in their document, “Moisture Control for Dense-Packed Roof Assemblies in Cold Climates: Final Measure Guideline” (Schumacher and LePage 2012). They provide an overview of the problem, citing previous literature:

Many contractors and cellulose sales people falsely believe that dense-pack assemblies are “airtight”. This has been shown not to be the case (Derome 2005, Schumacher 2011) – with disastrous consequences in cold and mixed climates where roof rafters have been “dense packed” with no provision for rafter ventilation (to remove moisture) or for control of condensing surface temperatures (to minimize moisture accumulation) (Lstiburek 2010b). Approximately two assemblies in ten fail – typically within 10 years (Fitzgerald 2010).

Schumacher and LePage also provide hygrothermal analysis of a variety of assemblies, showing the moisture risks associated with unvented dense-pack roofs. They suggest that failures are not endemic because post-retrofit houses only achieve moderate airtightness. As a result, interior moisture generation is sufficiently diluted by wintertime air leakage to result in low wintertime interior relative humidity levels. They provide several options for moisture-safe roof assemblies that utilize dense-pack cellulose, as follows:

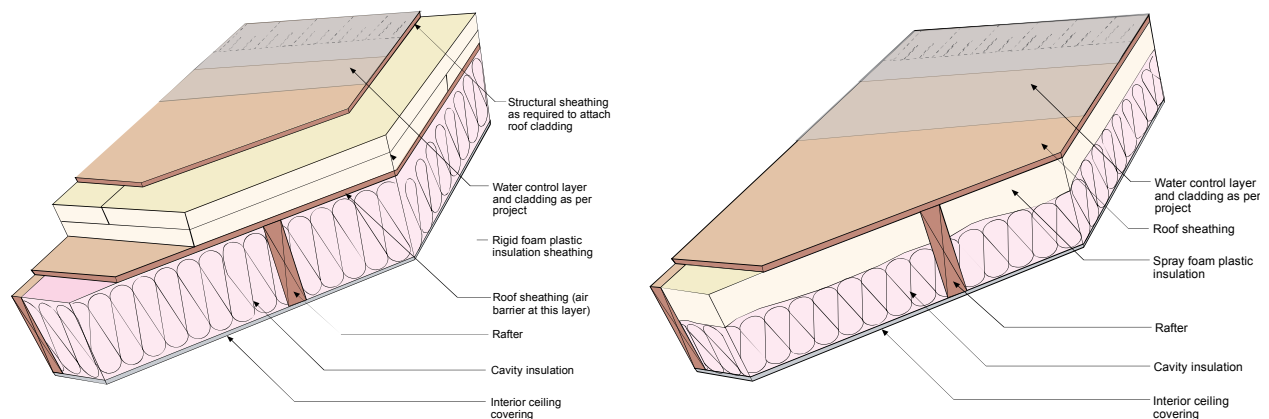


Figure 4: Unvented roof hybrid insulation options: rigid foam overclad (left) or spray foam (right)

1. Exterior Insulation: roof deck overclad, as per Figure 4 left
2. Hybrid Insulation: spray foam at roof deck with fibrous insulation as per Figure 4 right
3. Bottom-Ventilated Decks: air space or rafter ventilation chutes underneath the roof deck, outboard of insulation, as per Figure 5
4. Top-Ventilated Decks: air space underneath the asphalt shingles/roof cladding, thus creating a drained and ventilated cavity, as per Lstiburek (2010a) and Straube & Burnett

(2005), per Figure 6. This assembly is not a common assembly with asphalt shingles, and was considered somewhat experimental or conceptual.

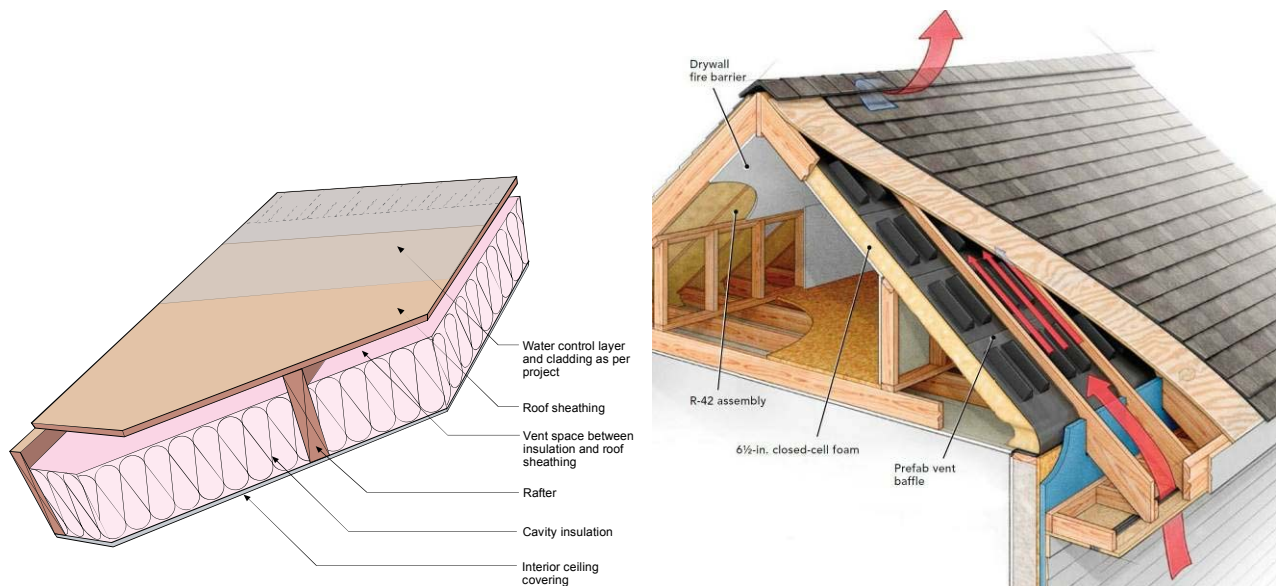


Figure 5: Bottom-ventilated roof deck; right figure from Lstiburek (2011)

The “top ventilated” deck warrants further explanation; Schumacher and LePage (2012) provide a description of the design, with recommendations for implementation; a conceptual illustration is shown in Figure 6.

A number of low-rise residential roofing systems incorporate ventilated gaps between the roofing and the roof deck (e.g. clay roof tiles, concrete roof tiles & slate tiles installed on strapping; cedar shakes installed over drainage/ventilation mat). The top-ventilated deck strategy might be considered for dense-pack insulation retrofits where the existing ceiling must be kept but exterior insulation cannot be added (e.g. due to historical preservation considerations, spatial limitations or cost constraints).

When a ventilation gap is incorporated above the roof deck, the roofing can dry to the underside. If a vapor permeable underlayment is used, the roof sheathing can also dry to this ventilated gap; however, the rate of drying through the sheathing is limited by the vapor permeance of the sheathing and the drainage plane installed on top of the sheathing.

Top-ventilated retrofit roofs may provide better moisture performance than common retrofit roofs; however, further research is needed to better understand and establish the sensitivity to sheathing and underlay vapor permeance. At this point in time the likely moisture performance of top-ventilated retrofit roofs is not expected to be as good as the other three retrofit strategies: exterior insulated, hybrid-insulated and bottom-ventilated retrofits. Builders are encouraged to employ one of the first three strategies. If a top-ventilated retrofit must be implemented, it should be completed using plywood sheathing and high vapor permeance underlayment.

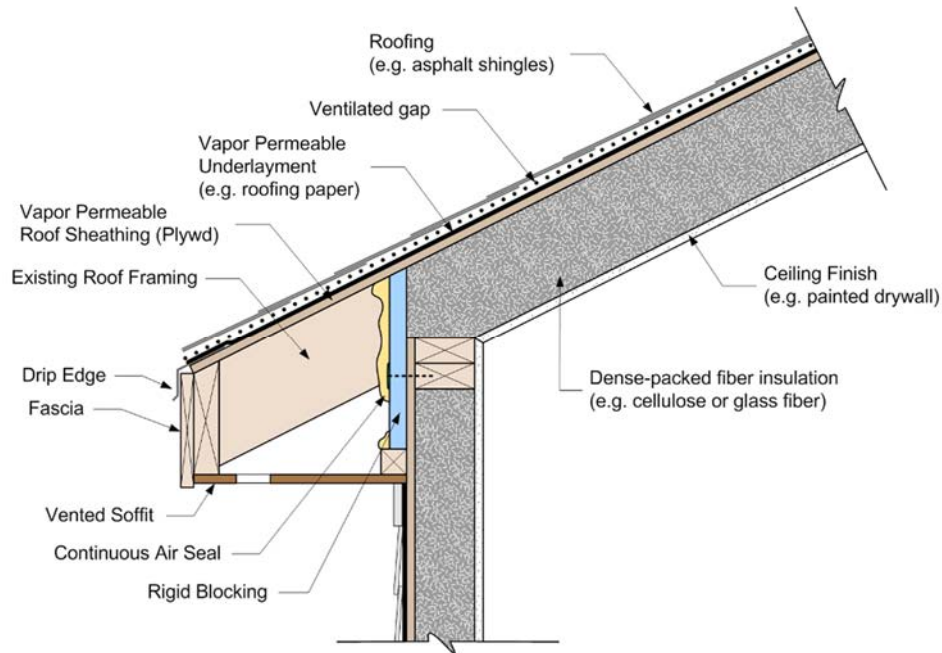


Figure 6: Top-ventilated dense-packed roof assembly (Schumacher & LePage 2012)

2.2 Field Experience in Houston, TX and Jacksonville, FL (CZ 2A)

BSC made discoveries on unvented roof behavior in hot humid climates during field implementation; several of these roofs were built in the Houston TX area circa 2001 (IECC climate zone/CZ 2A). The typical roof assembly was asphalt shingles, roofing felt, OSB sheathing, and netted and blown cellulose insulation (see Figure 7 left). Netting was attached to the underside of the dimension lumber (2x8 to 2x12) rafters.

However, during the first fall of operation, the homeowner reported seeing reflections of moisture condensation and dripping from the ridge of the unvented attic, from the interior. Site investigations (see Figure 7 right) revealed that at the ridge, there were elevated wood moisture contents, and evidence of previous condensation (such as rusted staples).



Figure 7: Netted and blown cellulose roof insulation in Houston; moisture content at roof ridge

In addition, the cellulose insulation at the peak had a noticeably “packy” or compactable texture, as opposed to the “fluffy” texture of dry cellulose. This failure was localized at the peak of the roof. These moisture issues were remediated by removing the insulation at the roof ridge; of course, there was a thermal penalty associated with this modification.

A similar type of issue occurred in two production homes in Jacksonville, FL (CZ 2A), circa 2000. Again, the roof assembly was asphalt shingles, roofing felt, OSB sheathing, and netted and blown cellulose insulation (Figure 8, left). The house was relatively airtight for the climate (2.5 ACH 50).

During a site visit, the cellulose and roof sheathing above were wet to the touch, and the steel truss plate was corroded; however, there was no wood decay. In response, the insulation was removed near the ridge (roughly two feet, per Figure 8, right), to increase surface temperatures at the condensing roof sheathing surface. This roof has been rechecked over time (circa 2003, and as recently as March 2014); roof sheathing conditions remain dry with this assembly.



Figure 8: Netted and blown cellulose roof insulation in Jacksonville; corrosion of ridge truss plate

2.3 Field Experience in Northern California (CZ 3C)

Moisture issues in unvented roof assemblies often manifest in the form of damage to the sheathing at the ridge of a sloped roof, colloquially known as “ridge rot.” An example is shown in Figure 9, which was a dense pack cellulose roof in a northern California location (CZ 3C Marine).



Figure 9: Ridge sheathing degradation with dense pack cellulose in northern California

These issues occurred soon after construction (first winter); the problems were manifested as paint blistering at the interior gypsum board near the roof (Figure 10, right), due to dripping of accumulated condensation. The issue was definitely localized at the ridge of the roof; disassembly at lower portion of the roof showed dry sheathing conditions (Figure 10, left). Air barrier imperfections at the interior gypsum board (in particular, at the ridge board interruption) were a contributing factor.

The pattern of moisture accumulation seen here and in Zone 2A influenced the experimental design: sensors were concentrated near the roof ridge, where problems appear to be prevalent.



Figure 10: Dry sheathing lower at roof (L), and interior ridge conditions (R)

2.4 Salonvaara et al. (2013): Modeling Unvented Roofs in CZ 1-4

Salonvaara et al. (2013) studied unvented attics with simulations in CZ 1 through 4. They first presented an overview of unvented (or sealed) attics, with the positives and negatives of this design, compared to conventional vented attics.

The authors calibrated their models against field monitoring results from Boudreaux et al. (2013). One factor noted when comparing modeled and monitored results was the difference between the high temperature (140°F/60°C) sorption isotherm (relationship between relative

humidity and moisture content), compared with the room temperature isotherm. Slightly better correlation was achieved by using a temperature-dependent sorption response.

The authors then ran hygrothermal simulations (WUFI Pro) models of vented and unvented roof assemblies in various configurations, in climate zones 1 through 4. Interior RH levels were set at design conditions (higher than average/typical conditions); this exacerbates wintertime interstitial condensation risks. The roof assemblies consisted of asphalt shingles, felt paper, OSB sheathing, and insulation (ocSPF or fiberglass). Cases were run for no water intrusion and for a rainwater leak (1% of incident rain hitting the surface bypasses the water-resistive barrier) to the roof sheathing. The results are summarized, in the form of peak roof sheathing MCs, for the various cases in Table 1; peak moisture contents above 20% are highlighted in red. CZs 1, 3, and 4 results are shown to provide a range.

Table 1: Summary of simulation results (roof sheathing MCs) from Salonvaara et al. (2013),

Case	No Rain Leak (Peak MCs)			1% Rain Leak (Peak MCs)		
	CZ 1	CZ 3	CZ 4	CZ 1	CZ 3	CZ 4
Vented attic	8%	7%	7%	12%	12%	12%
Unvented, ocSPF (23 perm-in.)	8%	12%	15%	16%	24%	29%
Unvented, ocSPF (54 perm-in.)	8%	16%	22%	14%	27%	35%
Unvented, ocSPF (23 perm-in.) + 1 perm coating	6%	8%	9%	25%	49%	37%
Blown fiberglass, no interior vapor retarder	8%	19%	30%	13%	30%	-
Blown fiberglass, 10 perm interior vapor retarder	8%	14%	-	15%	26%	-

The authors concluded from these simulations that a vented attic assembly has greater drying ability in all climates than unvented assemblies. Most unvented ocSPF assemblies had safe MCs without rain leakage, but in colder climates (CZ 4) with very vapor-open ocSPF (54 perm-in.), peak MCs reached risky levels. With the addition of rain leakage, moisture contents were substantially higher, likely constituting failure (in most climate zones). The addition of a 1 perm coating (intumescent paint; 1 perm dry cup, 3 perm wet cup) on the interior side of the ocSPF resulted in lower MCs without rain leakage (reduction of interior-sourced vapor flow), but higher MCs with rain leakage (reduced ability to dry inward).

The two final cases use blown fiberglass insulation (100 perm-in.) instead of ocSPF; only CZ 1-3 were plotted. These results show that when vapor-open interior netting is used for installation, acceptable moisture contents were found in CZ 1 and 2, but riskier conditions were seen in CZ 3 and 4. Adding netting with a vapor permeance of 10 perms reduces risks to reasonable levels in CZ 1-3. The authors recommended that the current code requirement (IRC §806.4) for R-5 air impermeable insulation in CZ 1 and 2 be dropped, based on these results.

The authors then used whole-house energy simulations (WUFI-Plus) to study airflow issues between the interior conditioned zone, unvented attic, and exterior. They noted that although a house can have overall low enclosure air leakage, during the summer, stack effect will act downward, and exterior air will be drawn predominantly into the attic, if there is leakage to the outdoors. As a result, infiltration of hot-humid air can have a disproportionate effect on attic humidity conditions. In the simulations, air leakage resulted in high enough attic humidity to

cause concerns for mold growth. Although the common solution is addition of some space conditioning (summertime cooling and dehumidification) to the attic, the authors are wary of this solution for IAQ reasons (connecting non-cleaned attic space with interior air). The authors conclude that air sealing of the attic to the exterior is critical.

2.5 Boudreaux et al. (2013): Sealed Attic Monitored Performance (CZ 3A/4A)

The researchers presented data collected at eight houses in CZ 3A and 4A—four with vented attics, and four with sealed attics—in order to understand their moisture performance. The authors noted that there have reports of high humidity problems in unvented attics, from multiple practitioners and online sources.

Their data showed that attic absolute moisture contents (vapor pressures) were consistently higher in the sealed attics, compared with the vented attics. Similarly, the vapor pressures in the main spaces were higher in the sealed attic houses. When the individual house data were plotted, there was overlap between the two groups. The worst-performing unvented attic had the highest air leakage (10 ACH 50) of the sample; the authors described other factors influencing interior moisture levels, including occupant density and setpoint.

Plots of vapor pressure at various portions of the roof assembly indicated that the sealed attic roof typically had patterns of daytime drying (desorption, into the attic), and nighttime wetting (adsorption, from the attic air). Similar cycling was seen in the vented attic houses, but with a much smaller vapor gradient, given roof sheathing temperatures. The authors noted that the “spikes” in vapor pressure were associated with high solar gain days and/or roof sheathing temperature.

Vapor pressure measurements were combined with differential pressure and air leakage measurements to estimate moisture flow to and from the attic. Their calculations showed the strongest vapor drives (from attic to interior) during afternoon/early evening periods, and airflow downward (attic to interior) during the day, and upward at night.

The authors theorized that seasonally, moisture accumulates in the roof sheathing from summer to fall, and is then desorbed in the winter and spring.

Several sources of moisture for the sealed attic were discussed, including roof sheathing storage, solar-driven moisture from moisture stored in asphalt shingles (judged unlikely by the authors), exterior air leakage (likely, especially given downward stack effect in summer).

The authors used collected HVAC data to estimate the penalty associated with directly conditioning the sealed attic to control humidity. They noted a 7% increase in energy use, which cuts into the performance improvement associated with bringing the ductwork within the conditioned space. The authors recommended that alternatives other than sealed attics be used to bring ductwork within the conditioned space.

2.6 Lstiburek (2014): Humidity Behavior of Unvented/Sealed Attics

Lstiburek (2014) clarified some background and terminology for unvented attics, proposing the alternate, more descriptive term of “conditioned attic.” In earlier construction, attic ductwork was typically leaky, and supply leakage would slightly pressurize the attic, resulting in air leakage from the attic to the main space (a.k.a. “communication”, see Figure 11 left). This air

communication would result in dehumidification of the attic space; the moisture load in the attic was driven primarily by interior sources. Moisture would concentrate in the attic (top of the building) due to the buoyancy of moisture-laden air (which has a lower density than dry air).

The author cites Houston-area field research studying the effect of moisture vapor permeable and impermeable shingle underlayments on inward vapor drives (Figure 11 right); the study found no measurable differences between these roof test bays. Therefore, he notes that shingle inward drive issues are not a significant moisture source.



Figure 11: Air leakage communication from unvented attic to main space (L), and Houston-area roof underlayment study (R) (Lstiburek 2014)

However, as airtight HVAC ductwork became more common, incidental space conditioning provided to unvented attics and communication between attic and main space was reduced. The resulting problem has been higher humidity levels in unvented/sealed attics, especially with vapor-open insulation materials, such as open cell spray polyurethane foam. Interior moisture is adsorbed and desorbed from the roof sheathing with daily warm/cold cycles; without communication to remove the moisture, it accumulates due to moisture buoyancy.

The proposed solution to this issue is to add space conditioning (both supply and return) to the attic space, at 50 cfm (24 L/s) per 1,000 ft² (93 m²) of ceiling area. However, this has the potential to cause conflicts due to code fire separation requirements; one option is to add a return duct smoke detector that shuts down the attic air handler when smoke is detected.

2.7 Smegal and Straube (2014): Monitoring & Simulation of SPF Insulated Roofs

This research covers over two years of monitoring data (2010-2012) for seven vented and unvented roof assemblies, installed in a test hut in Waterloo, ON (CZ 6). Interior conditions were set at 68°F/20°C and 50% RH, which is a high moisture level that will stress assemblies due to wintertime condensation risks.

All assemblies were cathedral (compact) roofs, with roughly R-30 insulation, OSB roof sheathing, black asphalt shingles, and latex paint on gypsum board as an interior finish. They roof assemblies are described in detail in Table 2. All roofs face east.

Table 2: Test roof assemblies monitored in Smegal and Straube (2014)

Assembly	Short name	Vented/ Unvented	Vapor Control (lowest perm interior layer)
Unvented Closed Cell	NCC	Unvented	ccSPF
Vented Closed Cell	VCC	Vented	ccSPF
Vented Fiberglass	VFG	Vented	Latex paint & GWB
Unvented Painted Open Cell	NOCP	Unvented	Paint on ocSPF, latex paint & GWB
Vented Open Cell	VOC	Vented	Latex paint & GWB
Unvented Open Cell	NOC	Unvented	Latex paint & GWB

Ventilation in the vented roof assemblies was achieved with a polystyrene foam baffle installed under the roof sheathing, which connected to soffit and roof vents low and high. Sensors were installed to measure assembly temperatures, RH, MC, and boundary conditions (interior and exterior). Wetting systems were installed between the roof sheathing and shingle underlayment, to determine drying ability of the assemblies after a wetting event.

Sheathing moisture contents were plotted: most roofs had a seasonal swing, with drier (5-10%) MCs in summer, and wetter (8-13%) in winter; all of these levels are well within the safe range for durability. However, the MCs for unvented ocSPF (NOC) and painted unvented ocSPF (NOCP) exceeded 20% each winter. In the first winter, the interior was at 40% RH, and 20-28% MC peaks were seen. The second winter had 50% RH conditions, and higher (20-34%) MCs were seen. However, in each following summer, sheathing MCs in these ocSPF roofs fell to safe levels. This indicates that ocSPF roof assemblies in CZ 6A face some durability risks, even with the addition of a painted vapor control layer on the ocSPF.

RH levels within the roof assemblies were examined:

- In the ccSPF roofs (NCC/VCC), RHs within the foam were in the safe range. In the vented ccSPF roof (VCC), the ventilation chute RH levels were similar to outdoor conditions.
- In the fiberglass roof (VFG), ventilation chute RH levels were similar to outdoors. Cavity RHs fluctuated on a daily basis, showing moisture movement through the assembly (convective looping, diurnal heating/moisture drive, or air leakage).
- In the unvented ocSPF roofs (NOCP, NOC), RHs on the exterior side of the cavity rose and fell seasonally, similar to sheathing MCs. The latex painted foam had a slightly drier exterior-side RH (by 5%), which is possibly insignificant, but might reflect the slight increase in vapor resistance in assembly NOCP.
- In the vented ocSPF roof (VOC), the RH on the exterior side of the cavity was very high (peaks at 95% and 100%) during the two winters), with possible condensation risks. The low vapor permeance of the polystyrene foam chute and the lack of moisture storage (compared to OSB sheathing) may contribute to these high RHs.

The wetting system was used in the summer and fall of 2010; the applied wettings (multiple 30-60 mL wettings; 240 mL total) produced only small increases in sheathing MCs, remaining well within the safe range.

The monitoring work was followed by hygrothermal simulations (WUFI 5.1 Pro) of the assemblies; reasonable correlation was obtained between the model and measured data. The roof assemblies were simulated in other Canadian climate zones and various interior RH levels (low/medium/high), using worst-case (north/12:12 roof pitch) orientation.

The ccSPF roof assemblies worked well under most conditions; the cases that were at risk of failure were high interior RH (50%) in colder climates. Note these risks are seen for worst-case orientation; at a south orientation, these assemblies have no risk.

The vented ocSPF roofs worked well under all conditions; however, this assumed no vapor resistance for the baffle/chute, which seemed to affect conditions in the monitored data.

The unvented ocSPF roofs showed risks in many climate zones with latex paint (Class III) as interior vapor control. Polyethylene (Class I) reduced risks substantially, but at the cost of eliminating inward drying. An ocSPF roof with a Class II (1 perm) vapor retarder worked in conditions as cold as Ottawa, with “medium” RH levels.

The vented fiberglass roof showed excellent performance in the simulation; however, this simulation did not include the effect of air bypass leakage from the interior, which is likely in practice, and will add significant moisture load to the roof assembly.

The authors provided overall recommendations for construction, and for further research on the permeance effects of ventilation baffles/chutes.

3 Cold Climate (Chicago) Experimental Setup

3.1 Overview

The cold-climate test house was located in Bolingbrook, IL, roughly 35 miles southwest of Chicago (Zone 5A). It is a model house, provided by K. Hovnanian Homes. The house was unoccupied during the testing period; it also served as a demonstration/test house for meeting Challenge Home requirements in a production builder setting.

The test bed for the experimental roofs was the attic of the attached garage (third garage bay; Figure 12, in red). The gable end wall of the garage faces south; the two test roof orientations are east and west. There are seven rafter bays that were used as experimental test bays.



Figure 12: Test home with attached garage used for experimental roof

The roof assemblies were measured for temperatures, wood moisture contents/MCs (both sheathing and framing), and relative humidity/RH at various locations. Interior and exterior temperature and relative humidity conditions were measured on-site; exterior data was supplemented with airport weather data (e.g., precipitation and wind). Measurements were collected in a central data acquisition system (connected to the wired sensors); measurements were taken at 5-minute intervals, and hourly averages recorded.

Instrumentation listing and specifications can be found in Appendix A.

Data were collected via cellular modem; one advantage of this communication connection was that interior temperature and relative humidity setpoints could be adjusted remotely.

3.2 Experimental Roof Assemblies

A cross-section of the experimental roof design is shown in Figure 13; the assemblies are described in Table 3 (with color codes used later as identifiers). The roofs are set up with one experimental assembly per rafter bay; each bay extends east-west, so that each experimental rafter bay pair is a complete cross section of a roof, including eaves and ridge.

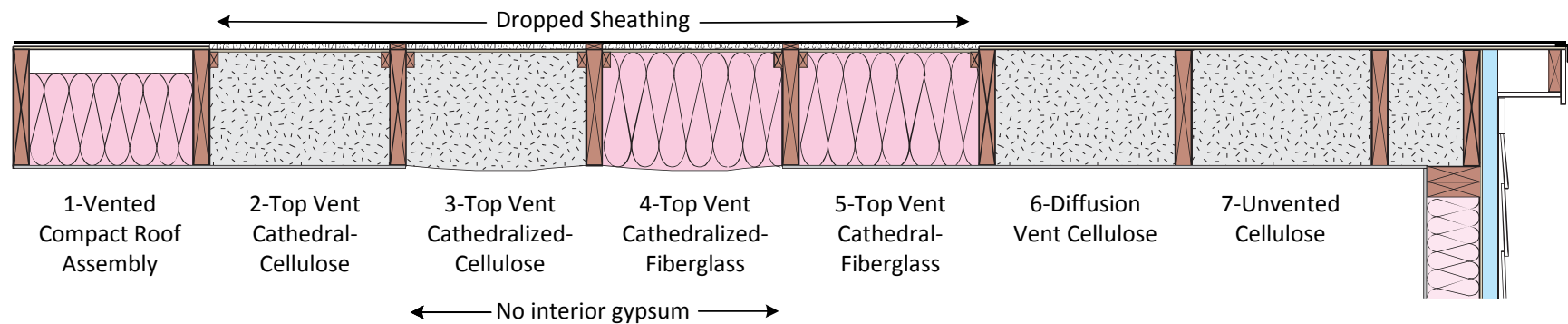


Figure 13: Chicago experimental roof test bays, showing materials

Table 3: Description of Chicago experimental roof test bays

#	Description	Interior	Rafter Bay	Exterior	Roof Ventilation
1	Vented compact roof	½ in. gypsum board, latex paint	R-30 fiberglass batt, 4 in. airspace	7/16 in. OSB, #30 felt, asphalt shingle	4 in. air space ventilated at eave and ridge
2	Top vent cathedral-cellulose	½ in. gypsum board, latex paint	R-38 cellulose, dense packed	7/16 in. OSB, mesh, asphalt shingle	Breather mesh ventilation from eave to ridge under shingles
3	Top vent cathedralized-cellulose	None (open)	R-38 cellulose, dense packed	7/16 in. OSB, mesh, asphalt shingle	Breather mesh ventilation from eave to ridge under shingles
4	Top vent cathedralized-fiberglass	None (open)	R-38 fiberglass batt	7/16 in. OSB, mesh, asphalt shingle	Breather mesh ventilation from eave to ridge under shingles
5	Top vent cathedral-fiberglass	½ in. gypsum board, latex paint	R-38 fiberglass batt	7/16 in. OSB, mesh, asphalt shingle	Breather mesh ventilation from eave to ridge under shingles
6	Diffusion vent cellulose	½ in. gypsum board, latex paint	R-38 cellulose, dense packed	7/16 in. OSB, #30 felt, asphalt shingle	Ridge “diffusion vent” (glass fiber faced gypsum board)
7	Unvented cellulose	½ in. gypsum board, latex paint	R-38 cellulose, dense packed	7/16 in. OSB, #30 felt, asphalt shingle	Ridge sealed with self-adhered membrane; unvented

Further explanation of the assemblies described in Table 3 is provided below.

3.2.1 Vented Compact Roof (Roof 1)

This is a typical code-compliant cathedral roof (§R806.1 through R806.3), with a ventilated air space above the fiberglass insulation. An R-30 batt was chosen for installation in the 2x12 (11-1/4 in.) rafter bay, leaving roughly a 4 in. airspace (Figure 15). The ridge ventilation detail was somewhat unconventional, with a “doghouse” built up of 2x framing and OSB sheathing; however, it was necessary for a similar appearance between experimental roof assemblies.

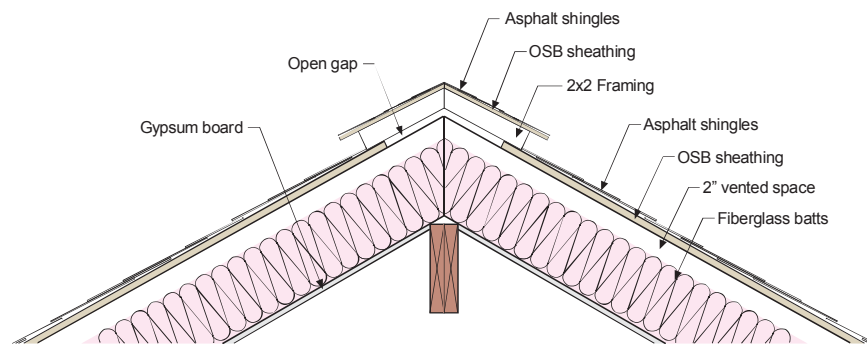


Figure 14: Ridge condition at Roof 1-Vented compact roof



Figure 15: Roof 1-Vented compact roof insulation, showing airspace/ventilation detail

3.2.2 Top Vent Cathedral-Cellulose (Roof 2)

This is one of four roof assemblies that utilize a “top vent” strategy, as described by Schumacher and LePage (2012). In this type of assembly, if a vapor-permeable water-resistive barrier (WRB) is used (or if the WRB is omitted), the sheathing can dry upwards to the air space, and moisture will be removed from the assembly by ventilation. The ventilation space under the shingles was created using a polypropylene “breather mesh” or “spacer mesh” commonly used for drainage and ventilation under cedar shingles. This mesh was sufficiently strong to support shingles without damage, and created a reliable airspace. However, the completed roof showed some degree of waviness of the shingles at joints between roof bays (Figure 29), which might not be acceptable in practice.

In addition, this assembly allows drying of the shingles to the underside (into the air space).

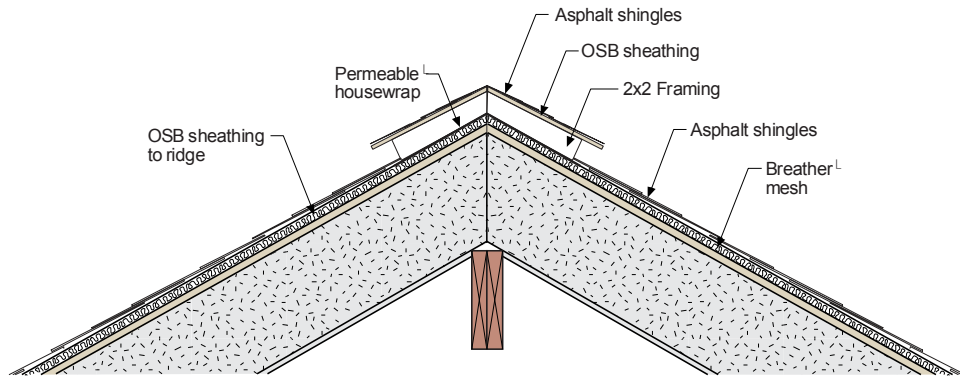


Figure 16: Ridge condition at Roof 2- Top vent cathedral-cellulose (3, 4, and 5 similar)

At the soffit, air enters the ventilation space at a gap between the fascia and the sub-fascia created by the breather mesh (Figure 17 and Figure 18).

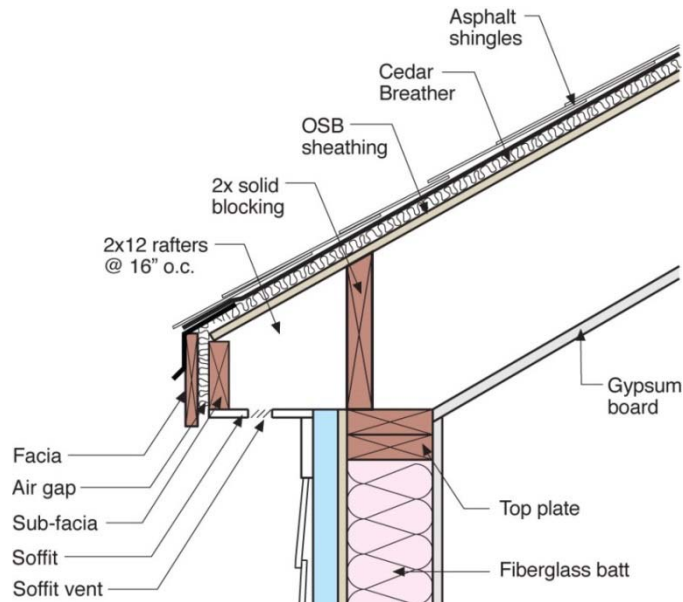


Figure 17: Soffit condition at Roofs 2, 3, 4, and 5 - Top vent cathedral/cathedralized

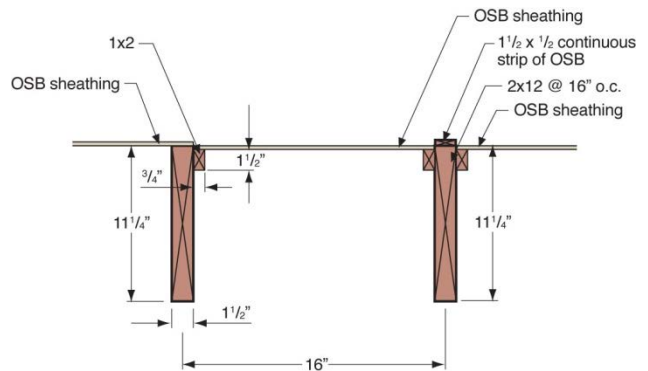
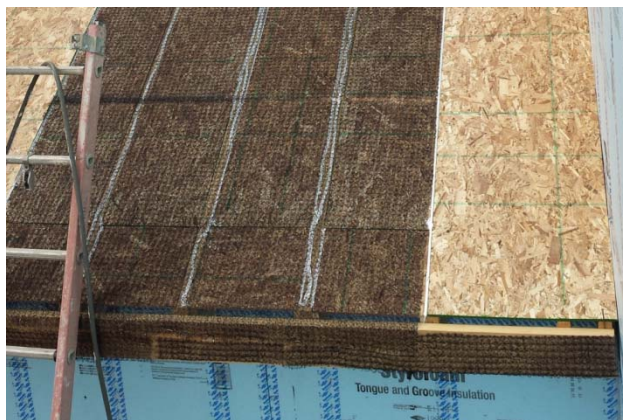


Figure 18: Dropped sheathing and breather mesh at roof deck of Top vent roofs (2, 3, 4, 5)

At the ridge, the breather mesh was covered with a vapor permeable housewrap, which sheds water blown into the “doghouse” ridge (Figure 16). However, in order to allow escaping airflow from the breather mesh, holes were cut into the housewrap (roughly 3 in. x3 in.), per Figure 19.



Figure 19: Top vent roof (2, 3, 4, 5) ridge housewrap covering and cut openings

The roof sheathing was “dropped” flush with the top of the rafters at the “top vent” assemblies (per Figure 18, right), to create a flat plane/substrate for asphalt shingles across all test bays. Additional nailers (1x2s) were required to support the sheathing between rafters at these bays.

This system was implemented with no underlayment or WRB below the asphalt shingles. This was done to provide a “best case” scenario that provided the maximum drying of the OSB sheathing, without the reduction in permeance due to the vapor resistance of a WRB.

3.2.3 Top Vent Cathedralized-Cellulose (Roof 3)

This assembly is identical to Roof 2 (Top Vent Cathedralized-Cellulose), except that the interior gypsum board was omitted, creating a “cathedralized” (vs. cathedral) roof/ceiling assembly.



Figure 20: Top vent cellulose roofs (roofs 2 and 3)

This roof shows the effect of omitting the interior air barrier in the assembly; the cellulose netting was left exposed at the interior. Images of the cellulose installation and the finished assembly are shown in Figure 20.

3.2.4 Top Vent Cathedralized-Fiberglass (Roof 4)

This assembly is identical to Roof 3 (Top vent cathedralized-cellulose/no gypsum board), with fiberglass batt replacing the dense pack cellulose.

3.2.5 Top Vent Cathedral-Fiberglass (Roof 5)

This assembly is identical to Roof 2 (Top vent cathedral-cellulose/gypsum board), but with fiberglass batt replacing the dense pack cellulose. Installation of the R-38 batt in these roofs is shown in Figure 21; note that even with careful installation, there is some “buckling” of the batts away from the roof sheathing (not Grade I installation).



Figure 21: Top vent fiberglass roofs (roofs 4 and 5)

3.2.6 Diffusion Vent Cellulose (Roof 6)

This assembly has rafter bays dense packed with cellulose insulation (similar to the unvented roof/Roof 7), except that at the ridge, an 8 in. wide strip of OSB sheathing was replaced with vapor permeable glass fiber faced exterior gypsum board, as shown in Figure 22 and Figure 24. This gypsum board section is intended to function as a “diffusion vent,” as described below.

In previous field experience, sloped compact roof assemblies have moisture problems predominantly at the ridge, where moisture accumulates due to thermal/moisture buoyancy and convective looping. The intent of the diffusion vent is to dry this accumulated moisture via vapor diffusion, while still acting as an effective air barrier. Installing a diffusion vent over a small portion of the roof would likely be a simpler and lower cost retrofit than a full top-ventilated deck. Air barrier connections are made with tape adhered at joints.

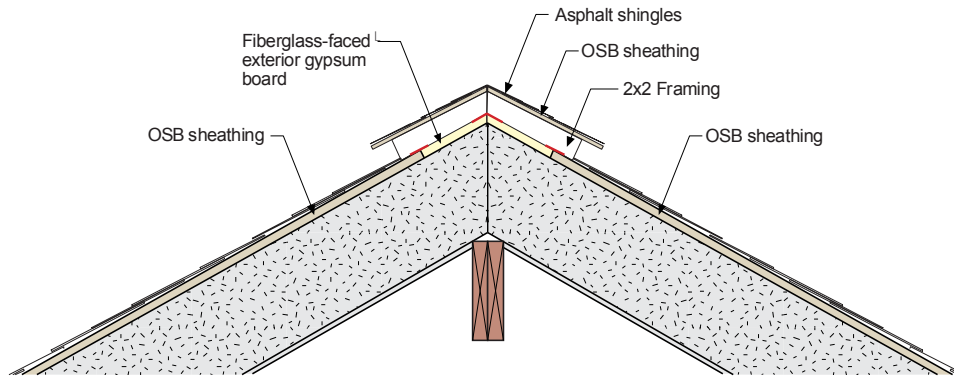


Figure 22: Ridge condition at Roof 6-Diffusion vent cellulose

The vapor permeance (in perms) of the exterior gypsum sheathing is stated in the manufacturer’s literature as 23 perms (dry cup/ASTM E96 Procedure A). However, further permeance testing data over a range of humidities was obtained from ORNL, and plotted in Figure 23. The manufacturer’s permeance is plotted for reference (“Spec Value”), with values for other structural sheathings (OSB and plywood) and ½ in. unpainted gypsum board, from ASHRAE (2009a) data. This demonstrates that the exterior gypsum sheathing would allow significantly more drying than plywood or OSB.

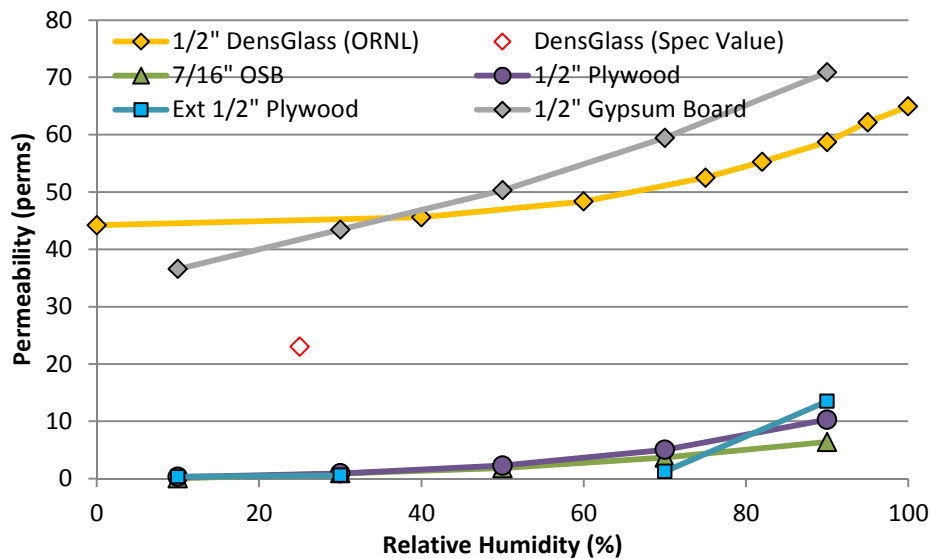


Figure 23: Ridge condition at Roof 6-Diffusion vent cellulose

3.2.7 Unvented Cellulose (Roof 7)

This assembly is the unvented dense-pack cellulose roof that has been shown to fail in previous work. This bay was intended as a control, and to provide a comparison between previous known failures and the experimental assemblies.



Figure 24: Diffusion vent (6) and unvented (7) ridge conditions

3.3 Roof Bay Instrumentation

The roofs were instrumented with temperature, wood moisture content, and relative humidity sensors as per Straube et al. (2002). A typical instrumentation package for a “top vented” roof is shown in Figure 25.

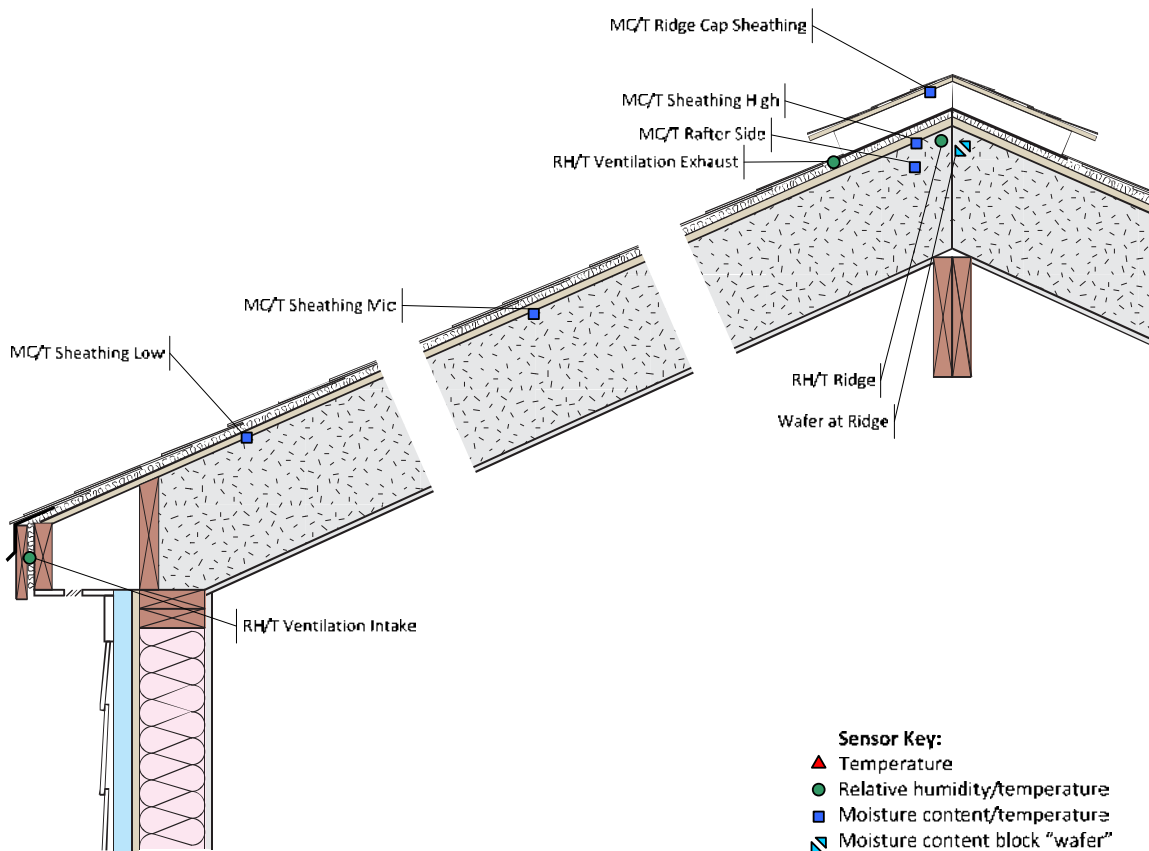


Figure 25: Instrumentation setup for Roof 2-Top vent cathedral-cellulose (3, 4, and 5 similar)

The sensors are described in the following groups:

- **Sheathing Sensors:** Rotting or damage of sheathing is the most common type of moisture-related failure seen in building assemblies. Given the “ridge rot” issues (moisture accumulation at the peak) described earlier, measuring moisture content and temperature (MC/T) at the sheathing at multiple locations is useful to understand the spatial variations. Therefore, MC/T sensors were installed at low, middle, and high points in the sheathing, on both east and west orientations.
- **Ridge Sensors:** Ridge moisture accumulation issues were also studied with sensors installed near the peak. The sensors included a temperature/relative humidity (T/RH) sensor, moisture content at the ridge framing, and a “wafer” sensor, which is a small wood sample measured for moisture content. The wafer sensor uses the relationship between RH and MC (the sorption isotherm) to act as a surrogate humidity sensor that tracks long-term patterns; see Ueno and Straube (2008).
- **Ventilation Cavity T/RH:** To examine the effect of heat and moisture removal from the ventilation cavity, temperature/relative humidity (T/RH) sensor were installed at the eave intakes and the ridge exhaust.
- **Doghouse Sensors:** To determine whether there is any risk of moisture release from the roof accumulating at the sheathing of the “doghouse” detail, the moisture content and temperature (MC/T) of the sheathing were measured at the underside of the “doghouse.”

The instrumentation at the vented compact assembly (Roof 1) is similar to the top vent package, except that the ventilation cavity T/RH sensors measure conditions at the 4 in. deep ventilated space, not the mesh air space of the top vent roofs.

The instrumentation package for the diffusion vent (Roof 6) and unvented cellulose (Roof 7) assemblies is reduced from the “top vent” package (Figure 26), given the lack of a ventilation cavity. The remaining sensors are parallel to those found in the “top vent” assemblies.

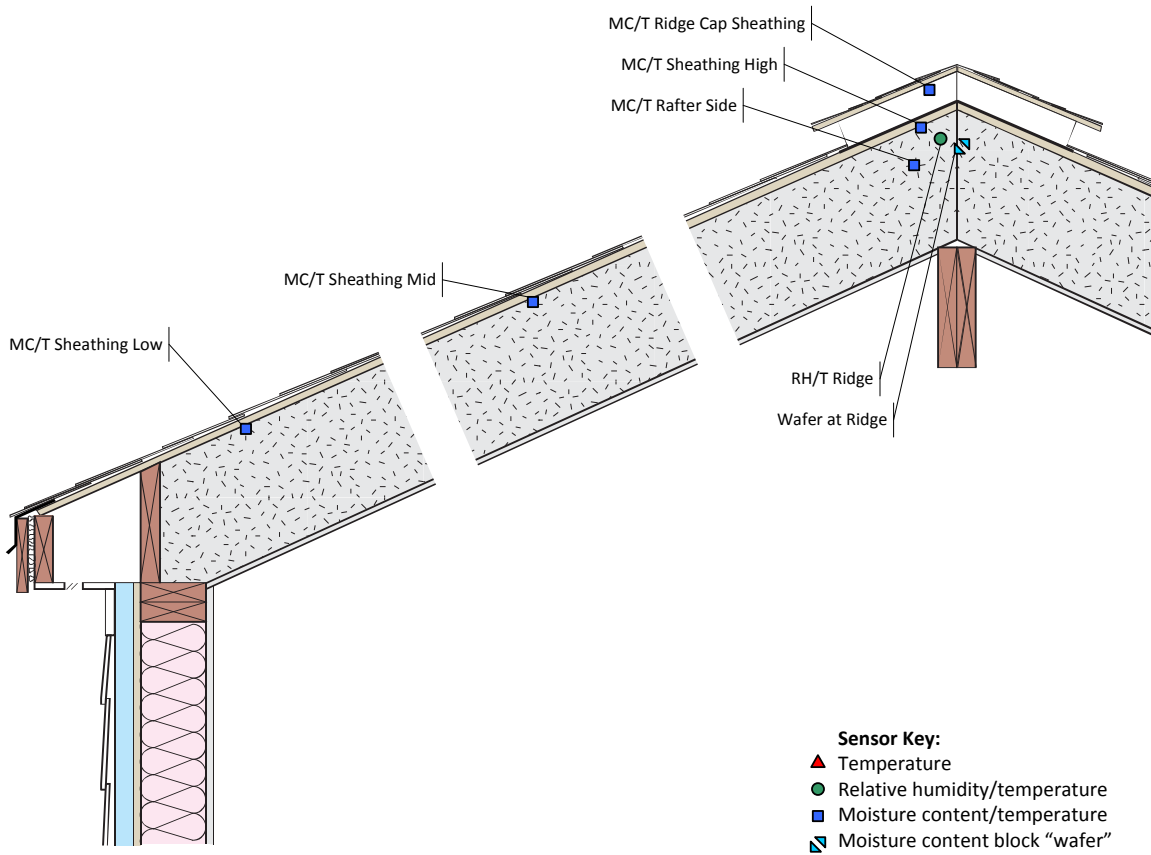


Figure 26: Instrumentation setup for Roof 7 – unvented cellulose

3.4 Interior Space Conditioning

The experimental attic was set up to run at constant temperature and humidity conditions through the winter. Electric resistance space heating was installed in the attic space (Figure 27, left), controlled by the data acquisition system. A constant 72°F/22°C setpoint was used; no cooling was provided. To reduce the heating load on the attic unit, additional space heating (also controlled by the data logger) was installed in the garage space (Figure 27, right).



Figure 27: Experimental attic space heating (L), garage heating and relay box (right)

To stress the assemblies through the winter, the attic interior space was run at a high relative humidity; the target was 50% RH. Humidity conditions were maintained by a heated water reservoir-type humidifier (Figure 28), controlled by the data acquisition system.

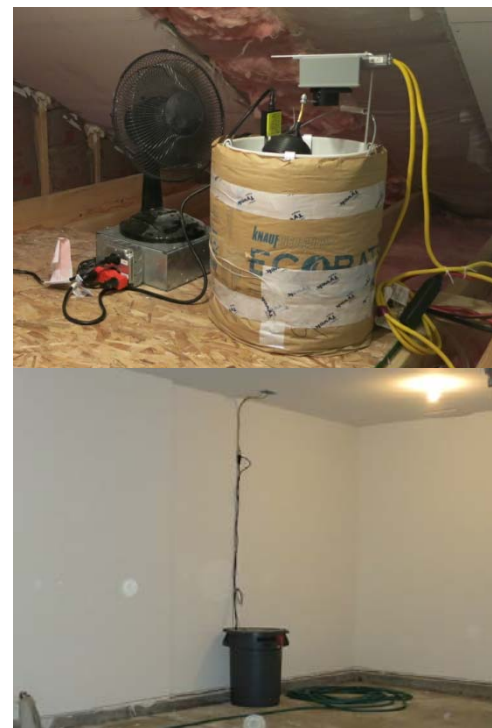
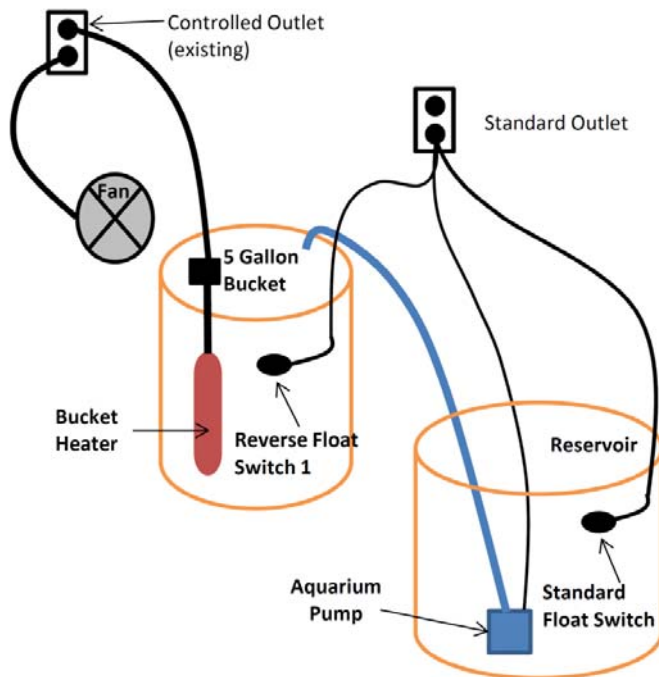


Figure 28: Schematic and photos of humidification setup; heated bucket and reservoir at right

3.5 Overview of Roof Installation

The completed roof assembly is shown in Figure 29 (left); the “doghouse” ventilation detail was partially assembled in order to install instrumentation (Figure 29, right), and then reassembled.



Figure 29: Completed test attic over garage (L), and disassembled “doghouse” detail (R)

The experimental roof bays were sealed against lateral air movement/communication with air barrier detailing that included caulk or expanding foam at the sheathing-to-framing joints and framing connections, and compressible gaskets at the interior faces of the rafters (Figure 30, left). Rafter bay leakage to exterior was controlled with similar foam and caulk details (Figure 30, right).



Figure 30: Interior of experimental roof bays, showing air sealing, gaskets, and instrumentation

The interior of all roof bays except 3 and 4 (top vent cathedralized-cellulose and fiberglass) were finished with ½ in. gypsum board, finished with a single coat of latex paint (possibly more permeable than a Class III vapor retarder; not tested), as shown in Figure 31 and Figure 32.



Figure 31: West (front) face of experimental roof bays interior



Figure 32: East (rear) face of experimental roof bays interior



Figure 33: South (gable end) face of test attic

The gable end wall and floor of the test attic were insulated with R-13 fiberglass batt.

The exterior of the roof was examined with infrared thermography, to determine if there was greater heat loss from any of the experimental assemblies. No discernable difference was seen between roof bays in cold conditions (26° F, albeit with some snow cover on the roof deck, Figure 34), or in milder conditions (47° F).

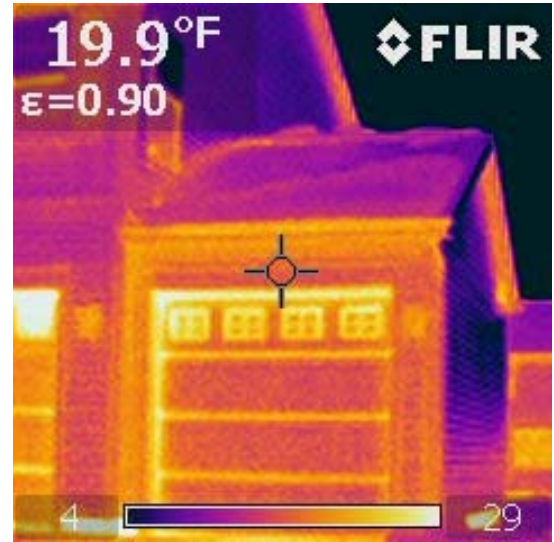


Figure 34: Infrared image of test roof (front) in winter conditions (26°F)

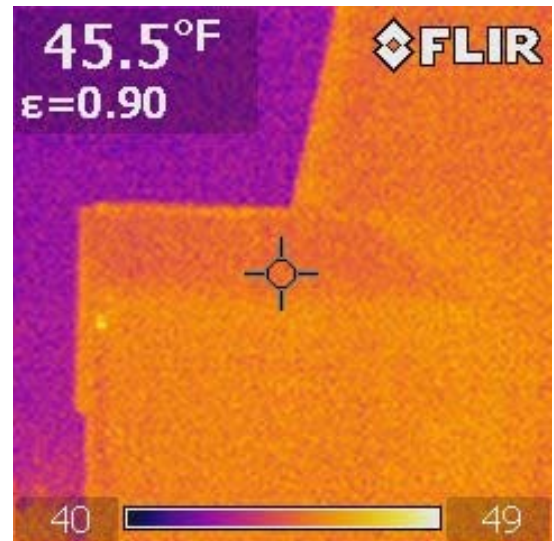


Figure 35: Infrared image of test roof (front) in mild conditions (47°F)

3.6 Roof Air Leakage Testing

The air leakage of the test attic was measured, for two reasons. One was to ensure that air leakage of the space was low enough that the electric resistance space heater (1000 W or 3400 Btu/hour) could maintain interior temperatures. Second, excessive air leakage in one experimental roof assembly (compared to others) would result in anomalies that create unwanted variations between assemblies.

The air leakage of the attic was tested with an Energy Conservatory Minneapolis Duct Blaster® Series B Fan, placed in a rigid foam filler panel in the attic hatch (Figure 39 left). The roll-up garage door was opened during the testing to relieve pressure. The initial tests, when combined with infrared thermography, revealed substantial air leakage at several portions of the roof (Figure 36, Figure 37, and Figure 38). These leaks were rectified as best as possible with available materials and tools.

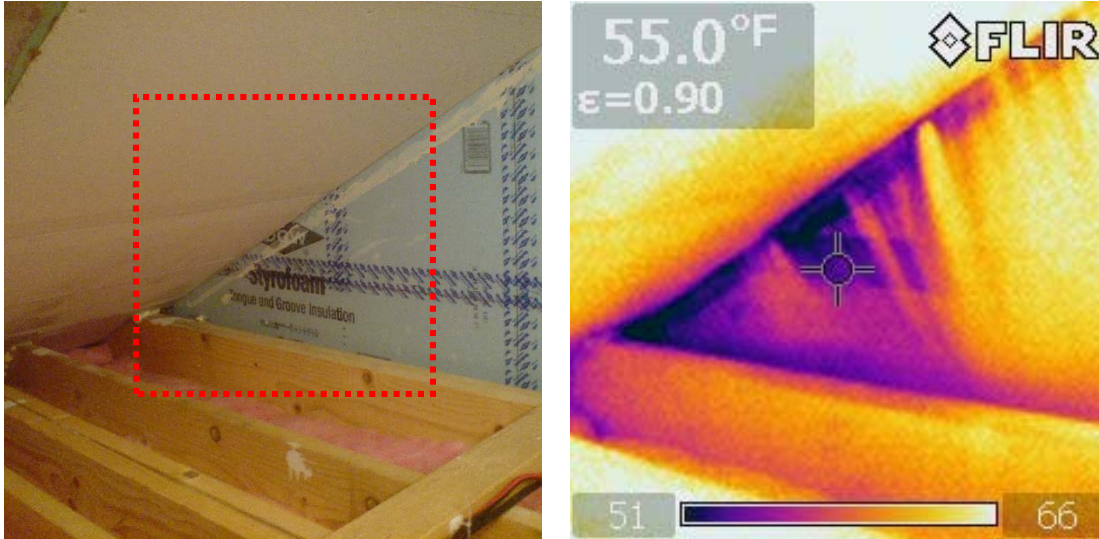


Figure 36: Air leakage at roof connection to main house (XPS sheathed wall)

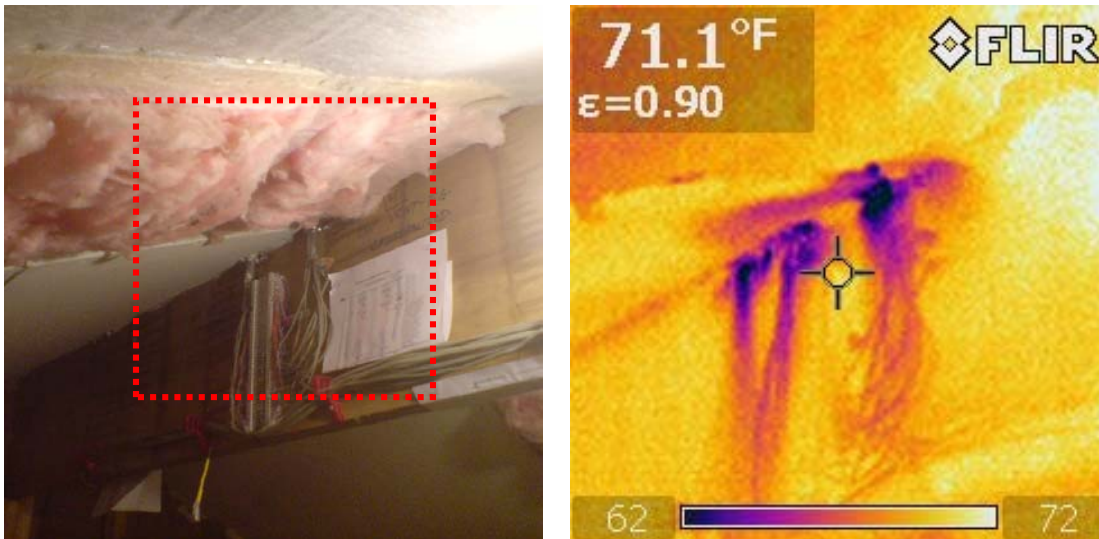


Figure 37: Air leakage at ridge and instrumentation wire penetrations

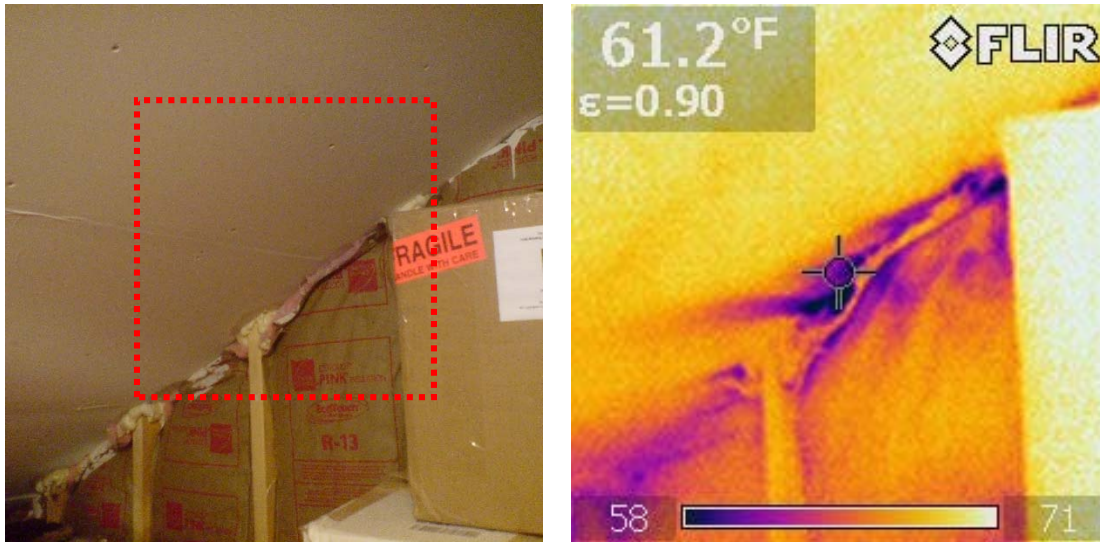


Figure 38: Air leakage at gable end rake wall (connects to unvented cellulose Roof 7)

After retrofit air sealing, a multipoint air leakage test was completed (results in Figure 39 right). The overall air leakage measurements are shown in Table 4, both in terms of raw measurement (cubic feet per minute at 50 Pascals/CFM 50), volume-normalized metric (air changes per hour at 50 Pascals/ACH 50), and surface-area normalized metric (CFM 50/square foot enclosure). The surface area normalized results are the most useful, and reflect higher air leakage than recommended for energy efficient construction, but not so high as to indicate a problem reaching interior setpoint. The ACH 50 figure is strongly distorted by the small volume of the attic space.

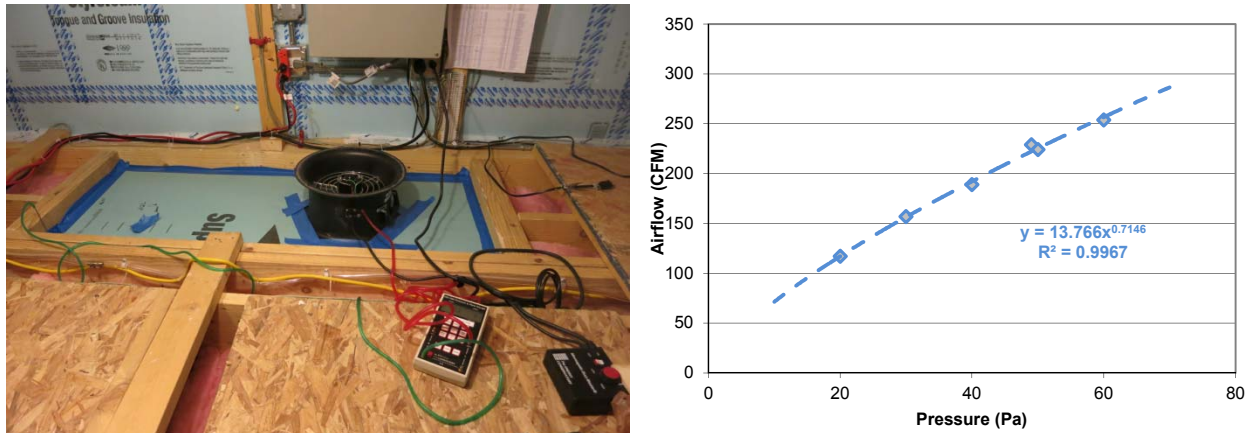


Figure 39: Air leakage testing of attic space (left), and multipoint test results (right)

Table 4: Results of test attic air leakage testing

Measurement	Metric	Normalizing metric
225	Cubic feet per minute at 50 Pascals (CFM 50)	
32.9	Air changes at 50 Pascals (ACH 50)	(411 cubic feet)
0.45	CFM 50/sf enclosure	(503 sf surface area)
23.2	Square inches leakage area (EqLA)	

Following the air leakage test, the attic was depressurized to -50 Pa, and the pressure difference (ΔP) across the ceiling gypsum board was measured for the various roof assemblies.

Measurements were taken low and high in the rafter bays, on both orientations (Figure 40). Roofs 3 and 4 (cathedralized) were not tested in this manner, as these assemblies have no interior gypsum board/air barrier.



Figure 40: Testing pressure difference (ΔP) across ceiling gypsum board in test attic

The measurements are shown in Table 5, with the average of the measurements, and the percentage of the interior-exterior pressure difference due to the interior gypsum board.

Table 5: Test attic air ΔP across gypsum board, with attic at 50 Pa

	1- Vented compact roof	2-Top vent cathedral cellulose	5-Top vent cathedral fiberglass	6-Diffusion vent cellulose	7-Unvented cellulose
East Upper	47 Pa	30 Pa	20 Pa	19 Pa	18 Pa
East Lower	46 Pa	28 Pa	21 Pa	17 Pa	10 Pa
West Upper	45 Pa	23 Pa	24 Pa	21 Pa	19 Pa
West Lower	47 Pa	13 Pa	25 Pa	19 Pa	19 Pa
Average	46 Pa	24 Pa	23 Pa	19 Pa	17 Pa
Avg. % ΔP	93%	47%	45%	38%	33%

One conclusion of the ΔP testing was that in the vented compact roof (Roof 1), the interior gypsum board is the majority (90%+) of the air barrier, as would be expected with a rafter bay ventilated to the exterior. The measurements do not seem to indicate gross differences in air leakage in the remaining bays that would make them non-comparable (17-24 Pa range). The top vent assemblies (2 and 5) had greater pressure differences across the drywall than the diffusion vent and unvented roofs (6 and 7). Based on later disassembly, this indicates that the “dropped sheathing” detail (at the top vent roofs) had more air leakage than the conventionally sheathed roofs.

Two of the roof bays (2 and 7) had a single measurement that was an outlier relative to the other measurements; both were “lower” air leaks in cellulose bays. A plausible explanation is that the airflow retarding properties of cellulose can result in a pressure difference across a nominally open rafter bay cavity.

An ideal measurement would have been a zone pressure diagnostic (ZPD, per Bohac 2002), which involves cutting a known-size hole through the interior gypsum board and repeating the pressure testing (measuring the difference). It would have provided estimates of (a) leakage area from the rafter bay to interior and (b) leakage area from the rafter bay to exterior. However, this was not done, due to time constraints and the need to repair the gypsum board after the work.

4 Cold Climate (Chicago) Monitoring Results

4.1 Boundary Conditions

Interior (test attic space), exterior, and garage temperatures are shown in Figure 41, for the test period. Attic space heating was only added in mid-November, 2013; garage space heating was added in mid-December. Weather data for Lewis University Airport/KLOT (Romeoville, IL; roughly 5 miles from the site) is also graphed as a comparison point.

Several control issues occurred over the course of the experiment, including temperature overshoot (due to equipment failures, site issues, and power failures). However, for the majority of the winter, the test attic ran at a constant 72°F/22°C setpoint. Garage heating was run from December through February.

Winter 2013-2014 was an exceptionally cold winter (7110 HDD 65°F vs. 6460 HDD normal), which provide ideal conditions for condensation-related failure. The lowest temperature measured on site (early January 2014) was -13.4°F/-25.2°C (can be compared to Aurora, IL 99.6% temperature of -2.0°F).

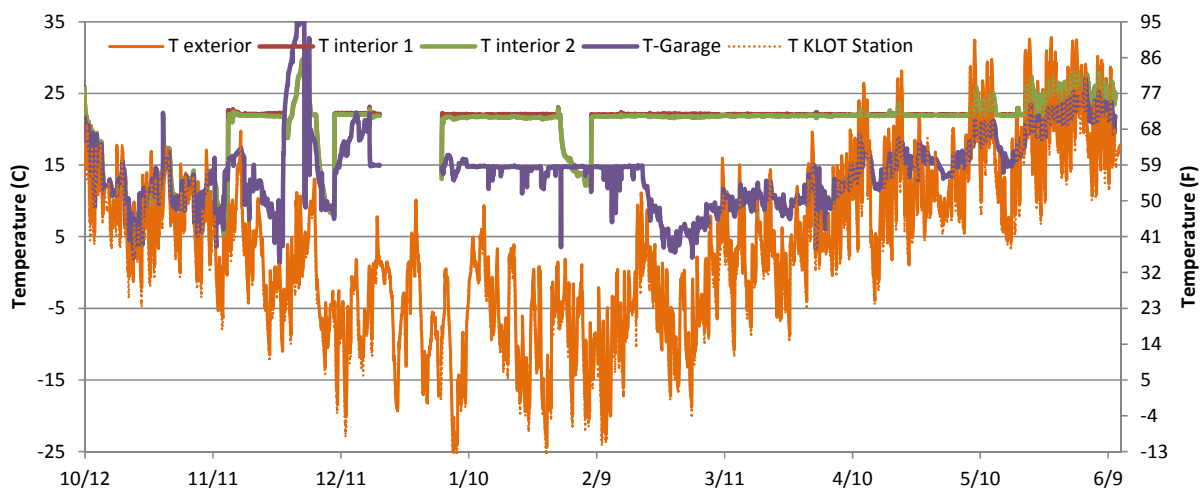


Figure 41: Test attic interior, garage, and exterior temperatures, winter 2013-2014

The test attic relative humidity is shown in Figure 42; although humidification was started in mid-November, again, control and site issues resulted in periodic failures and loss of control. However, conditions were maintained at 50% RH for most of the winter. In the spring, as outdoor temperatures rose, the inward temperature gradient caused moisture desorption from the sheathing, resulting in relative humidity levels above setpoint.

However, relative humidity data alone do not reflect the critical moisture condition of absolute air moisture content. This is indicated by dewpoint, which is graphed in Figure 43 for test attic and exterior conditions. It shows the net effect of the loss of temperature and humidity control; for instance, there were periods when humidity control was maintained but heating had failed. The periods showing constant dewpoint (51°F/11°C) are highlighted with the grey and green bar graphic. This graphic is used in later plots, to indicate periods at or away from constant interior moisture conditions.

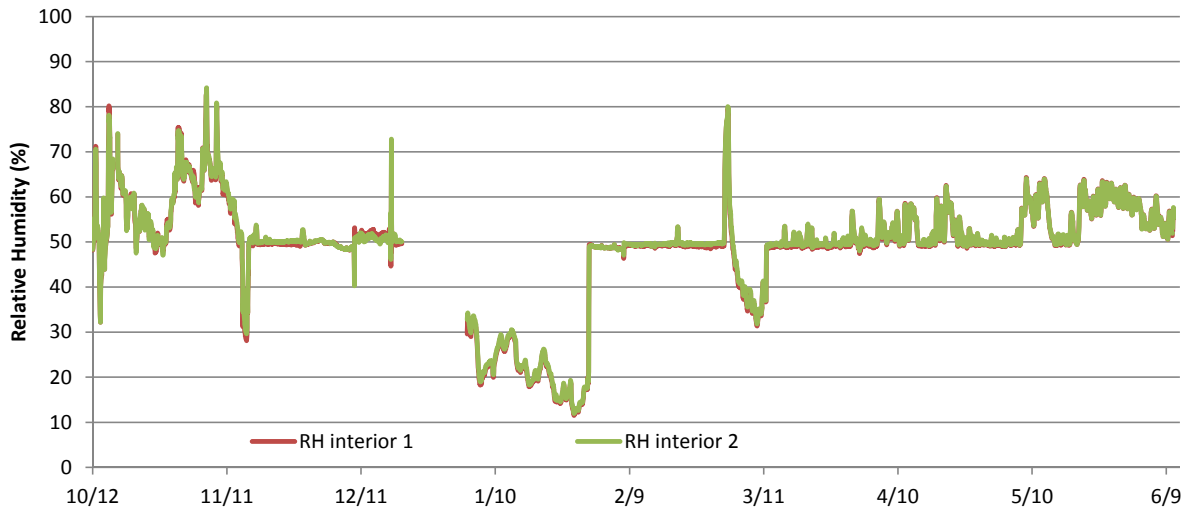


Figure 42: Test attic interior relative humidity, winter 2013-2014

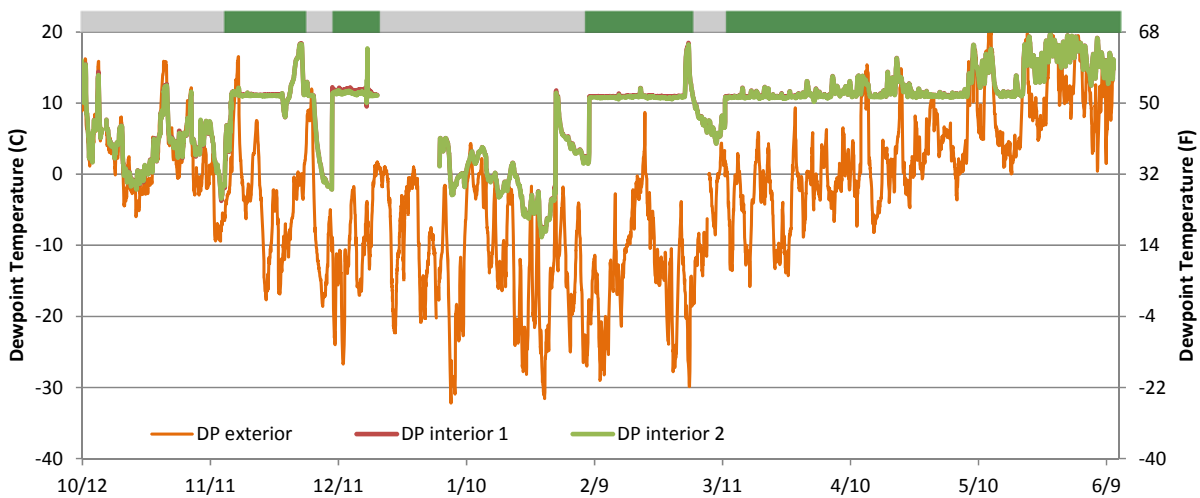


Figure 43: Test attic interior and exterior dewpoint temperature, winter 2013-2014

4.2 Sheathing Moisture Contents

OSB roof sheathing MCs are shown in the following graphs. Three measurements (upper/middle/lower) were taken on each (east/west) orientation. The results are shown in the graph using blue shades for the east-facing roof, and reds for the west-facing roof. Height is indicated by color intensity; low sensors are lighter shades, and high sensors are darker shades. Exterior temperature is also graphed for reference.

Sheathing MCs often exceeded the fiber saturation point (wood cell walls are saturated). The fiber saturation point is typically 30% MC in solid wood (FPL 2010), but lower (25-26%) in adhered wood products such as OSB (Glass 2013). From the fiber saturation point up to capillary saturation, the relationship between MC and electrical resistance is not well defined (James, rev. 1988), so the plotted values should not be taken as absolute measurements. However, the high values are useful to show greater wetness levels than lower values.

The results for Roof 1 (compact vented) assembly are shown in Figure 44. For the majority of the winter, moisture contents are well below 20%, which is in the safe range for mold growth. The occasional spikes to over 20% appear to be associated with precipitation events; it is plausible the spikes seen at the upper sheathing sensors are associated with wind-driven rain, blowing rain into the ridge vent. However, these wetting events quickly dried. The “safe” behavior of this roof is consistent with Smegal and Straube’s (2014) monitoring results.

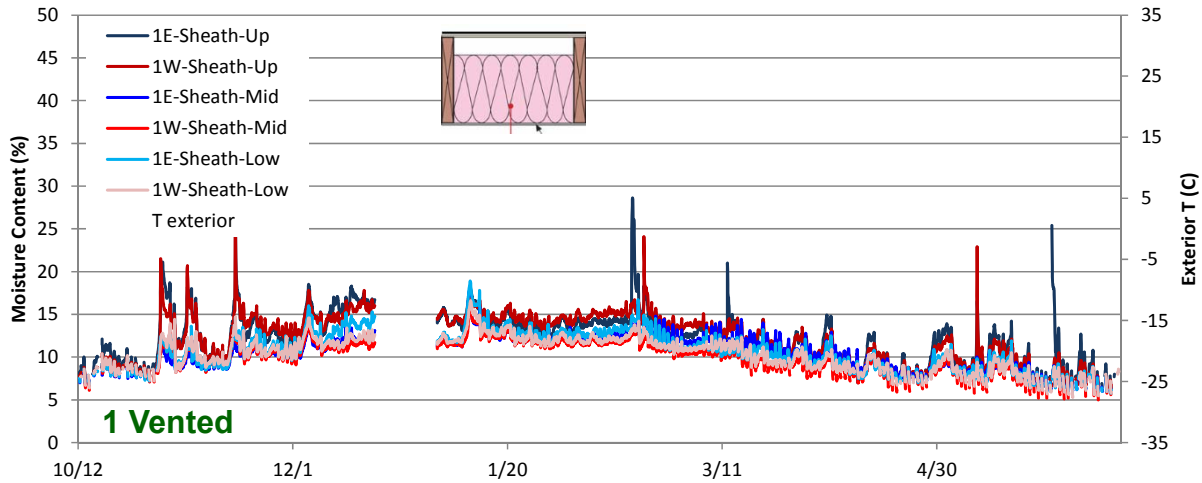


Figure 44: Roof 1 (vented) sheathing moisture contents

The results for unvented cellulose (Roof 7) and diffusion vent cellulose (Roof 6) are shown in Figure 45 and Figure 46, respectively. Moisture contents are much higher, with much of the winter well over 20% MC. In addition, both roofs show the expected spatial pattern: moisture levels are greater at the higher portion of the roof, with roof ridge moisture contents well over 40% (risk of rot and decay).

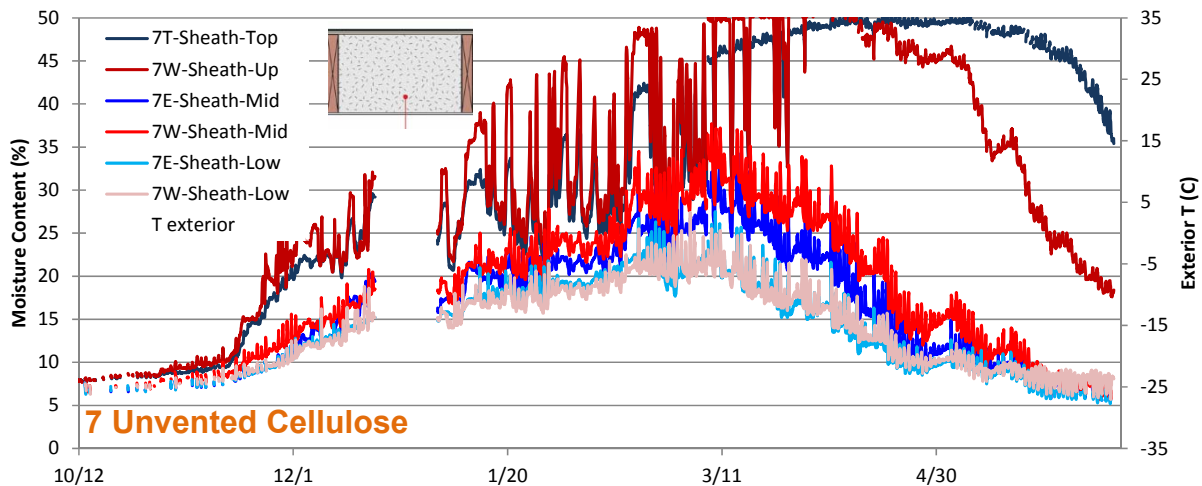


Figure 45: Roof 7 (unvented cellulose) sheathing moisture contents (unfiltered data)

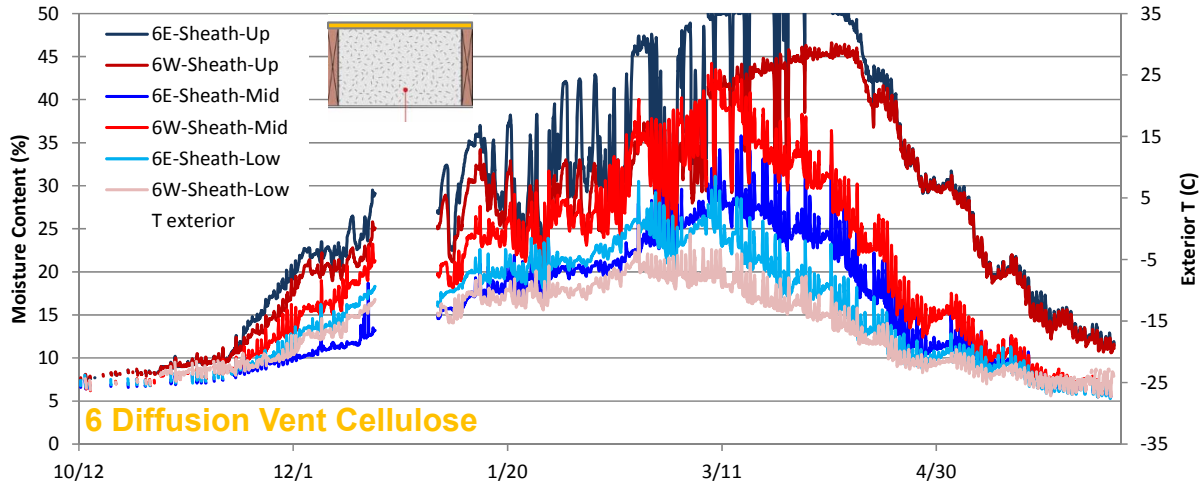


Figure 46: Roof 6 (diffusion vent cellulose) sheathing moisture contents (unfiltered data)

The upper moisture content measurements are difficult to read, due to the sudden shifts at high MCs. These MC anomalies coincide with freezing temperatures; it is likely that freezing of water in the sheathing results in inconsistent electrical resistance (and thus measured MC). The MC trends during non-freezing temperatures are more representative of actual conditions. Therefore, the previous data were filtered (only MC measurements above 32°F/0°C plotted) to make the graphs more readable; all remaining graphs are shown with filtered data. The filtered data for unvented cellulose (Roof 7) and diffusion vent cellulose (Roof 6) are shown in Figure 47 and Figure 48.

One marked difference between these two roofs is their dry-down period in the spring, highlighted in dashed grey rectangles. The moisture content in the diffusion vent (Roof 6) roof falls much faster, and to a lower level (12% MC) than the unvented roof (Roof 7) (17% and 35% MC). This is likely an indication of the greater drying available by diffusion in Roof 6.

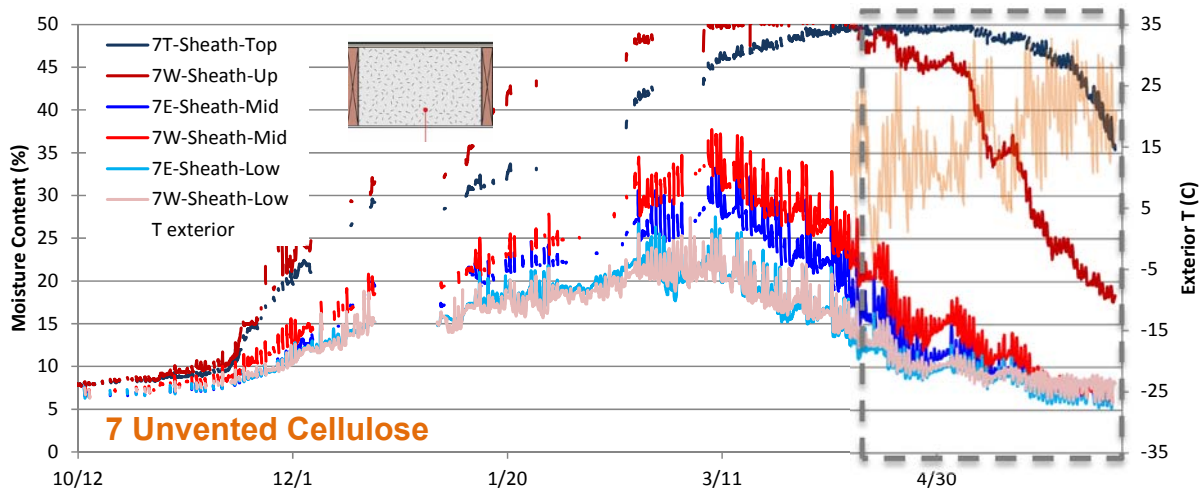


Figure 47: Roof 7 (unvented cellulose) sheathing moisture contents (filtered data)

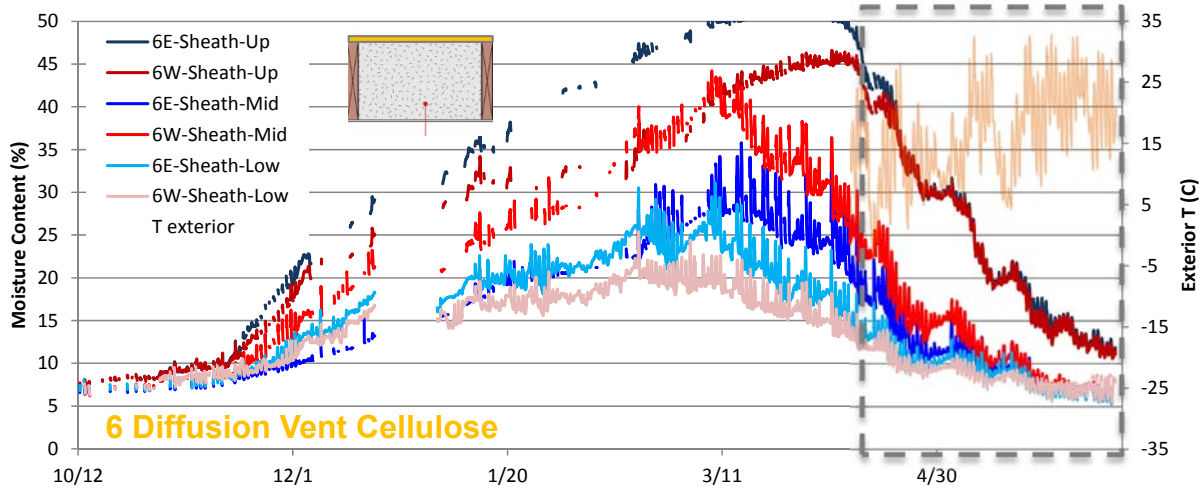


Figure 48: Roof 6 (diffusion vent cellulose) sheathing moisture contents (filtered data)

The results for the cellulose “top vent” (“breather” mesh netting under shingles) roofs are shown in Figure 49 (top vent cellulose with gypsum board) and Figure 50 (top vent cellulose, no gypsum board). The same high moisture contents and spatial patterns were seen (greatest moisture at roof peak). The gypsum board assembly (Roof 2) has drier moisture levels at the lower portions of the roof than the assembly without gypsum board (Roof 3). This is reasonable, given that the painted gypsum board provides some level of air leakage and vapor flow control. These roofs had springtime drying rates similar to the diffusion vent roof, possibly due to upward drying into the mesh air space.

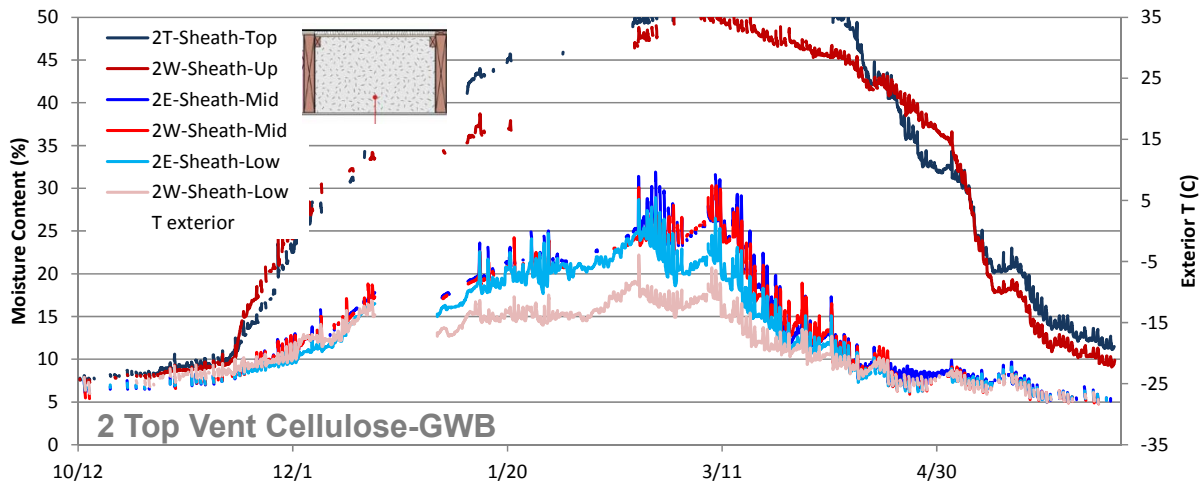


Figure 49: Roof 2 (top vent cellulose with gypsum board) sheathing moisture contents

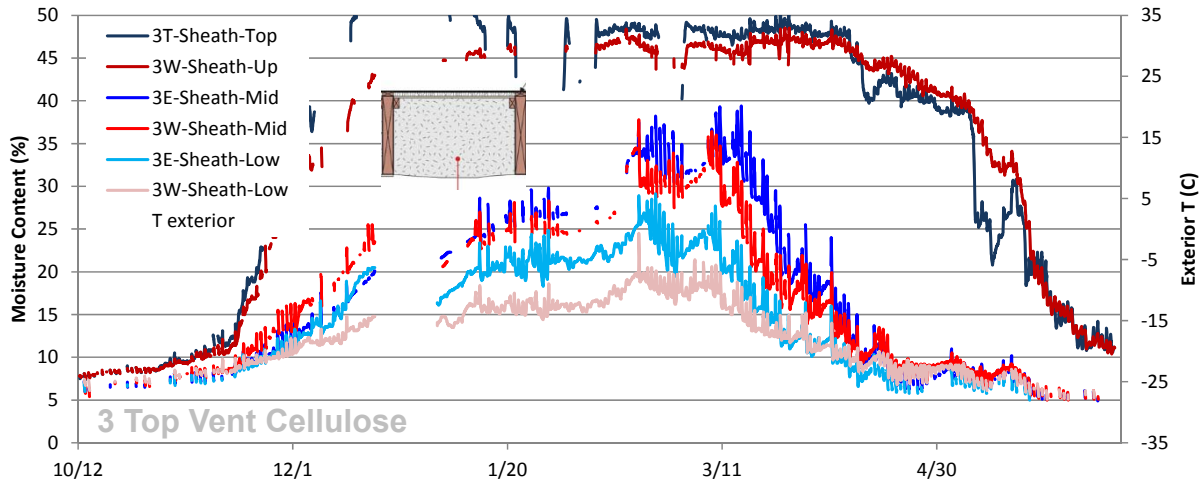


Figure 50: Roof 3 (top vent cellulose, no gypsum board) sheathing moisture contents

The results for the fiberglass “top vent” (“breather” mesh netting under shingles) roofs are shown in Figure 51 (top vent fiberglass with gypsum board) and Figure 52 (top vent fiberglass, no gypsum board). These measurements showed much greater variation in moisture levels over the winter, with sudden drops in moisture content. Therefore, these graphs were plotted with the constant dewpoint graphic; there is some correlation between periods of sudden drying and periods when humidification was not running.

The two assemblies show different responses: the gypsum board assembly (Roof 5) has some degree of stratification (higher MCs at upper parts of roof), while the no gypsum board assembly (Roof 4) showed high moisture contents at almost all locations.

The difference in behavior between the fiberglass and cellulose top vent roofs (2, 3, 4 and 5) may be a function of the hygric storage/moisture buffering effect of the cellulose insulation; fiberglass insulation has minimal moisture storage.

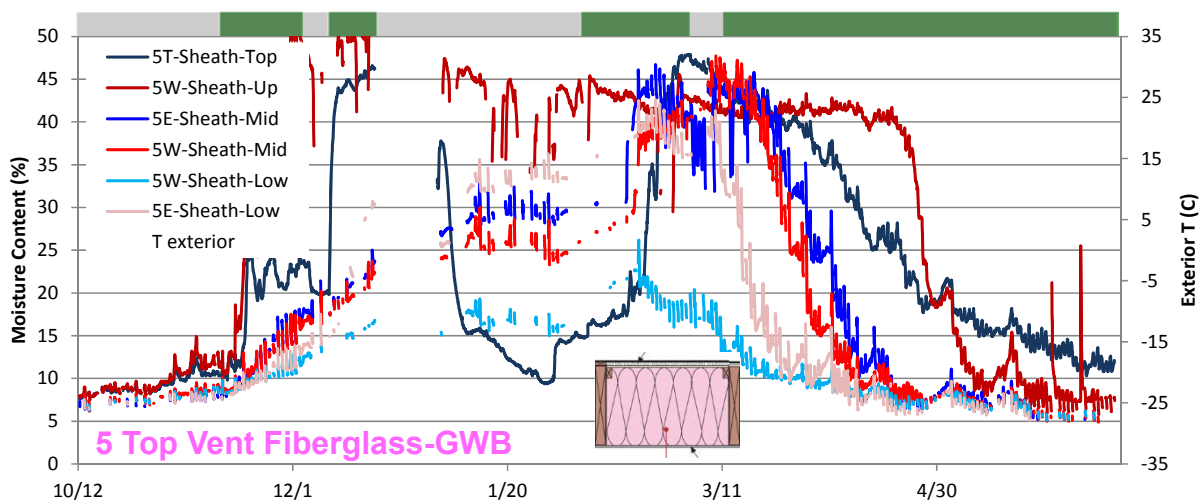


Figure 51: Roof 5 (top vent fiberglass with gypsum board) sheathing moisture contents

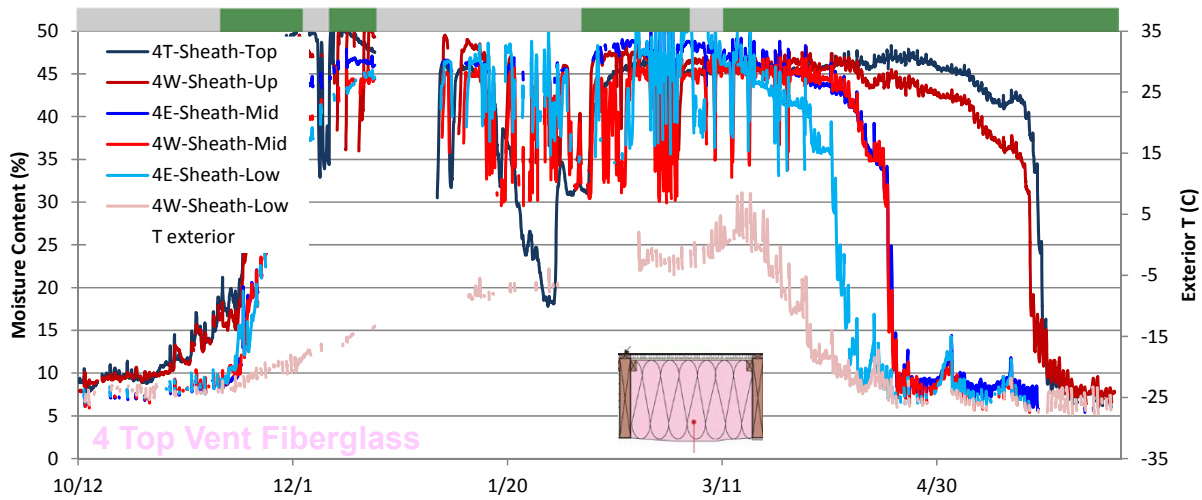


Figure 52: Roof 4 (top vent fiberglass, no gypsum board) sheathing moisture contents

When the roof assemblies dry in the spring, the uppermost portions of the roof stay wettest the longest, and the lower portions of the roof dry out first.

A mid-December site visit allowed verification that the monitoring data reasonably reflected reality. The top vent fiberglass assembly without gypsum board (Roof 4) was examined from the interior. A brown stain indicating water leakage (Figure 53, left) was found; when the batt was removed, very wet/saturated roof sheathing and fiberglass were observed (Figure 53, right).



Figure 53: Top vent fiberglass, no GWB (4) water leak (L) and wet fiberglass batt (R)

The sheathing was saturated with liquid water/condensation (Figure 54, left), and the fiberglass was saturated with condensation at the exterior surface as well (Figure 54, right).



Figure 54: Top vent fiberglass, no GWB (4) wet sheathing (L) and wet batt (R)

4.3 Roof Ridge/Peak Sensor Packages

Multiple sensors packages were installed at the roof ridge/peak, due to the localization of damage there, in previous observations. The data are plotted in parallel for multiple roofs; the color coding used for these graphs is shown in Table 6.

Table 6: Color code labels used for cold climate (Chicago) roof assemblies

#	Name
1	Vented
2	Top Vent Cellulose-GWB
3	Top Vent Cellulose
4	Top Vent FG
5	Top Vent FG-GWB
6	Diffusion Vent Cellulose
7	Unvented Cellulose

Both top vent cellulose roofs (2, 3) are shown in grey (of different shading), and both fiberglass roofs (4, 5) are shown in pink. The diffusion vent (6) and unvented cellulose roofs (7) are shown in gold and orange, respectively. Typically, the top vent roofs are plotted together, and the remaining roofs (1, 6, and 7) in another grouping.

4.3.1 Rafter Framing Moisture Contents

Rafter framing moisture contents reflect patterns similar to the previous roof sheathing MC measurements. Results for the vented (1), unvented (7), and diffusion vent (6) roof are shown in Figure 55 and the top vent roofs (2, 3, 4, and 5) in Figure 56.

The vented roof (1) shows consistently dry performance (all MCs below 15%), while roofs 6 and 7 MCs rise in winter, to peaks in the 40-45% MC range. However, the diffusion vent (6) roof dries more rapidly than the unvented (7) roof, and to a lower ending MC (8% vs. 15%).

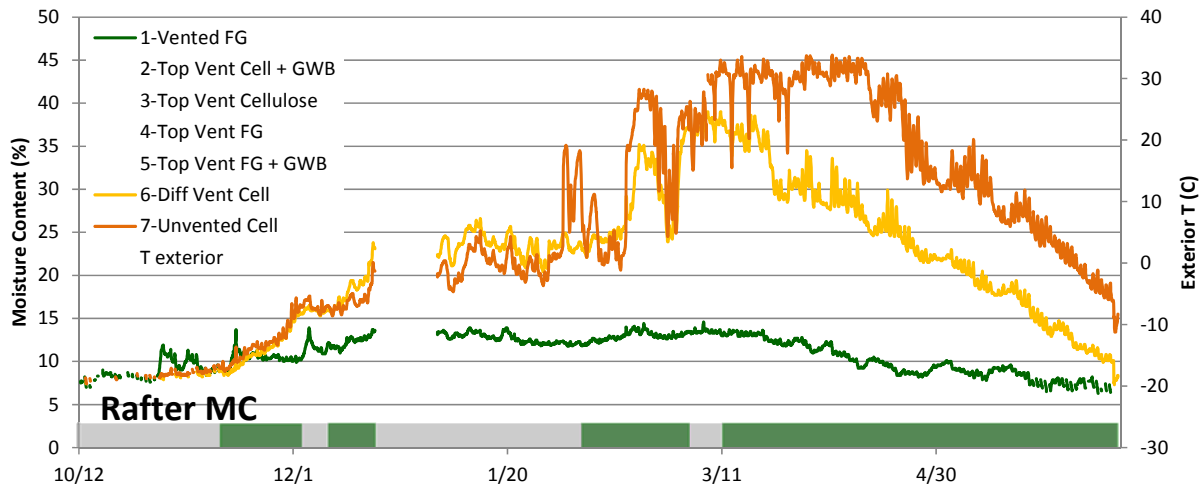


Figure 55: Rafter framing moisture content, vented (1), diffusion vent (6), and unvented (7)

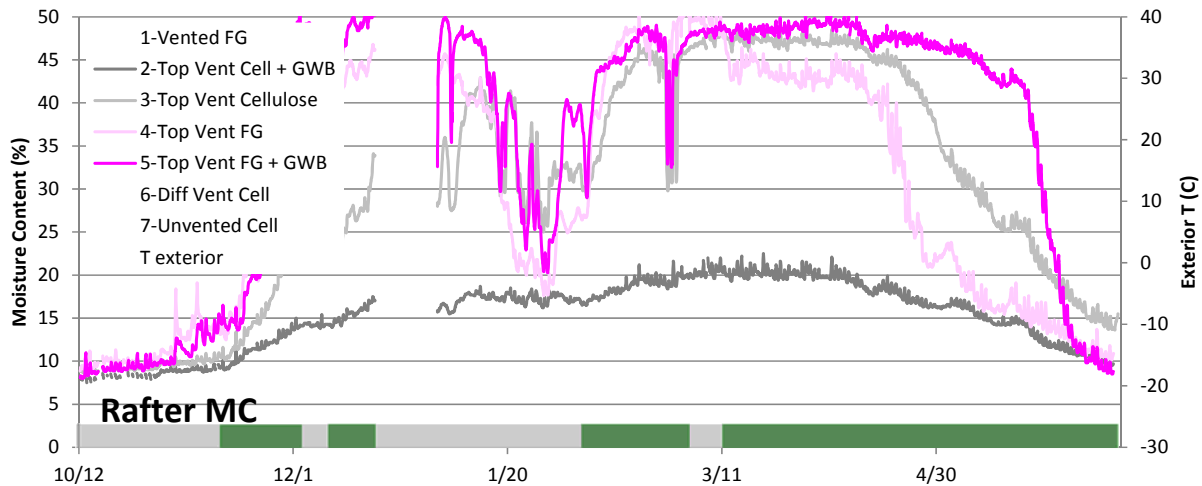


Figure 56: Rafter framing moisture content, top vent cellulose (2, 3) and fiberglass (4, 5)

The top vent roofs (Figure 56) show greater MC variations over the course of the winter, but three of the four roofs move roughly in parallel. The top vent cellulose with gypsum board (2) assembly stays much drier (peak ~21% MC) than the remaining roofs (45-50% MC). The MC rise and fall patterns can be roughly correlated with humidification system operation (green/grey bar). All top vent roofs dry in the spring to the 10-15% MC range. The top vent fiberglass with gypsum board (5) roof shows the slowest drying, but no clear reason is seen for this behavior.

4.3.2 Roof Peak/Ridge Relative Humidity

The relative humidity at the rafter bay peak is plotted for the unvented (7) and diffusion vent (6) roof in Figure 57 and the top vent roofs (2, 3, 4, and 5) in Figure 58. The vented roof is not plotted, because it largely reflects outdoor conditions.

The unvented and diffusion vent roofs both spike in RH after the installation of humidification, and remain at high RH (90-100%) through most of the winter. In the spring, the diffusion vent roof dries to safer levels, while the unvented assembly remains at high RH levels.

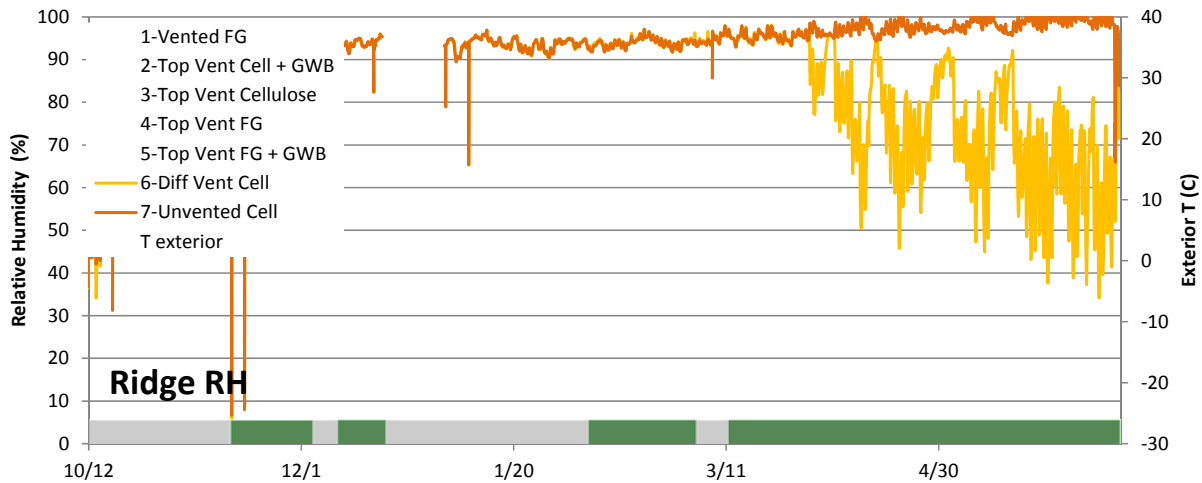


Figure 57: Roof ridge peak RH, diffusion vent (6) and unvented (7)

The top vent cellulose roofs (2 and 3) show similar behavior, with RH remaining in the 90-100% through most of the winter, and drying in the spring. The top vent fiberglass roofs (4 and 5) though show more variations, and Roof 4 (no gypsum board) shows extreme variations in RH (from 15% to 95%). These extreme variations were first interpreted as sensor failure: polymer capacitance-based RH sensors are known to have issues with high RHs and condensing conditions, consistent with the measurements at the roof ridge.

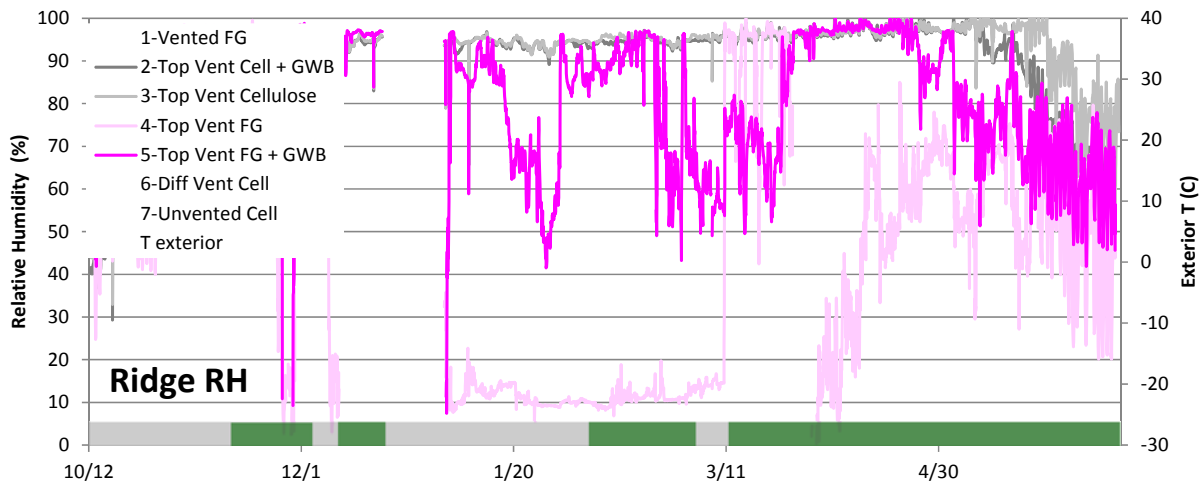


Figure 58: Roof ridge peak RH, top vent cellulose (2, 3) and fiberglass (4, 5)

4.3.3 Roof Peak/Ridge Wafer Sensor

Given the variations seen in the RH sensors, the wood “wafer” sensors were also checked as surrogates for relative humidity (Figure 59).

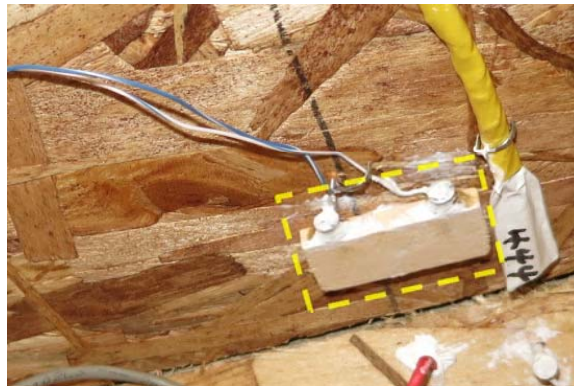


Figure 59: Roof ridge wafer sensor example, next to RH sensor

Wafer sensors have greater durability than RH sensors; although they are slow to respond, they can be useful for understanding seasonal moisture accumulation and release patterns. The response of these wood-based sensors should be understood when interpreting these results. In previous calibration (Ueno and Straube 2008), the “wafer” sensors come to equilibrium with 100% RH conditions (air in closed container over water) at 28%–30% MC. However, immersing the sensors in liquid water increases their MC to the 40%–45% range. Therefore, measurements above the 100% RH-equivalent range indicate liquid water condensation.

Roof peak/ridge wafer moisture contents are plotted for the vented (1), unvented (7), and diffusion vent (6) roof in Figure 60 and the top vent roofs (2, 3, 4, and 5) in Figure 61.

The vented roof (1) shows RHs that peak at roughly 100% RH-equivalent; with drier conditions for much of the winter. The unvented (7) and diffusion vent (6) roofs both show moisture contents well into the liquid water/condensation range; similar to previous results, the diffusion vent roof (6) dries much faster than the unvented (7) roof.

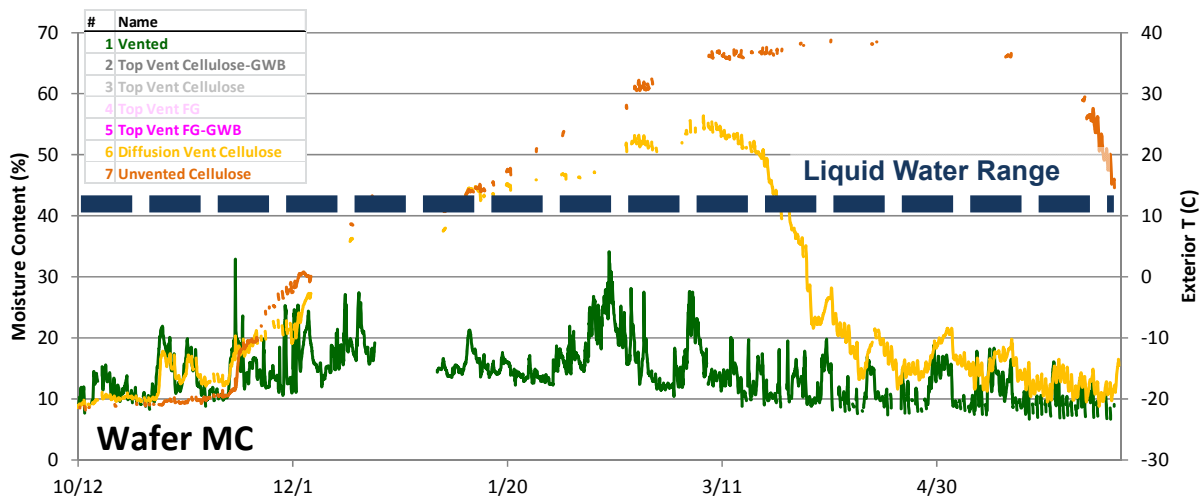


Figure 60: Roof ridge wafer sensor, vented (1), diffusion vent (6), and unvented (7)

The top vent cellulose roofs (2 and 3) both show quick rises into the liquid water/condensation range, with drying in the spring. The top vent fiberglass roof with gypsum board (5) has similar behavior, but with some variations (apparently linked with humidification operation). The top vent fiberglass roof without gypsum board, however, showed similar puzzling behavior as the RH sensor in the same assembly (dropping to very low RH in the winter). Both fiberglass roofs showed periods above the liquid water/condensation range.

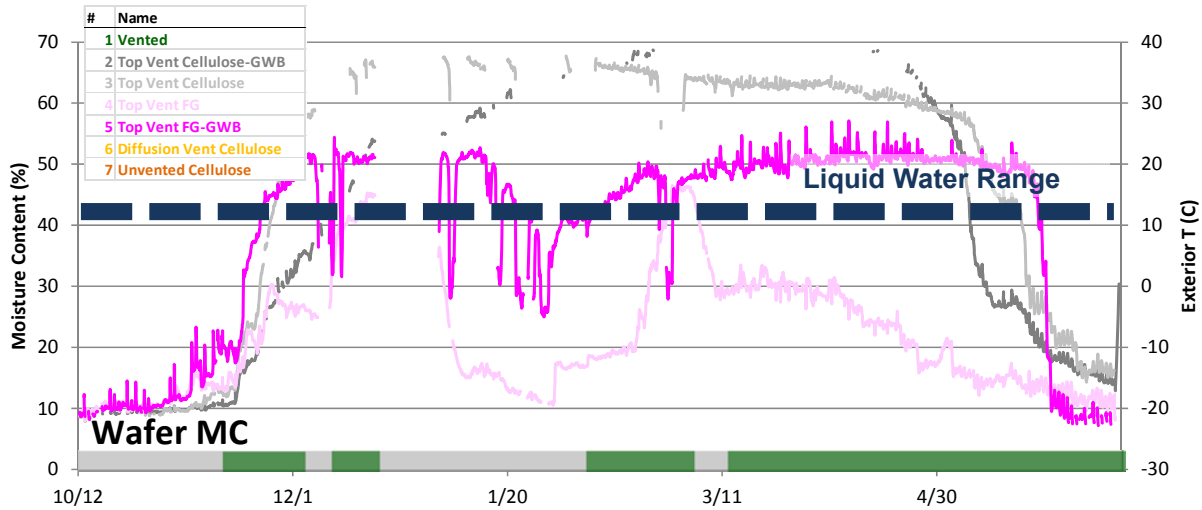


Figure 61: Roof ridge wafer sensor, top vent cellulose (2, 3) and fiberglass (4, 5)

4.3.4 Roof “Doghouse” Sheathing Moisture Content

Sheathing moisture content at the “doghouse” detail was measured (Figure 62). The principle of many of these roofs is that they release moisture at the peak: there is a risk that this moisture might condense on the underside of the doghouse detail, causing damage.



Figure 62: Roof “doghouse” sheathing moisture content sensor

The measured doghouse MCs are shown in Figure 63, with outdoor temperature for reference. MCs remain mostly below 20%, with some brief excursions above that range that dry quickly. However, the top vent fiberglass roof without gypsum board (Roof 4) showed much higher MCs, with peaks in the 40% range. Combined with the anomalies seen in rafter bay peak RH (and

matching wafer sensor), they suggest air leakage may be occurring at this test bay. Leakage of high humidity indoor air could result in the doghouse sheathing wetting seen here.

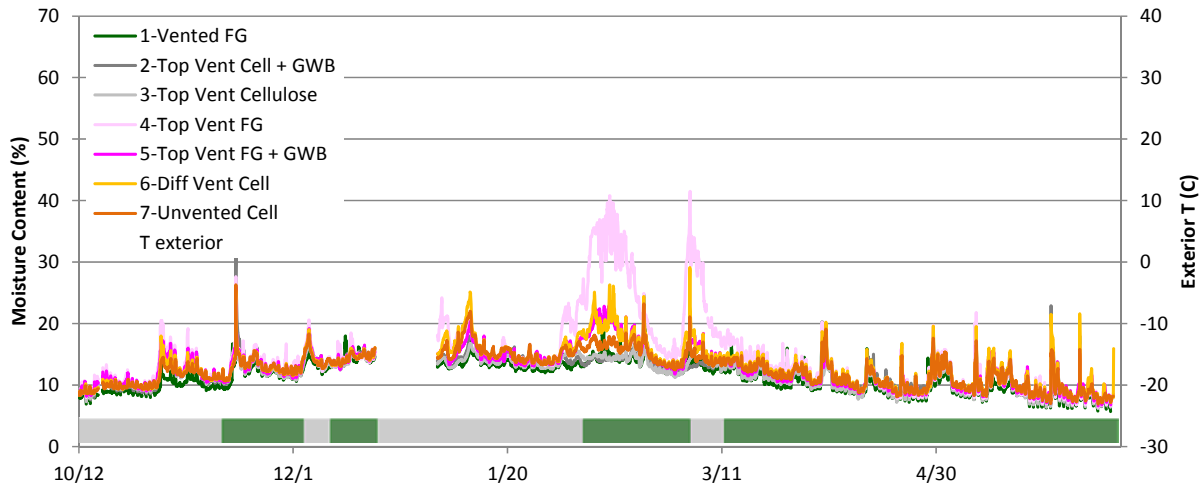


Figure 63: Roof “doghouse” sheathing moisture content measurements

There are multiple spikes in doghouse MC; they were plotted with precipitation data (taken from airport data) in Figure 64. The data seem to indicate some (albeit not perfect) correlation between moisture spikes and precipitation events. Improved correlation might be obtained by calculating driving rain (from precipitation and wind data) that would push rain through the doghouse detail (predominantly east-west).

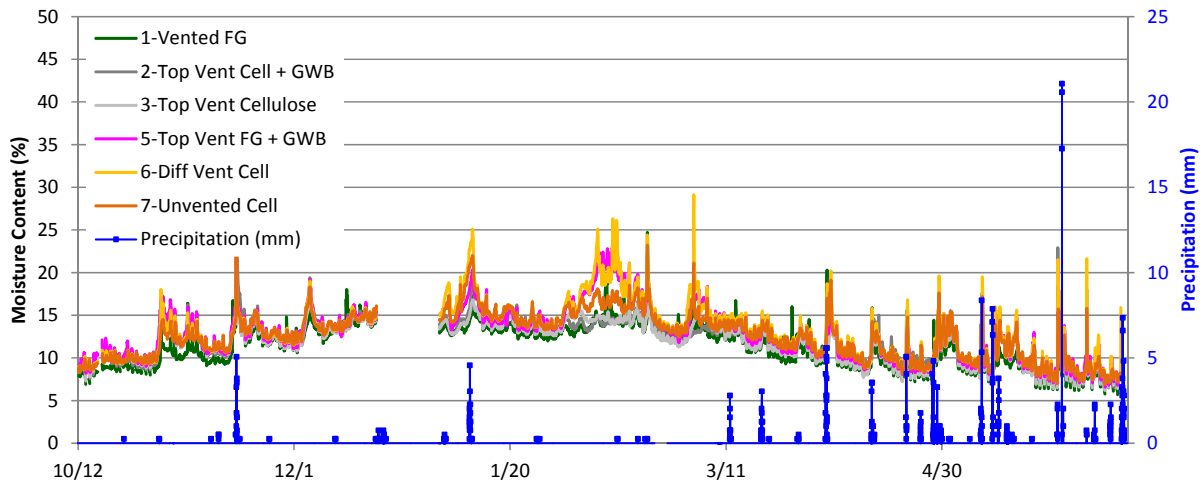


Figure 64: Roof “doghouse” sheathing moisture content measurements with precipitation

4.4 Ventilation Space Sensors

Temperature and relative humidity sensors were installed in the airstream of the ventilated roof assemblies (1 through 5), in order to provide some indication of whether moisture removal was occurring. Dewpoints were calculated and plotted, which generally seemed to indicate higher dewpoints at the exhaust points of the roofs. These plots are shown in Appendix B.

Unfortunately, not many conclusions can be drawn from the ventilation space measurements. Although higher dewpoints at the exhaust may indicate removal of moisture, they might also simply indicate static accumulation (and stratification) of moisture, if there is minimal airflow. To truly measure moisture removal, both intake/exhaust air moisture content and airflow would need to be measured. Given the limited ($\sim\frac{1}{2}$ in.) mesh airspace under the shingles, it seems plausible that the airflow might be relatively low. Measurement of the low velocity airflows occurring in ventilation cavities is difficult to monitor in-situ (Van Straaten 2003).

5 Cold Climate (Chicago) Disassembly

At the conclusion of any enclosure monitoring experiment, a useful step is to open the test assemblies and examine conditions. It is instructive to understand how the monitored data relate to actual damage or material durability. Therefore, the test roofs were disassembled at the end of the experiment (June 2014); the builder converted the garage attic back into a conventional vented geometry.

5.1 Ridge Exterior Conditions

Given the concentration of moisture at the roof ridge, the exterior disassembly proceeded from the ridge downward. Conditions after removing the “doghouse” sheathing, 2x4 standoffs, and housewrap ridge wrap are shown in Figure 65.

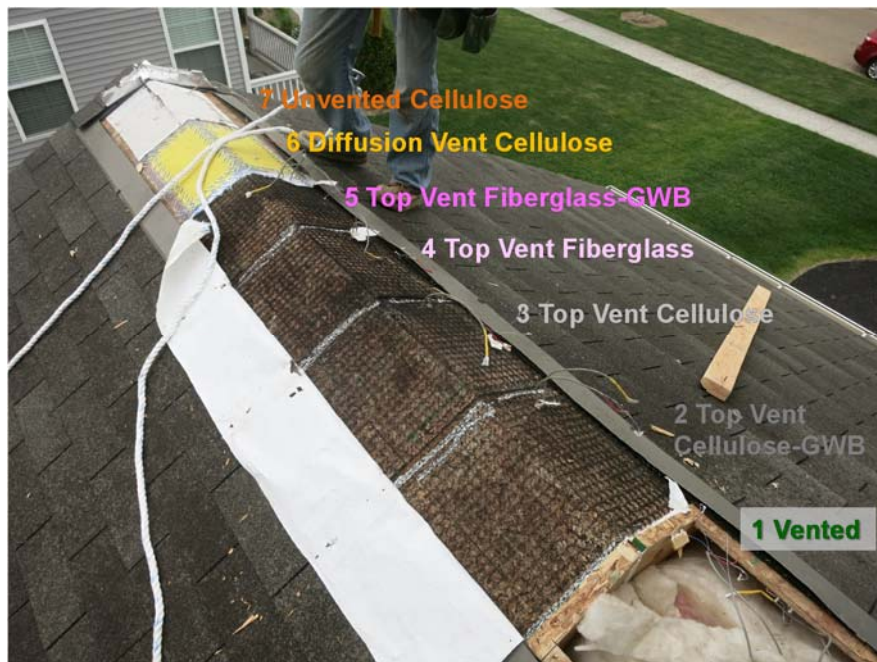


Figure 65: Ridge conditions, before removal of breather mesh



Figure 66: Ridge conditions, after removal of breather mesh

Conditions after removal of the “breather” mesh are shown in Figure 66 and Figure 67. The breather mesh was run continuously across all four “top vent” assemblies, so unintentional cross flow could occur here. The roof sheathing is not continuous across the four bays, due to the “dropped” sheathing detail.

There was apparent exterior moisture damage (stained, likely mold growth on sheathing), with the greatest damage concentration at the fiberglass bays.



Figure 67: Ridge conditions, after removal of breather mesh

The damage at the fiberglass bays was examined by probing the sheathing with a screwdriver (Figure 68). Although these stained areas appear heavily damaged, they are structurally intact.

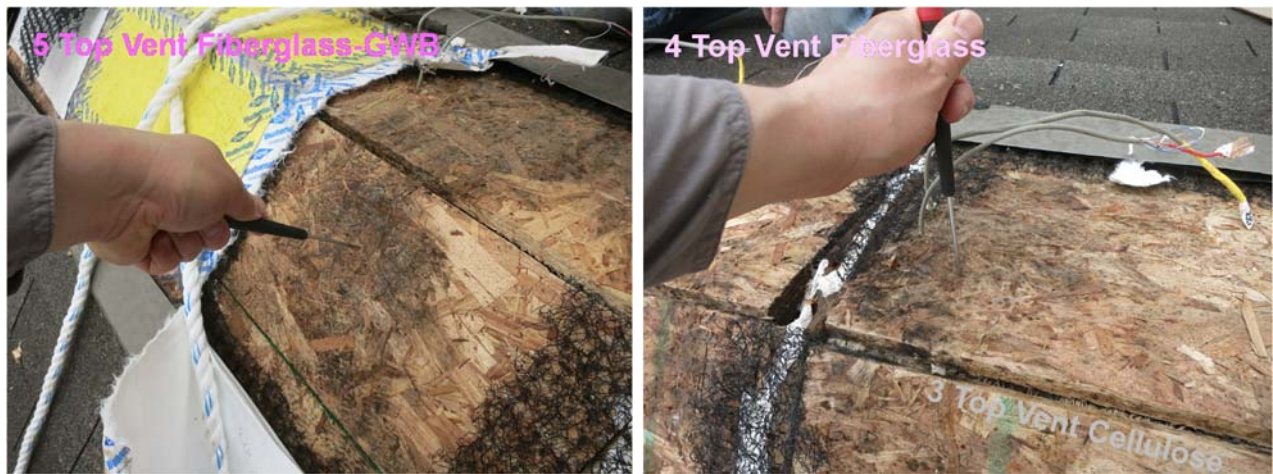


Figure 68: Ridge sheathing conditions (“screwdriver test”) for Roofs 4 and 5

There is damage to the sheathing at the top vent cellulose roof (3), shown previously in Figure 68. However, based on the damage pattern (adjacent to bay 4, top vent fiberglass), and the complete lack of top surface damage in the adjacent cellulose bay (top vent cellulose with gypsum board; Figure 69), it is likely that the staining on roof 3 is due to cross-airflow leakage coming from the adjacent fiberglass assembly.



Figure 69: Ridge sheathing conditions, Roofs 1, 2, and 3

5.2 Rafter Bay Peak Conditions

A strip of roof sheathing was removed at the peak, and conditions were examined on the top and bottom surfaces of the sheathing, and in the rafter bay.

The top and bottom of the sheathing in Roof 3 (top vent cellulose with gypsum board) is shown in Figure 70. The interior surface showed rusted fasteners, some discoloration, and grain raise/thickness swelling of the OSB, but no visual indication of mold growth. The top side, in contrast, showed the mold growth that is suspected to have originated from an air leak from the adjacent (fiberglass) bay.



Figure 70: Ridge sheathing bottom (L) and top (R) conditions, Roof 3

Conditions at Roof 2 (top vent cellulose, no gypsum board) are shown in Figure 71; interior sheathing had similar conditions to Roof 3 (no visible mold growth, rusted fasteners, grain raise of OSB).

The cellulose insulation had not settled over the course of a winter, and was not visibly damaged. There was some “caking” of the cellulose (adhesions to the roof sheathing), which is regarded as an indication of dried moisture accumulation (Rose and McCaa 1998, Derome 2005).



Figure 71: Ridge sheathing top conditions, Roof 2 (L); cellulose conditions (R)

In contrast, the top vent fiberglass roofs showed extensive damage. Sheathing conditions at Roof 4 (top vent fiberglass, no gypsum board) are shown in Figure 72; the exterior side is stained with suspected mold (near the assumed air leak), and the interior side has extensive staining and growth, with insulation adhered to the sheathing (Figure 72 left). Figure 72 (left) shows the east (rear) facing roof sheathing.



Figure 72: Ridge sheathing top (L) and bottom (R) conditions, Roof 4

Another image of the interior side of the east-facing roof sheathing is shown in Figure 73 (left); the west (front) face is shown in Figure 73 (right).



Figure 73: Ridge sheathing bottom conditions, Roof 4

Similar images are shown for Roof 5 (top vent fiberglass with gypsum board); both exterior and interior sides showed extensive damage and staining (wetter on the inside).



Figure 74: Ridge sheathing conditions, Roof 5

Within the rafter bays, there was apparent mold growth on the framing, concentrated at the exterior (colder in winter) side (Figure 75, Figure 76). In addition, although the fiberglass batts were installed meticulously from the underside, gaps between the batts and framing were evident from the top side, which would have left possible openings for airflow bypass.



Figure 75: Fiberglass batt conditions at ridge, Roof 4



Figure 76: Fiberglass batt and framing conditions at ridge, Roof 4 (L) and Roof 5 (R)

The gypsum sheathing at the diffusion vent roof (6) had no evidence of damage from the exterior. When disassembled, the gypsum sheathing appeared to be basically intact, with no evidence of staining or mold growth (Figure 77).



Figure 77: Ridge sheathing top and bottom conditions, Roof 6

The unvented cellulose assembly (7) showed no damage from the exterior, after removal of the self-adhered membrane (remnants are visible in Figure 78 left). When the sheathing was removed, only minor evidence of moisture issues (OSB grain raise, rusted staples, cellulose “caking”) were seen; no visual evidence of mold growth was found. The cellulose insulation did not settle over the course of the winter; it still filled the cavity to the ridge.



Figure 78: Ridge sheathing top and bottom; cellulose conditions, Roof 7

5.3 Conditions Away From Ridge

Following disassembly of the ridge, the roof cladding materials were stripped near the ridge; the front (west) face is shown in Figure 79. There is some degree of exterior staining at all of the top vent roofs, but it is more severe at the fiberglass batt roofs.



Figure 79: Sheathing away from ridge, west (front) face of roof

The same condition on the east (rear)-facing roof is shown in Figure 80, showing similar patterns (worse conditions at fiberglass batt roofs).



Figure 80: Sheathing away from ridge, east (rear) face of roof

At the top vent cellulose roofs (4 and 5) and dense pack cellulose roofs (6 and 7), the sheathing was largely intact (minor damage seen, of grain raise, “caking,” and fastener corrosion), as shown in Figure 81.



Figure 81: Sheathing away from ridge, Roofs 4 and 5 (L), Roofs 6 and 7 (R)

Similar to the ridge, the fiberglass batt roofs showed worse conditions than the cellulose bays, away from the ridge (Figure 82). The sheathing condition at Roof 4 (top vent fiberglass, no gypsum board) was worse than Roof 5 (top vent fiberglass with gypsum board).



Figure 82: Sheathing away from ridge, Roofs 4 (left) and 5 (right)

5.4 Interior Disassembly

The interior gypsum board was removed, revealing drip patterns in the fiberglass batt bays (condensation rundown), and further signs of mold on the roof framing (Figure 83).



Figure 83: Staining of ceiling gypsum board at (L); mold on framing (R), Roof 5

6 Cold Climate (Chicago) Analysis

6.1 ASHRAE 160 Analysis

ASHRAE Standard 160 (ASHRAE 2009b) provides guidance on moisture analysis for building envelope design, including the moisture performance evaluation criteria (in terms of mold growth risk). The failure criteria were refined in addendum (a) (ASHRAE 2011), giving the requirement of a “30-day running average surface RH over 80% when the 30-day running average surface temperature is between 5°C (41°F) and 40°C (104°F).” Other practitioners (Arena 2013, 2014) have found ASHRAE 160 criteria to be excessively stringent/conservative.

The measured temperature and relative humidity conditions at the roof ridge were analyzed using ASHRAE 160 criteria. Thirty-day running averages were calculated for each hour, and the resulting pass/fail results tabulated. In a strict interpretation of Standard 160, a single failing hour would constitute an assembly failure.

ASHRAE 160 is not being used as a design tool (per its intent) in this exercise; instead, the monitored data can be compared with the conditions of the roof assembly after one winter, based on the disassembly.

The graphs below show hours when the test assemblies fail ASHRAE 160 criteria (using point markers); exterior temperature and the 30 day average temperature at the roof ridge cavity are added for reference. The vented (1), unvented (7), and diffusion vent (6) roofs are shown in Figure 84 and the top vent roofs (2, 3, 4, and 5) in Figure 85.

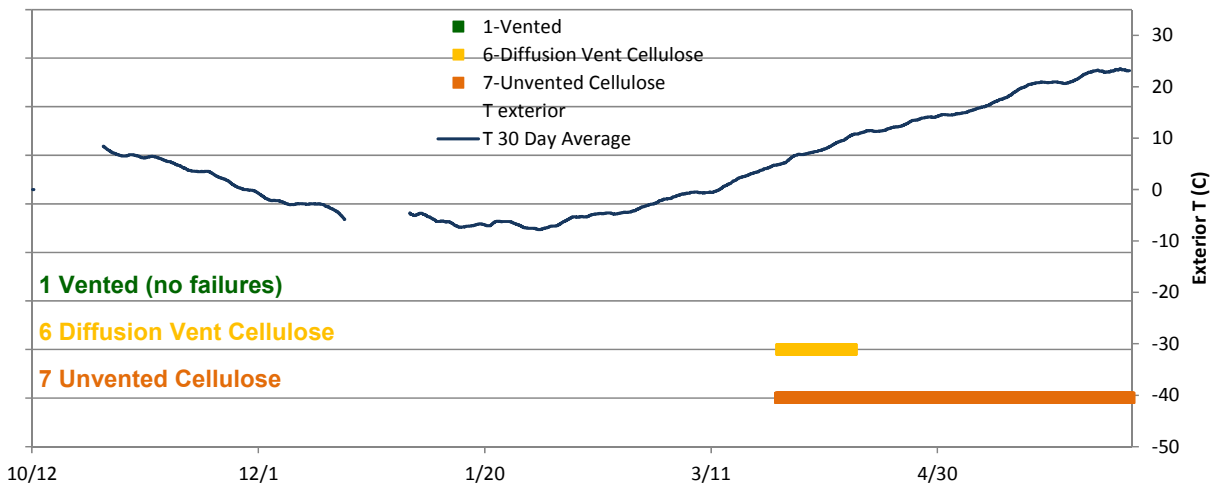


Figure 84: ASHRAE 160 failures, vented (1), diffusion vent (6), and unvented (7)

The vented (1) roof had no hours failing ASHRAE 160 during the test winter. The unvented (7) and diffusion vent (6) roofs had relative humidity levels that rose past 80% in the fall/early winter, but by that point, temperatures had fallen below the risk range (41°F/5°C). But in the spring, as the assemblies warmed, 6 and 7 had many failing hours. The diffusion vent roof (6) dried rapidly, reaching safe conditions (below 80% RH) by mid-April. However, the unvented assembly (7) remained wet, staying above 80% RH through the end of the monitoring period.

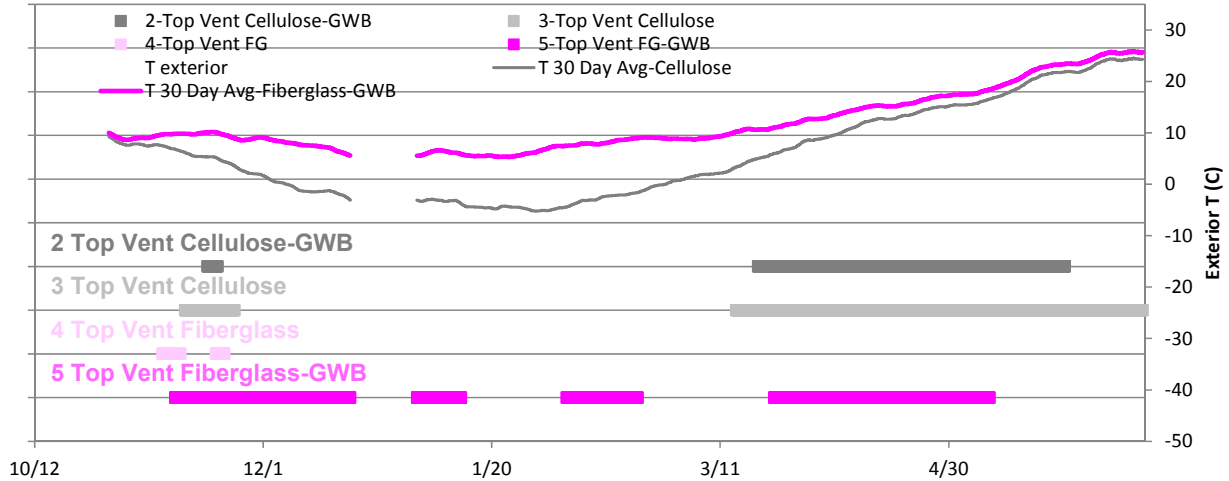


Figure 85: ASHRAE 160 failures, top vent cellulose (2, 3) and fiberglass (4, 5)

The top vent roofs (2, 3, 4, and 5) all showed periods failing ASHRAE 160 criteria in the fall, before temperatures fell below the risk range. Again, as temperatures warmed, the assemblies returned to ASHRAE 160 failure conditions. However, the top vent fiberglass roof without gypsum board (4) remained below 80% RH. This assembly had RHs and MCs with wide swings and dry conditions, apparently reflecting air leakage through the assembly.

The 30 day running average temperature at the ridge was calculated for the assemblies; there was a substantial difference between the various assemblies (top vent cellulose with gypsum board/Roof 2 and top vent fiberglass with gypsum board/Roof 5 plotted above). This is covered in more detail in the following section.

A tabulation of the hours failing ASHRAE 160 criteria is provided in Table 7.

Table 7: Number of hours roof ridge T/RH failing ASHRAE 160 criteria

#	Assembly	# Hours Failing ASHRAE 160	% of Hours Fail ASHRAE 160
1	Vented	0	0%
2	Top Vent Cellulose-GWB	1667	29%
3	Top Vent Cellulose	2396	41%
4	Top Vent FG	129	2%
5	Top Vent FG-GWB	2659	46%
6	Diffusion Vent Cellulose	374	6%
7	Unvented Cellulose	1852	32%

6.2 Ridge Average Temperature

Per the previous section, when the 30 day running averages temperatures at the roof ridge were calculated, noticeable differences were seen between assemblies, despite them having similar nominal R values (all R-38 except R-30 vented roof/Roof 1). The 30 day averages are plotted with outdoor temperature in Figure 86.

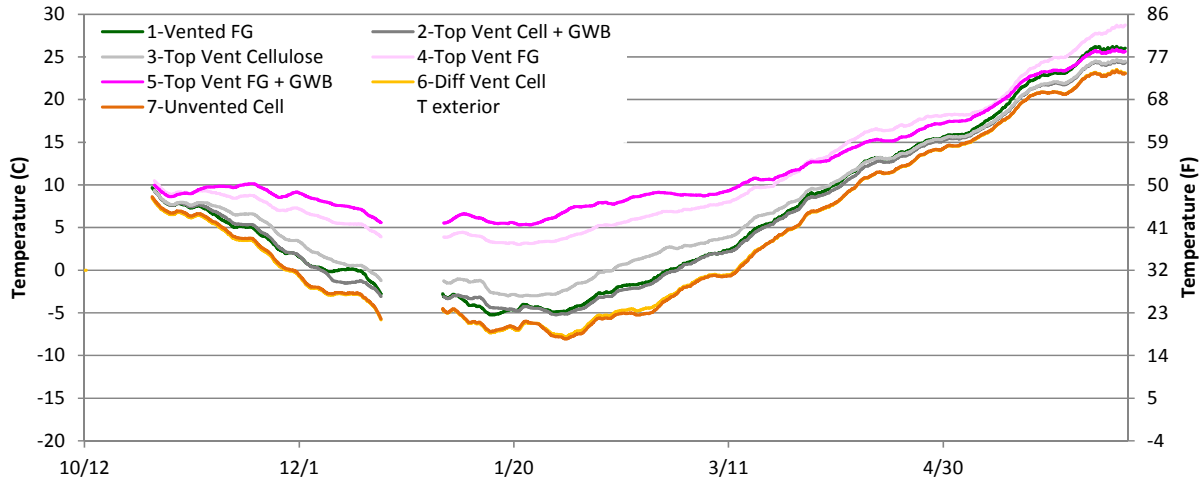


Figure 86: 30-day running average temperatures at ridge (T/RH sensors) for all roofs

Temperatures were close during milder weather, and then separated as the winter grew colder. The unvented (7) and diffusion vent (6) assemblies had essentially identical behavior, and the top vent cellulose (2, 3) and vented (1) assemblies had slightly warmer but also similar temperatures. The two top vent fiberglass roofs (4, 5) had much warmer temperatures at the roof ridge.

These differences may be due to airflow (interior-to-exterior air leakage, transporting interior heat to the ridge), which is consistent with other measurements and site observations (moisture damage on top side of fiberglass roofs, pressure differential measurements).

6.3 Sheathing Temperatures and Ventilation Space Behavior

Examination of dewpoint temperatures of the ventilation spaces (in the top vent roofs) gave inconclusive results (see Section 0): the difference in dewpoint might reflect moisture removal, or simply moisture accumulation. Another way of gauging whether effective ventilation is occurring through the “top vent” mesh is to examine the sheathing temperatures. Ventilation air movement up the roof might carry some heat with it, possibly cooling the lower roof surfaces (or the entire roof surface), relative to the analogous unvented roof.

Detailed graphs are provided in Appendix C; however, the temperature measurements show little indication of the “top vent” detail having an effect on sheathing temperatures. The fully ventilated cathedral roof had cooler summer sheathing temperatures, consistent with airflow.

6.4 Conclusions for Cold Climate (Chicago) Test Roof

Combining the monitored data, the disassembly of the assemblies, and further analysis, the following conclusions can be drawn from this work.

6.4.1 Boundary Conditions (Interior Humidification)

One potential criticism of this work is that 50% interior RH in a Zone 5A climate is a severe loading. It is definitely above commonly observed interior RH levels: for instance, Arena et al. (2010) measured winter monthly average RHs of 36-38% in a survey of Zone 5A (Massachusetts/Connecticut) newly constructed houses.

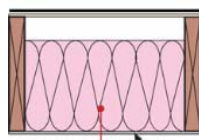
However, greater airtightness (in energy efficient housing) increases risks of high interior RHs, especially in cases when controlled mechanical ventilation is not installed or operated. For instance, Ueno and Lstiburek (2015) measured RHs in the 40-50% range for much of the winter in a low air leakage (under 1 ACH 50) house in a Zone 5A climate with an inoperable ventilation system.

More importantly, the 50% RH loading was used to accelerate moisture-related failures of the assemblies; this is a commonly used technique, as covered in Rose and McCaa (1998), Wilkinson et al. (2007), Straube et al. (2009), and Smegal and Straube (2014). An ideal experiment would have first run these roof assemblies under “typical” interior RH conditions (e.g., 30% RH) for one winter, followed by a second winter at the extreme loading (50% RH). However, the roof was available for only one winter of monitoring, which eliminated that option.

6.4.2 Overview of Assemblies

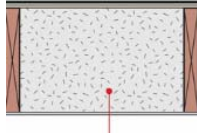
The test roof assemblies are discussed below not in numerical order, but in an order that provides some logical flow between relative performances of these assemblies.

Some patterns were seen consistently across the assemblies. When moisture accumulation and/or damage occurred, it was concentrated and most intense at the roof ridge, consistent with previous field observations. In addition, moisture accumulation within the assembly was essentially driven by interior relative humidity and exterior temperature; periods when the humidification system failed had less accumulation or even moisture removal.



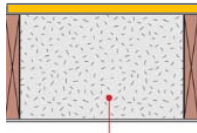
1 Vented

The “control” roof, or compact vented roof assembly (Roof 1) showed excellent performance, with low wood moisture contents, RHs well within the safe range, and no sign of damage during disassembly. This is especially impressive given the high interior RH conditions (50% RH at 71°F). That being said, the roof ventilation in this assembly was likely better than achieved in the field. The air space cavity above the insulation was a full 4 inches (substantially above the code-mandated 1”), and the ridge ventilation opening had very low restriction, with a large opening (see Figure 69), and no restriction from ridge mesh or netting.



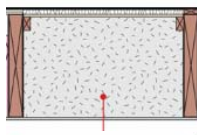
7 | Unvented Cellulose

The unvented cellulose roof (Roof 7), a.k.a. “dense pack cellulose roof,” showed long-term accumulation of moisture, especially at the ridge, as indicated by high sheathing moisture contents, high relative humidity, and wafer sensor measurements indicating condensation or liquid water. In addition, the assembly showed a long-term failure of ASHRAE 160 criteria (from mid-April through the end of monitoring in June). However, when the roof was disassembled, although there were definite signs of moisture accumulation, the damage was by no means severe. No visible mold growth was found on the underside (interior) of the roof sheathing; damage was restricted to grain raise/thickness swelling of OSB flakes, corrosion of fasteners (both structural nails and wiring staples), and “caking” of the cellulose insulation. No settling was seen in the cellulose insulation. However, this disassembly was conducted after only a single winter; annual cycles of wetting to this level are likely to have worse effects on durability.

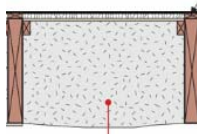


6 | Diffusion Vent Cellulose

The diffusion vent roof (Roof 6) had similar performance to Roof 7, with high moisture conditions during the winter (including liquid water condensation), especially at the ridge. However, all measurements (sheathing MC, ridge RH, wafer sensor) showed that this assembly dried much more rapidly during warmer spring weather than Roof 7, due the outward drying available through the fiberglass-faced gypsum board at the ridge. As a result, this assembly had a considerably shorter period that failed ASHRAE 160 criteria. Disassembly showed no evidence of mold growth on the gypsum board at the ridge, or on the OSB further from the ridge. Similar to Roof 1, this roof did not show massive material failures, but it had moisture levels much higher than levels recommended for durability.



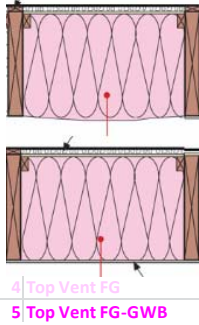
2 | Top Vent Cellulose-GWB



3 | Top Vent Cellulose

The top vent roofs insulated with cellulose (Roofs 2 and 3) behaved similarly to Roofs 6 and 7, but with some small differences. Overall, similar high moisture contents were seen. In addition, the sheathing moisture content measurements gave no consistent indication of greater drying due to ventilation through the “breather” mesh/air space. Roof 2 and 3 MCs largely overlapped Roof 6 and 7 results. These two roofs also had hours failing ASHRAE 160 in the early winter, and the late winter/spring. The extent of failures into the spring was closer to the unvented (Roof 7) assembly than the diffusion vent (Roof 6) assembly.

The underside of the ridge roof sheathing showed similar conditions to Roofs 6 and 7. Suspected mold damage was seen on the top surface of the ridge sheathing at Roof 3. However, it was ascribed to cross-contamination air leakage from the adjacent fiberglass batt roof (Roof 4). This was based on the fact that no other cellulose roofs showed this type of damage, and the fact that the pattern was seen only on the side of the rafter bay adjacent to the fiberglass rafter bay.



The top vent roofs insulated with fiberglass batt (Roofs 4 and 5) had similar moisture levels to Roofs 2 and 3, with some exceptions. Roof 4 (fiberglass, no gypsum board) had roof sheathing moisture contents that remained very high for much of the winter (liquid water/condensing conditions), at lower, middle, and upper locations. Roof 5, on the other hand, showed more stratification.

Some measurements (roof peak RH and wafer sensor) in Roof 4 showed some anomalies (rapid variations between low and high RH, or much lower RH than expected), which were ascribed to air leakage issues. Air leakage from Roof 4 is consistent with the “doghouse” sheathing moisture content data.

During disassembly, the sheathing conditions were much worse than the cellulose roofs, even though measured moisture levels were often comparable. The interior side of the sheathing showed extensive wetting, staining, and evidence of mold growth. However, although there was extensive damage, the OSB sheathing was still structurally sound. Sufficient water accumulated at the sheathing to wet the fiberglass batt, and also drain/run down to the gypsum board.

6.4.3 Cellulose vs. Fiberglass Performance

The top vent roofs gave a comparison of cavity insulations: dense pack cellulose vs. fiberglass batt. An ideal comparison would have compared dense pack cellulose with blown-in fiberglass, eliminating the installation variable. The batt installation was imperfect, with air leakage paths and voids, allowing for air bypass of the insulation (and thus greater damage).

In general, the moisture measurements were comparable, or in some cases, the instrumentation in the fiberglass bays showed lower moisture levels. However, during disassembly, it was clear that the roof sheathing and framing in the fiberglass batt roofs suffered much more moisture-related damage, including staining, mold, and mold growth, relative to the cellulose roofs (Figure 87).



Figure 87: Top vent roofs, no interior GWB, East/front face; cellulose (L) and fiberglass (R)

ASHRAE 160 analysis indicates that both the cellulose and fiberglass top vent roofs have many hours above failure conditions, but there is a stark difference in resulting sheathing and framing conditions.

The dense pack cellulose insulation provides protection for the adjacent materials in the assembly; the mechanisms likely include the following:

- Dense-packed cellulose, if properly installed, has sufficient airflow resistance that it significantly reduces airflow through assemblies (Lstiburek 2010b, Schumacher 2011). This is particularly noticeable if there are air barrier failures in other portions of the assembly. Reducing airflow decreases wintertime wetting by interior-sourced humidity.
- Cellulose fiber insulation contains borates, which act both as a fire retardant and preservative/antifungal agent. Previous field observations have provided evidence that these preservatives can migrate into adjacent materials (e.g., sheathing or gypsum board), thus providing them with some protection.
- Cellulose insulation is able to absorb and adsorb moisture safely, resulting in a moisture storage/buffering effect in an assembly.

Rose and McCaa (1998) observed this type of protective effect in a three-year in-situ monitoring study of fourteen wood frame walls in Zone 5A (Champaign, IL). Three walls were configured with only Class III vapor control (latex paint on gypsum board); cavity fill insulation materials were fiberglass batt, blown-in fiberglass, and cellulose (dry-blown behind netting). Interior relative humidity was run at either 50-55% RH or 40% RH (over multiple winters). When these three walls were disassembled, the fiberglass batt had severe mold growth; blown in fiberglass had medium mold growth, and cellulose had mild mold growth (albeit with corrosion on metal fasteners, due to reactions with ammonium sulfate cellulose preservative).

6.4.4 Top Vent Assemblies

The concept behind top ventilated insulated roof deck assemblies is covered by Schumacher and LePage (2012); the design intent is that interior-sourced moisture will diffuse through the roof sheathing, into the ventilated air space (provided by the spacer/“breather” mesh), and be removed from the assembly.

However, the results indicated no significant drying or durability benefit for the top vent cellulose roofs (2 and 3), when compared with the unvented roof (7). One reason why these roofs had disappointing performance was the permeance of the sheathing. The moisture vapor permeance of OSB and plywood sheathing as a function of relative humidity is shown in Figure 88. At higher moisture levels, such as the wet wintertime conditions seen in the test assemblies, plywood is much more vapor permeable (20-35 perms) than OSB (5-8 perms).

OSB sheathing was chosen for the experiment because it is the commodity material used by production builders. Keeping the sheathing material constant across all roof bays eliminated an experimental variable, simplifying analysis. If this experiment had demonstrated adequate performance with OSB, plywood would clearly also perform well. If additional research work is conducted on top vent roofs, a more permeable sheathing material than OSB is recommended.

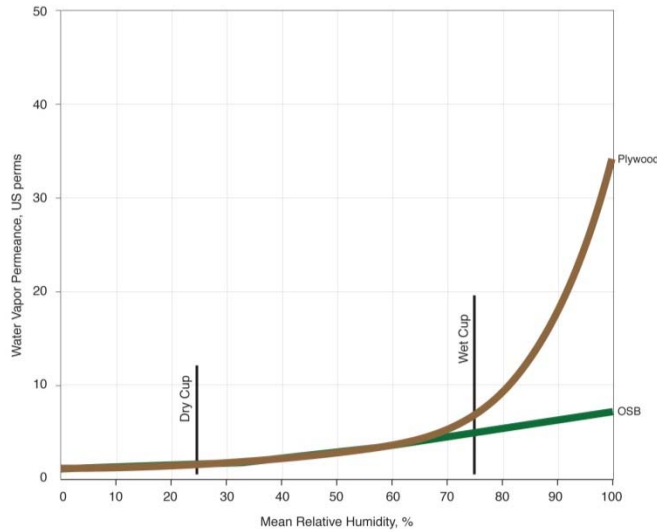


Figure 88: Vapor permeance of plywood and OSB sheathing as a function of RH

Another possible issue is that airflow through the ventilation space was likely restricted. Airflow had to occur through the ½ in. thick space created by the spacer mesh, as well as the openings cut into the housewrap “cap” at the ridge. A reduction in airflow would cause a commensurate reduction in available drying.

Overall, this research demonstrated that a top vent system is not viable in a Zone 5A climate with OSB sheathing, and a relatively small air space. If further research is considered on this topic, changing variables such as sheathing materials and air space size should be considered.

6.4.5 Air Leakage (Fiberglass Roofs)

The monitored data and roof conditions during disassembly all indicate air leakage at the two fiberglass top vent roofs (4 and 5). The 30-day average temperature data indicated that the two fiberglass roofs were outliers, running much warmer than the remaining roofs.

This leakage was due to insufficient air sealing at the “dropped sheathing” detail that was added to keep the asphalt shingles in a flat plane. In addition, despite careful installation of the fiberglass batts, a “blind” installation from below results in air gaps between the batts and framing, which result in air leakage pathways. The worse leakage was seen in Roof 4 (top vent fiberglass, no gypsum board), based on the doghouse moisture content measurements. This issue was not found during air leakage pressure difference (ΔP) measurements, given the lack of gypsum board on the interior. A pre- and post- gypsum board leakage test would have been ideal; however, it was not feasible in this experiment, given that the vented assembly (Roof 1) has rafter bays directly connected to outdoors.

6.4.6 Interior Vapor Control

One potential criticism of this research is that insufficient interior vapor control was used: the gypsum board was finished with a single coat of latex paint (likely more permeable than a Class III (10 perm to 1 perm) vapor retarder). Additional air leakage and vapor control should nominally reduce wetting from the interior.

Although vapor retarders can reduce sheathing wetting, vapor control in itself is by no means a recommended approach for unvented roof assemblies in cold climates. Unless the vapor barrier is detailed perfectly as an air barrier, incidental leakage of interior air will result in wetting of the assembly. An interior vapor barrier such as polyethylene (Class I, 0.06 perm) would completely eliminate drying to the interior. This combination results in an assembly that performs well in theory (and in one-dimensional simulations), but is not at all robust in real-world conditions.

This was demonstrated, for example, in a pool building investigated in a Zone 3A climate (Wilmington, NC; Figure 89). An interior polyethylene vapor barrier was installed, but connections were not made at the roof truss purlins. As a result, this roof failed due to air leakage from the pool, resulting in liquid water condensation at the ridge, which drained and ran out of the roof, creating visible interior staining.



Figure 89: Ridge condensation issues; Zone 3A pool with interior polyethylene vapor barrier

7 Hot-Humid Climate (Houston) Experimental Setup

7.1 Overview

The hot-humid test home is located in Friendswood, TX, roughly 30 miles southeast of Houston (CZ 2A), provided by David Weekley Homes. The house plan is two stories, slab on grade, with 4028 sf. It is a model house that has been unoccupied during the testing period; overview images are shown in Figure 90 and Figure 91. The front of the house faces north; the house is on a corner lot, with street sides on north and east sides.



Figure 90: Front and side views of Houston-area test house

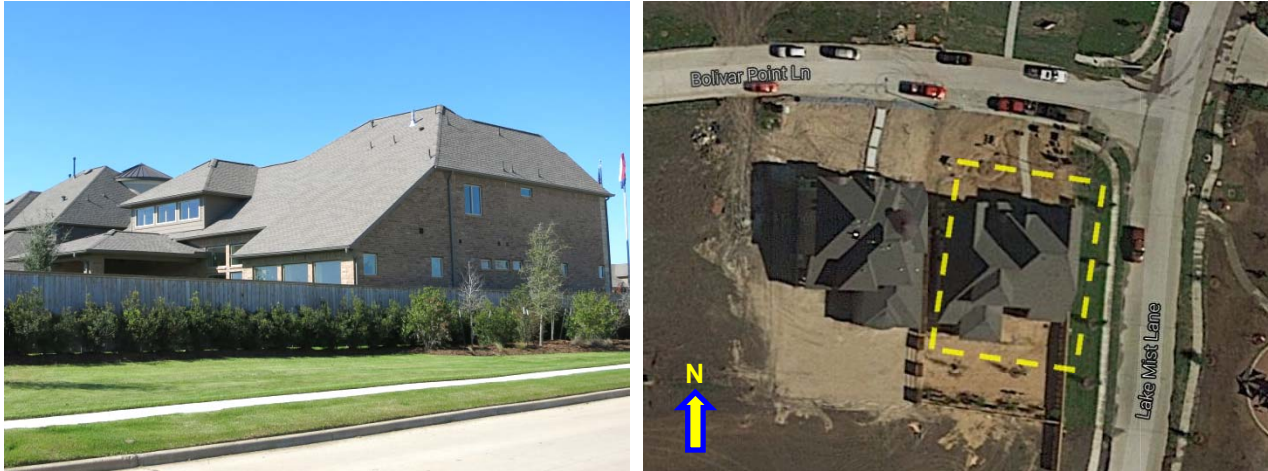


Figure 91: Rear quarter and overhead views of Houston-area test house

7.2 Unvented Roof Assembly and Geometry

The test house was configured with an unvented/sealed attic, insulated at the roofline. Unlike the cold-climate roof, the entire roof was insulated with a single material (spray-applied/adhered fiberglass; Johns Manville Spider[®] Spray-in Custom Fiber Glass Insulation System, 1.8 pounds/cubic foot density). The roof assembly section consists of asphalt shingles; underlayment (#15 asphalt saturated felt); 7/16" OSB sheathing, and spray-applied fiberglass at R-38 (9 in. @ R-4.2/in.), encapsulating the 2x8 (typical) rafters (Figure 90). No interior finish or air barrier material was installed; the fiberglass was left exposed inside the attic.



Figure 92: Interior of spray-applied fiberglass insulation in conditioned attic

At roof-to-wall connections, closed-cell spray foam was used to transition the air barrier from the roof sheathing to the wall, prior to roof deck insulation installation (Figure 93).



Figure 93: Spray foam used for roof-to-wall air barrier connection

The roof extends over the garage (normally unconditioned, but conditioned as a sales office at the model). The garage roof was insulated at the roofline and the floor of the attic, bringing the entire attic into the conditioned space (rather than dividing the attic into sealed vs. vented portions, with more complicated detailing), per Figure 94, left.

At the large porch overhang at the rear of the house, the porch roof was built as unconditioned space, outside of the sealed conditioned attic. Therefore, a short wall was built, insulated, and air sealed to separate the two areas, as shown in Figure 94, right. The attic over the porch was equipped with soffit vents, to connect it to the exterior.

No intentional dehumidification or space conditioning was provided in the unvented attic space. The space “floats” at conditions between interior setpoint and exterior conditions, which is common for this type of roof assembly. Operating conditions were monitored, and are a function of duct leakage, air leakage connection to the interior space, and air leakage from the attic to the exterior.

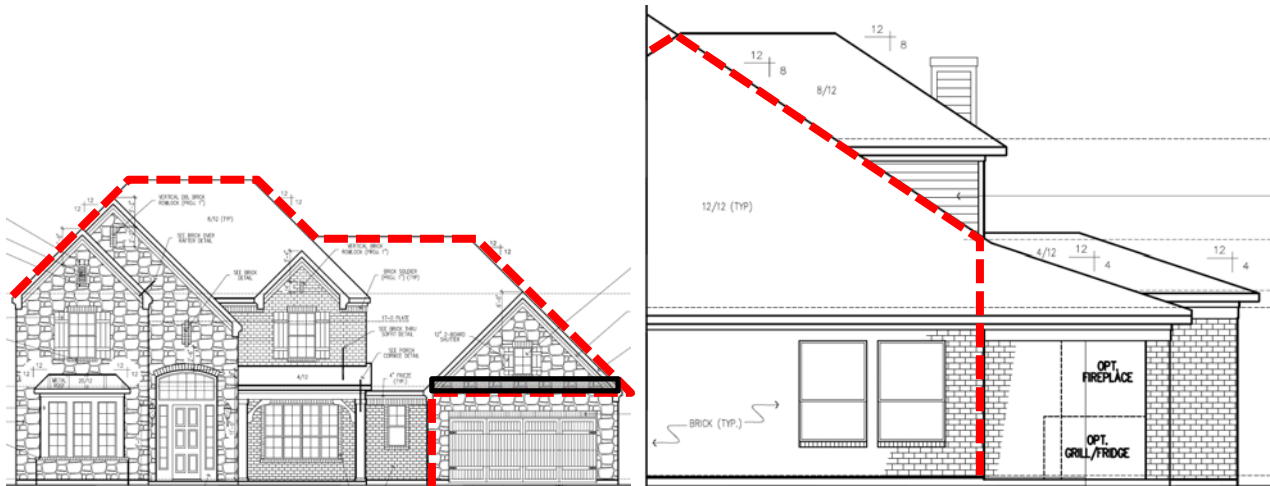


Figure 94: Air barrier/conditioned space line for unvented attic, front (L) and side (R)

7.3 Diffusion Port Assembly

The experimental roof assembly at this site is a “diffusion vent” detail, which allows for vapor diffusion drying at the ridge and tops of hips, while still functioning as an air barrier. The detail is used at the peak of the roof rafter bay cavities (at both the ridge and hip conditions), as shown in Figure 95; it was not used at the roof valleys.

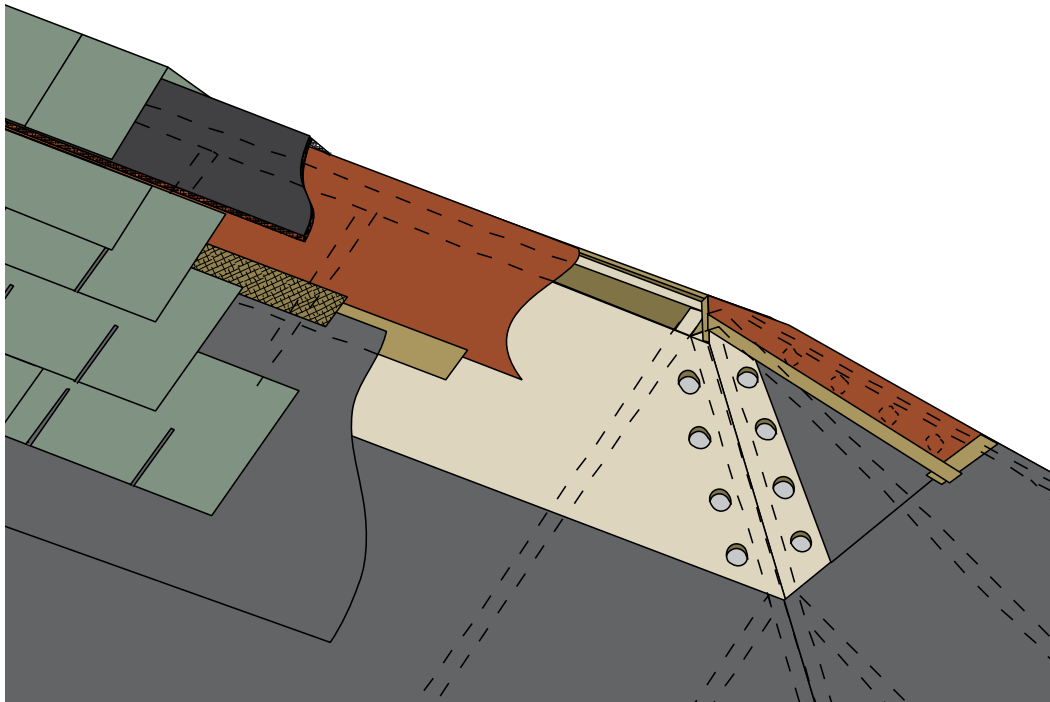


Figure 95: Diffusion vent design at roof ridge and hip

The components and details at the diffusion vent are the following:

- “Diffusion ports” are created at the ridge and hip of the roof:
 - At the ridge, a ± 3 in. strip of roof sheathing is omitted on each side, similar to a typical detail for a ridge vent. This leaves an opening of ± 2 in. on either side of the ridge beam (Figure 96, left).
 - At the hips, a series of 2 in. diameter holes were drilled in the roof sheathing at the top 2-3 ft. of the hip. The structural engineer did not accept the omitted sheathing detail at the hips, stating that a structural connection was required at the hip rafter. However, he accepted the drilled hole detail (Figure 97, left).
- The diffusion ports are covered with a strip of a highly vapor permeable roof membrane (tear-resistant polyethylene terephthalate/PET fabric with a diffusive, waterproof dispersion coating; 214 perms dry cup, 550 perms wet cup); this material is Cosella-Dörken Delta-Foxx (Figure 96, right, and Figure 97, right).



Figure 96: Open ridge (“diffusion port”) detail (L); permeable membrane applied over ridge (R)



Figure 97: Hip “diffusion port” drilled hole detail (L); permeable membrane applied at hips

- The edges of the permeable roof membrane are taped to the OSB roof sheathing to create an air barrier (while allowing vapor diffusion). Based on multi-substrate adhesion testing (Holladay 2013), a high performance acrylic adhesive flashing tape (3M 8067 All Weather Flashing Tape) was used.
- The field of the roof is dried in using the builder's typical underlayment for asphalt shingles (#15 asphalt saturated felt).
- The top edge of the roof underlayment creates a reverse lap situation (for bulk water drainage) at the intersection with the permeable roof membrane. This is addressed by taping the connection (with the same acrylic adhesive flashing tape; see Figure 95).
- The asphalt shingles are installed on the roof as per typical practice.
- The ridge is covered with a typical attic ridge exhaust vent material, which is in turn covered by ridge cap shingles (Figure 98).



Figure 98: Venting detail at ridge (L) and hip (R), showing vent profile

As a control comparison, some portions of the roof were built as typical unvented roofs, which experienced failures in Houston in previous work (see Section 2.2). Vapor-impermeable membrane (self-adhered bituminous roofing membrane) was installed over the ridge at these portions, rather than the diffusion port detail. These areas are shown on the roof plan in Figure 100. The goal was to demonstrate whether failure occurs at the control roof, and then whether the experimental (diffusion vent) roofs have sufficient drying to avoid failure.

7.4 Roof Monitoring Setup

The roof plan of the test house is shown in Figure 100, with the ridges, hips, and valleys marked, and roof slopes shown by blue arrows (pointing uphill). The areas that were constructed as typical unvented roofs (no diffusion port) are shaded.

The measurement locations are also shown in Figure 100: the instrumentation was set up to capture a sampling of orientations and roof assembly types. Typically, there is a ridge “package” of several sensors (orange stars in Figure 99); this sensor package is concentrated at the ridge due to the typical accumulation of moisture at the peaks. The notation in the figure calls out DV (diffusion vent) and UV (conventional unvented) monitoring packages.

The ridge monitoring “package” is shown in Figure 99, Figure 101, and Figure 102. Sheathing moisture contents were measured as high as practical (on both orientations), near the top edge of the roof sheathing. In addition, at the ridge top, a temperature/relative humidity sensor and moisture content “wafer” (small wood sample measured for moisture content, to act as a surrogate humidity sensor; see Ueno and Straube 2008) are installed. Finally, the sheathing moisture contents were measured on both orientations, roughly 16 in. downhill from the ridge, to capture the extent of the wetting.

In addition, at each bay with a ridge “package,” sheathing temperature and moisture content are measured downslope (in the same rafter bay at the sheathing), in one or two locations (blue squares in Figure 99). This measures moisture accumulation in the rafter bays with the same condition, but lower on the roof. The number of “lower” roof sheathing MC sensors is based on roof geometry (length of unobstructed rafter bays).

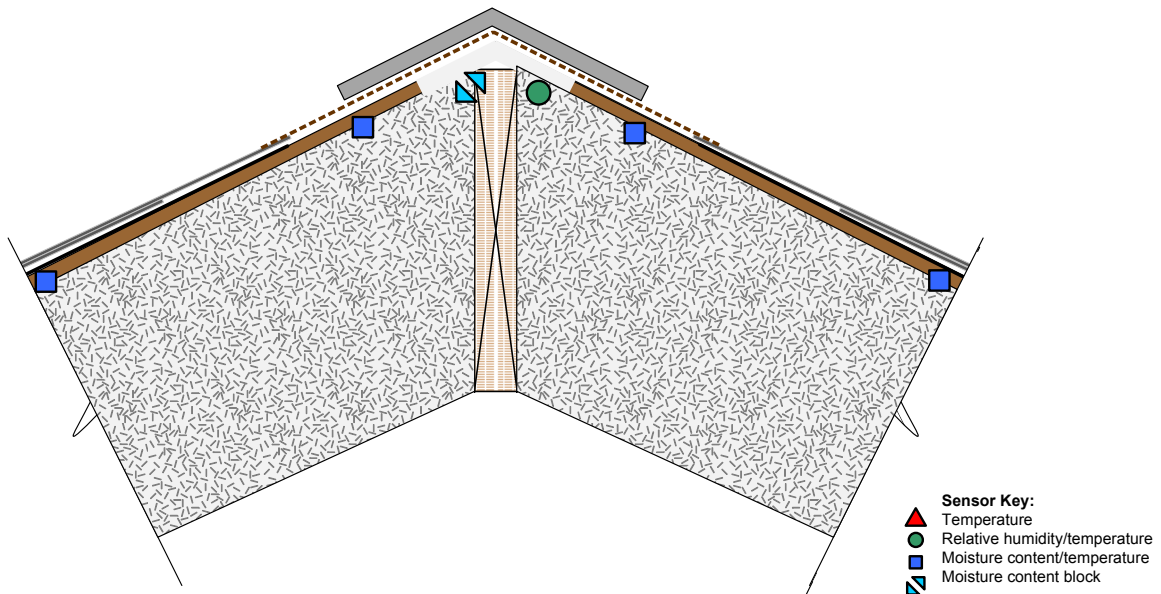


Figure 99: Ridge monitoring “package” (sensors at ridge and hip peaks)

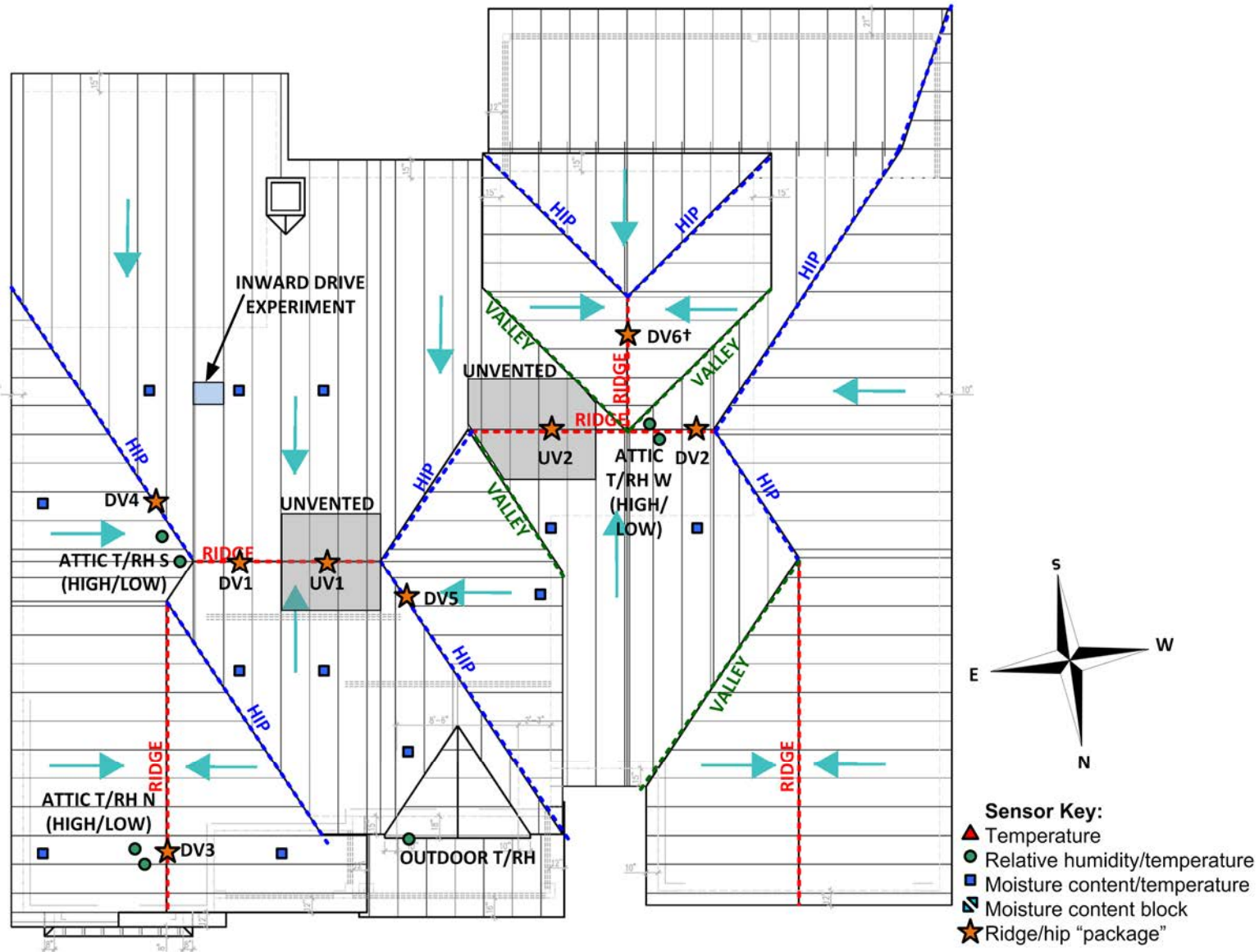


Figure 100: Houston roof plan, showing ridges, hips, and valleys, and measurement locations



Figure 101: Typical ridge monitoring package, with sensors highlighted



Figure 102: Ridge sheathing T/MCs and T/RH (L); ridge T/MC and wafer sensor (R)

Attic (i.e., interior) temperature and RH are measured at three locations in the sealed attic (Figure 103, left, and green circles in Figure 99); measurements are paired high and low, to capture the effects of thermal and/or moisture stratification in the attic space. Interior main space T and RH are measured at a sensor in the return duct of the space conditioning system, near the interior grille. Exterior T and RH are also measured on site, with a sensor mounted under the north soffit (Figure 103, right).

Measurements are taken at five-minute intervals, and averages are recorded on an hourly basis. Data are periodically downloaded remotely via cellular modem, to ensure data collection quality.



Figure 103: Interior attic temperature/RH sensor (L); exterior T/RH sensor under north soffit (R)

7.5 Inward Vapor Drive Experiment

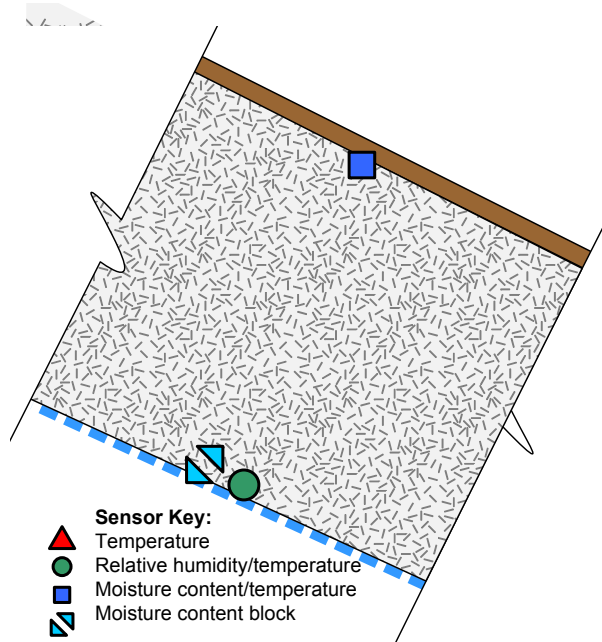
Water accumulating in shingle laps (due to capillarity) and inward solar moisture vapor drives have been considered as a contributor to attic humidity problems. This mechanism was discounted by hygrothermal modeling by Boudreaux et al. (2013), and by a field comparison of underlayments by Lstiburek (2014). However, given this opportunity, the issue was studied further with a small sub-experiment, described below.

A 2 ft. by 2 ft. section of a south-facing roof rafter bay was isolated using 1 in. extruded polystyrene foam blocking (Figure 104, left), covered with construction/ housewrap tape (polypropylene film tape with an acrylic adhesive), to reduce its vapor permeance. The foam was then air sealed to the adjacent rafters with both caulk and tape.

After insulation, the interior side was covered with a layer of 0.093 in. clear acrylic plastic (“plexiglass”) and sealed at the perimeter with flashing tape (Figure 104, right), to isolate the test area in an airtight manner. The acrylic plastic was added partway through the experiment; the date is indicated on subsequent graphs.



Figure 104: Inward drive “box” before insulation (L); after insulation and clear plastic cover (R)



The sensors installed within the isolated area are shown in Figure 105; they were:

- Roof sheathing MC and T (exterior side of cavity)
- Insulation-to-acrylic plastic RH and T (interior side of cavity)
- Insulation-to-plexiglass (acrylic plastic) wafer sensor (interior side of cavity)

Figure 105: Inward drive sensor package

The intent of this monitoring was to capture moisture driven through the exterior side of the assembly (shingles, underlayment, and sheathing) into the isolated area. Inward-driven moisture would tend to accumulate at the insulation-to-acrylic plastic interface; the accumulation would be measured the T/RH and wafer sensors. Sheathing MC is measured to determine whether moisture within the system increases over time, as moisture is driven from one side to the other seasonally.

This experiment is not intended to capture any diurnal or seasonal increase of moisture contents (i.e., “ratcheting”) due to increasing storage of interior-sourced moisture in the sheathing. Instead, it is intended to capture inward-driven moisture only from the exterior source, due to the “closed” system.

The initial sheathing moisture content was measured with a handheld meter (Tramex Moisture Encounter) at 8-9% MC.

7.6 Roof Air Leakage and Pressure Testing

Air leakage (blower door) and duct leakage testing were initially conducted by a third party rater, as part of the builder’s quality control process. The results are summarized in Table 8.

Table 8: Third party air leakage and duct leakage test results

Measurement	Value	Normalization
Enclosure air leakage	1993 CFM @ 50 Pascals	-
Volume-normalized leakage	2.8 ACH 50	42,910 cubic ft. volume
Area-normalized leakage	0.21 CFM 50/sf enclosure	9550 sf surface area

Measurement	Value	Normalization
System 1 Duct Leakage (Total)	179 CFM 25 (4.5% of floor area)	3981 sf conditioned floor area
System 1 Duct Leakage (to Exterior)	119 CFM 25 (3.0% of floor area)	3981 sf conditioned floor area

This was followed by the research team’s detailed air leakage measurements of the attic, main space, interconnections, and localization of air leakage.

Multipoint air leakage testing was conducted in the finished house (Figure 106 left), with the attic hatch either open or closed. The results of this testing are shown in Figure 106 (right) and Table 9.

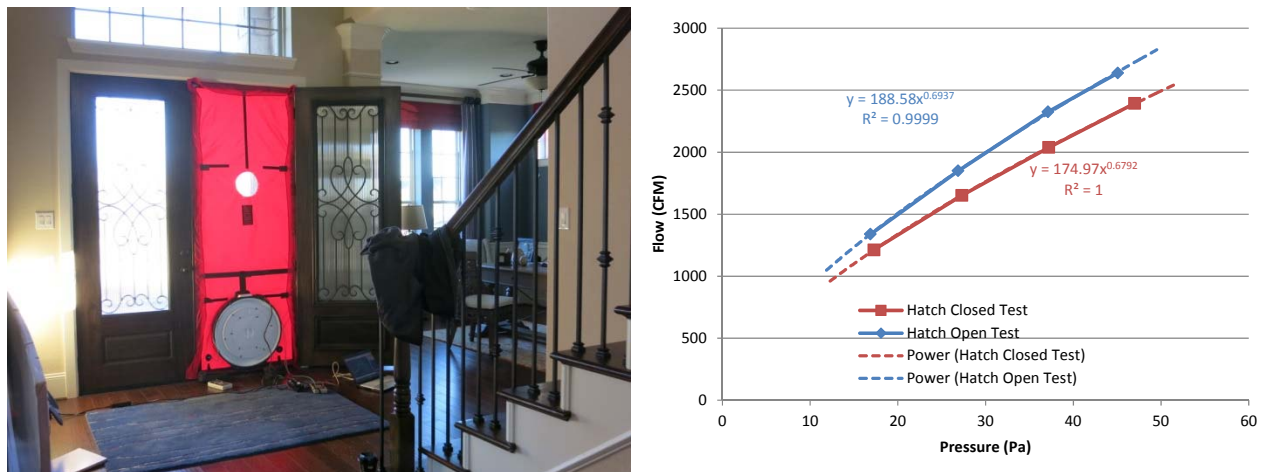


Figure 106: Air leakage (blower door) testing (L); multipoint hatch open/closed results (R)

The air leakage measurements are normalized based on an area/volume takeoff that includes the entire attic, assuming 11,594 ft² surface area and 67,876 ft³ volume. Results are shown normalized by volume (ACH50), surface area (CFM50/sf enclosure area), and stated in terms of Equivalent Leakage Area/EqLA, in square inches.

Table 9: Houston test house hatch open and closed air leakage measurements

Test	C	n	CFM 50	ACH 50	CFM50/sf	EqLA (sq. in.)
Hatch Closed	175.0	0.68	2494	2.2	0.22	257
Hatch Open	188.6	0.69	2846	2.5	0.25	293

Opening the hatch resulted in an increase of air leakage of 14%, or a relatively small amount. In either case, air leakage was less than 0.25 CFM50/sf, and below 2.5 air changes per hour at 50 Pascals (half or less than the 5.0 ACH50 requirement in the 2012 IECC, for Climate Zones 1 and 2).

The pressures across closed hatches (to the three sub-attics) were measured with the main space at -50 Pa, to demonstrate relative leakage connection to interior vs. exterior (Table 10). The

attic-to-exterior pressure drop was 76-86% of the total, which is consistent with the hatch open/closed results (i.e., relatively tight attic).

Table 10: Houston test house hatch open and closed air leakage measurements

Location	ΔP (Pa)	% Interior	% Exterior
Main attic over 2 nd floor	11.8	76%	24%
Rear attic over MBR	7.1	86%	14%
Attic over garage/sales office	12.2	76%	24%

The main attic hatch open/closed test and pressure measurements were used as inputs for zone pressure diagnostic or “add a hole” testing (per Bohac 2002), shown in Table 11. However, results had very a high uncertainty (see minimum vs. maximum in Table 11). The relative leakage areas from attic to exterior vs. interior are consistent, though. The team also attempted a guarded/nulled test, but the results were inconclusive and are not presented here.

Table 11: Houston test house zone pressure diagnostic (ZPD) calculation results

Metric	Minimum	Maximum	Units
House to attic leakage	1173	3247	sq. in.
Attic to exterior leakage	415	821	sq. in.
Leak ratio	2.8 : 1	4.0 : 1	-

The attic and main space were examined with an infrared camera during depressurization, in an attempt to localize air leakage. Exterior conditions were cold (40-45°F/4-7°C) during this test, so exterior air leakage was evident as cold areas or plumes.

Overall, the roof plane was relatively airtight; few thermal anomalies were seen at the roof plane, except for uninsulated or unsealed gas appliance exhausts.

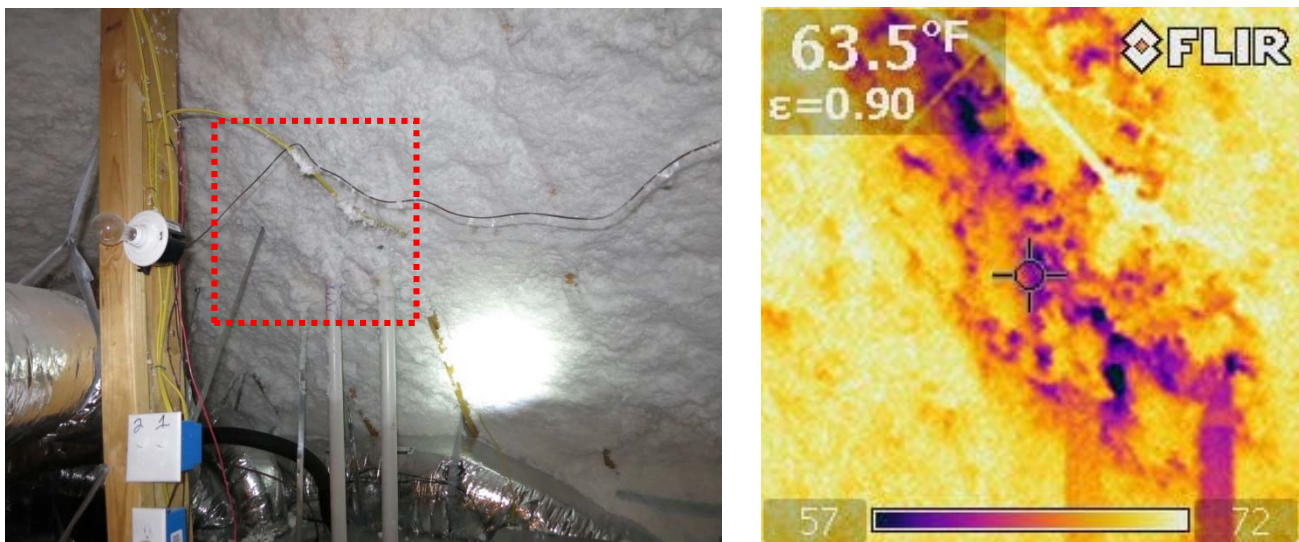


Figure 107: Unsealed gas appliance exhaust/intake, with evidence of air leakage

The roof peaks were examined for any sign of air leakage at the diffusion vent details; no evidence was found. However, leakage often occurred at transitions and connections between roofs and walls, especially at complicated details with multiple intersecting planes. For instance, leakage was evident at dormer and gable end intersecting planes at the front of the house (Figure 108 and Figure 109), and roof-wall connections at the rear of the house (Figure 111). These and the following leaks are keyed to Figure 110.

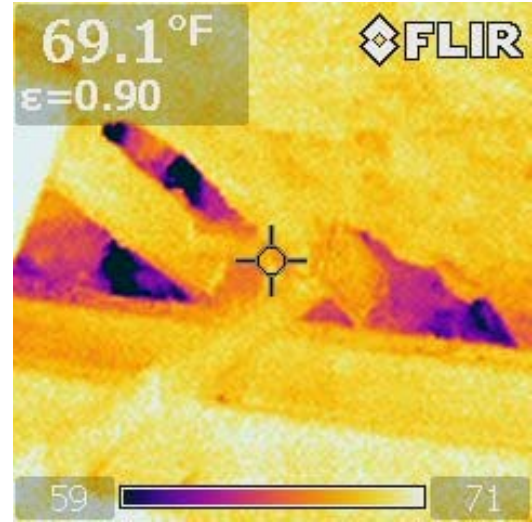


Figure 108: Air leakage at roof-to-wall details at dormer/intersecting roofs (Location A)

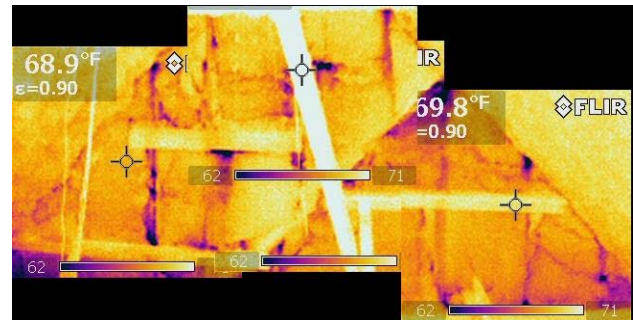


Figure 109: Air leakage at front attic gable end (Location B)

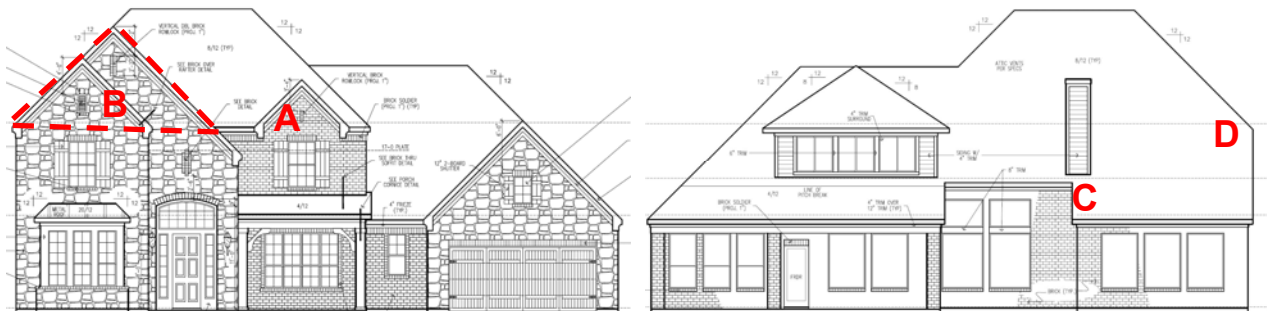


Figure 110: Front and rear elevations, showing air barrier failure locations

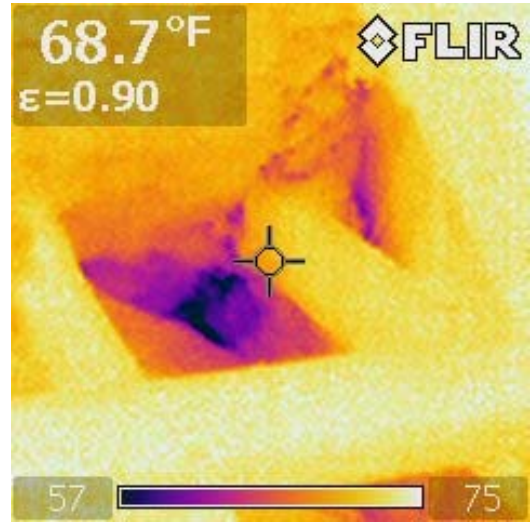


Figure 111: Air leakage at roof-to-wall details at roof-wall intersection (Location C)

Noticeable leakage was found at top of roof-wall intersection at small rear attic over master bedroom, at an interior-to-attic wall (Figure 112). This occurred despite the use of closed cell spray foam to seal these connections; apparently, not all key areas were sealed.

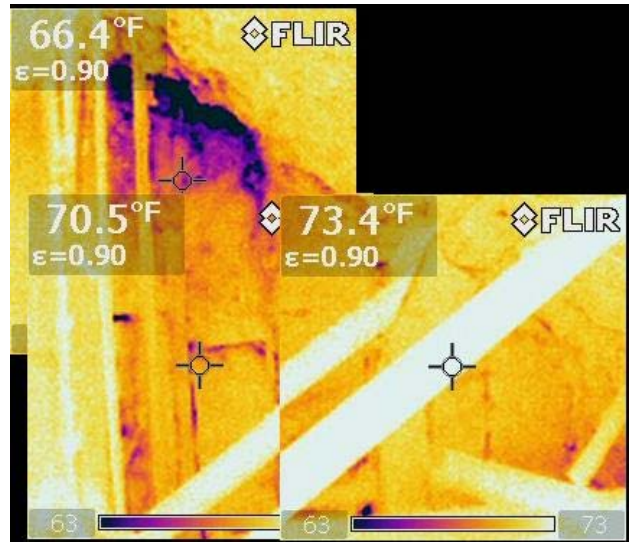


Figure 112: Air leakage at rear attic over master bedroom (Location D)

Observations from below corroborated that air leakage was occurring at roof framing connections/penetrations, at the roof-to-wall connection (Figure 113 and Figure 114).

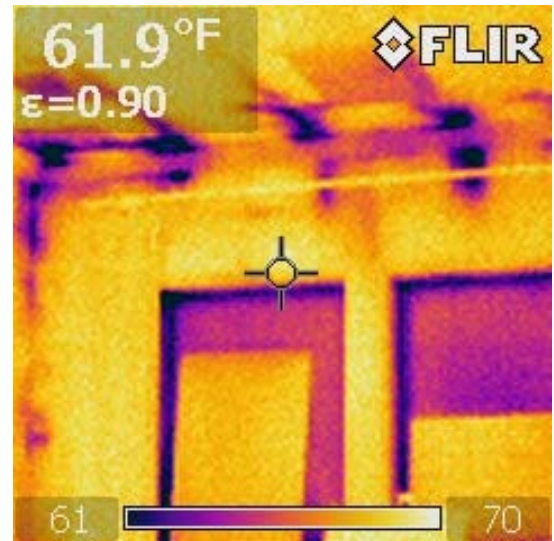


Figure 113: Air leakage at roof-to-wall connections, from interior space (first floor)

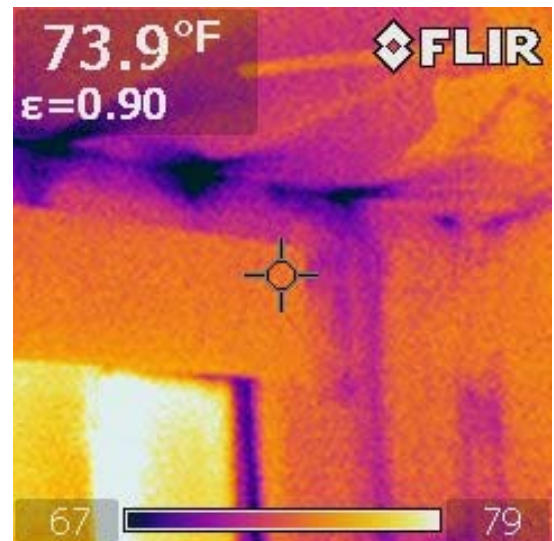
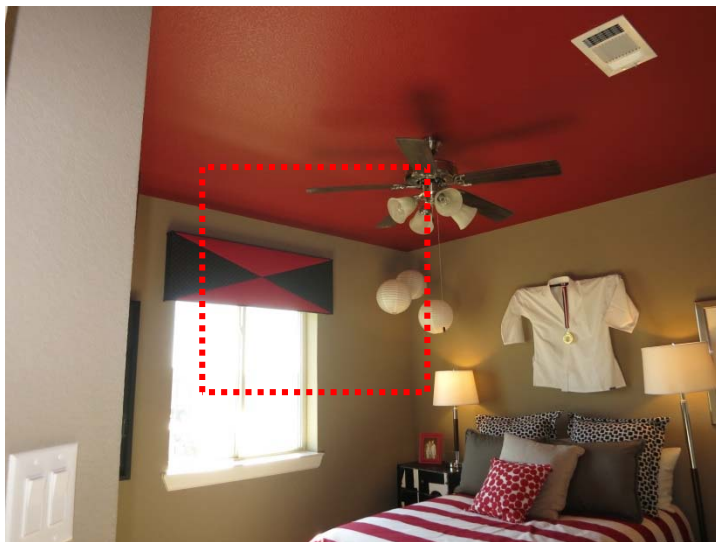


Figure 114: Air leakage at roof-to-wall connections, from interior space (second floor)

8 Hot-Humid Climate (Houston) Monitoring Results

8.1 Boundary Conditions

Data have been collected from February 2014 through June 2015 (16 months); data were not collected from mid-February 2014 through late March 2014, due to site power availability. Interior and exterior temperatures are plotted in Figure 115. Exterior temperatures include site-measured, and airport (Houston Hobby/KHOU) data. Interior temperatures include six conditioned attic measurements, at three pairs of vertical “stacks,” and main space (HVAC return) conditions (“Interior Downst.”).

The temperature excursion in mid-November 2014 during cold exterior conditions appears to be an interior setpoint issue; later winter data at similar exterior temperatures show warmer interior conditions.

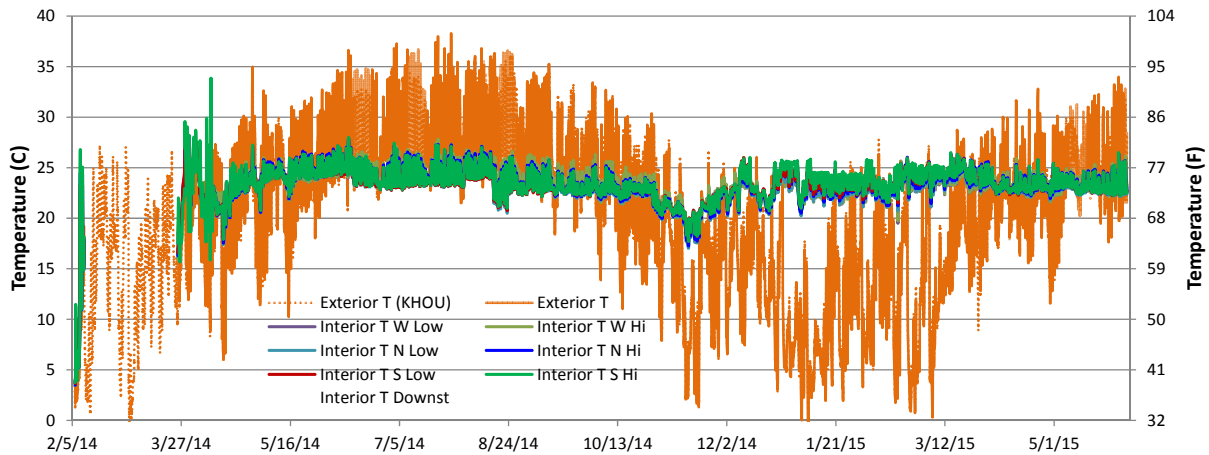


Figure 115: Houston exterior, attic, and main conditioned space temperatures

Monthly HDD and CDD data for Houston are plotted in Figure 116; recent data are close to climate normals. 2014 HDD were 2% higher than normal, and 2014 CDD 5% higher than normal. The past 12 months were 96% of normal HDD, and 110% of normal CDD.

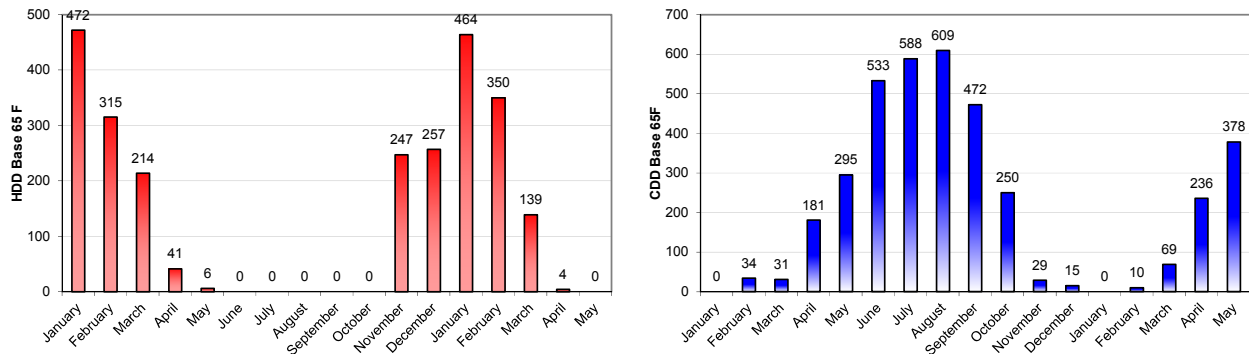


Figure 116: Heating degree days (L) and cooling degree days (R) for Houston (IAH airport)

Attic/interior summertime temperatures for two weeks in July 2014 are shown in Figure 117; conditioned attic temperatures are warmer than interior/return conditions, but still closer to interior temperatures than outdoors (typically daily cycles between 73-81°F/23-27°C, with the interior 73-75°F/23-24°C).

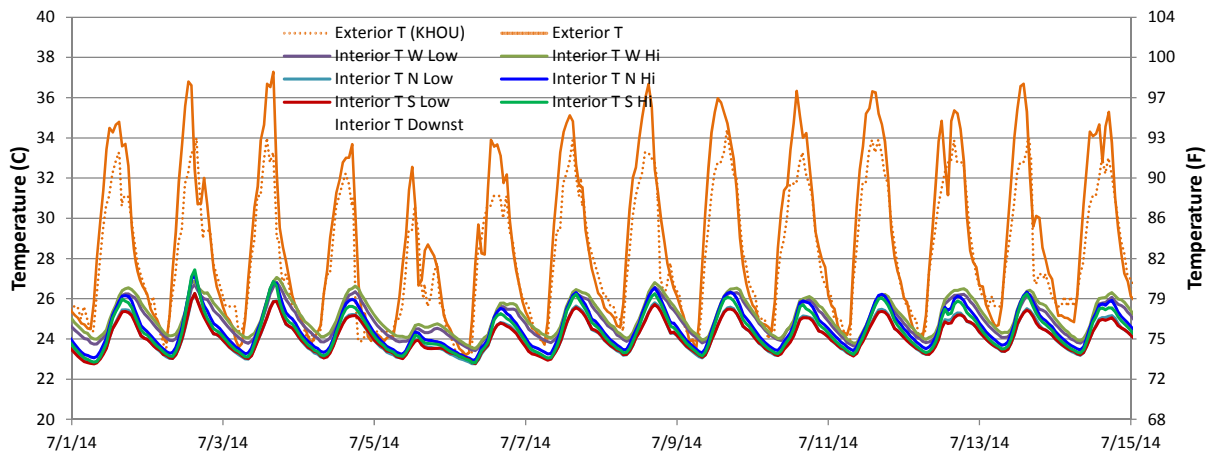


Figure 117: Houston temperatures, summertime (July 2014) detail

There are differences between conditioned attic temperatures; the west side sensors (both high and low) are the warmest, and are the slowest to cool in the afternoon/evening. This could be explained by the placement near the west face of the attic space (which has afternoon solar gain; Figure 119). These temperatures might also show the relationship between duct leakage, thermal coupling to the interior space, and heat gain/loss from the exterior. The next two warmest are the north and south “high” sensors; which is consistent with temperature stratification.

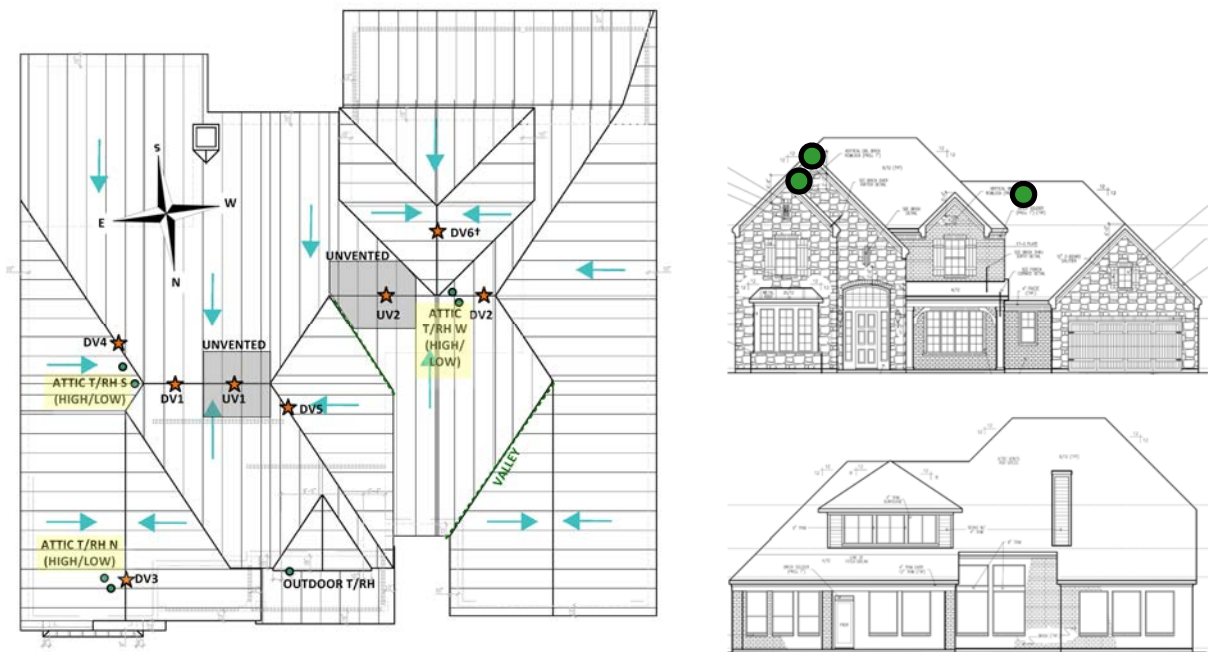


Figure 118: Attic T/RH locations highlighted in plan (L) and front/rear elevations (R)

There is a difference of roughly 2°F/1°C between the warmest and coolest temperatures. The conditioned attic sensors were installed at roughly the 1/3 and 2/3 points of the attic height, so they do not capture the extremes of stratification.

A similar plot for wintertime conditions (two weeks in January 2015) is shown in Figure 119. Interior temperatures clearly show a nighttime setback schedule. The main space conditions are typically warmer than the conditioned attic space, which is expected given minimal conditioning in the attic (duct leakage only; no intentional supply). The coldest temperatures are west high and low, followed by north low; the maximum difference is roughly 4°F/2°C. The west sensors are the outliers in both heating and cooling seasons, so temperature differences are likely explained by the ratio of incidental space conditioning vs. losses/gains to exterior.

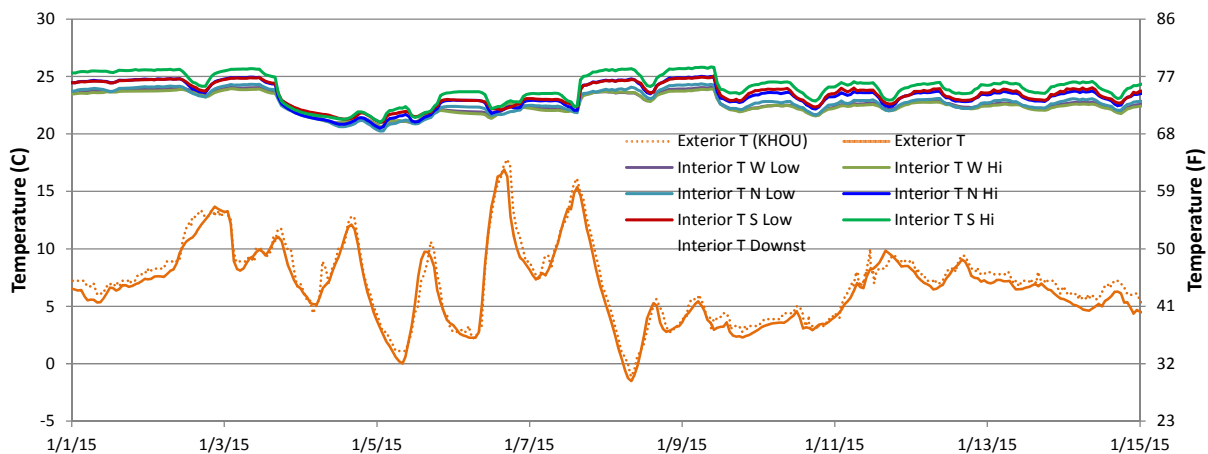


Figure 119: Houston temperatures, wintertime (January 2015) detail

Exterior and interior dewpoint (absolute air moisture content) conditions are shown in Figure 120; similar to temperatures, conditioned attic dewpoints operate between interior and exterior conditions in the summer. In the winter, interior dewpoints roughly track outdoor conditions (extremes are damped by house airtightness). There is no interior moisture generation, because the house is an unoccupied model.

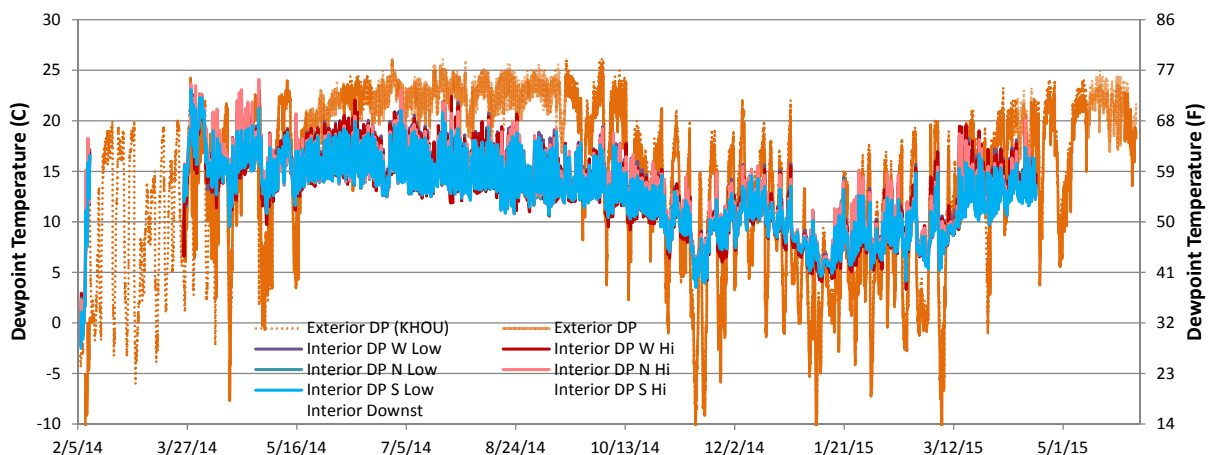


Figure 120: Houston exterior, attic, and main conditioned space dewpoint temperatures

Attic/interior summertime dewpoint temperatures for two weeks in July 2014 are shown in Figure 121; interior main space dewpoints remain at a relatively stable level (50-54°F/10-12°C dewpoint).

Attic conditions are wetter than interior (again, the space is not directly conditioned or dehumidified), with a strong diurnal cycle. The peaks occur in the 3-6 PM range, which is consistent with moisture adsorbed in sheathing being driven out by solar gain and dry bulb temperature difference. After sunset, the sheathing would tend to adsorb moisture from the air, pulling down dewpoint.

The data show stratification: the south high sensor shows the highest peaks, which is consistent with its location at the highest spot in the attic (Figure 118). North low and south low sensors showed the lowest peaks, again consistent with moisture stratification.

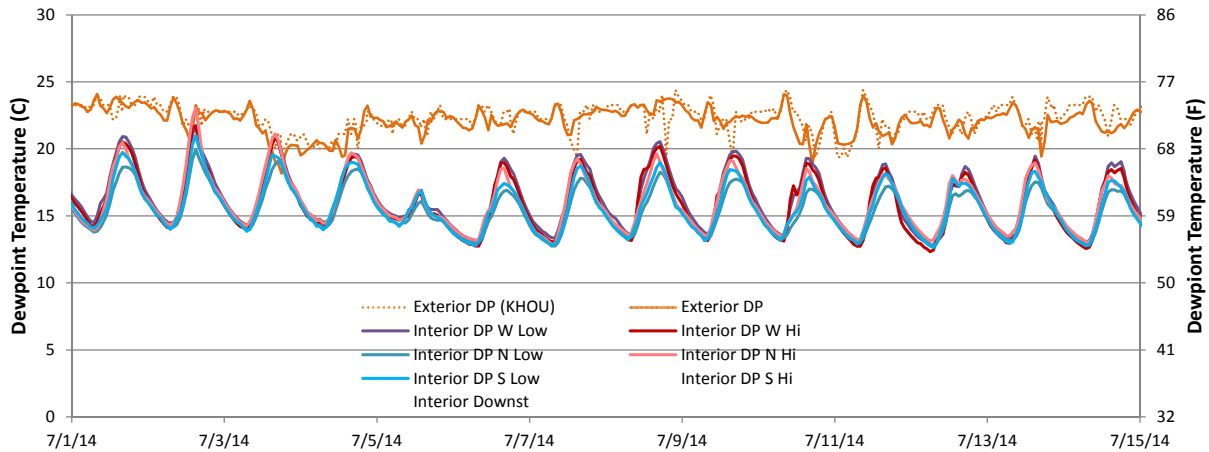


Figure 121: Houston dewpoint temperatures, summertime (July 2014) detail

Interior RH levels are shown in Figure 122; the initial data after the “gap” (semi-conditioned construction period) has very high RHs (60-90%), which is consistent with the moisture-generating construction activities (drywall mudding, interior painting) that occurred in the gap.

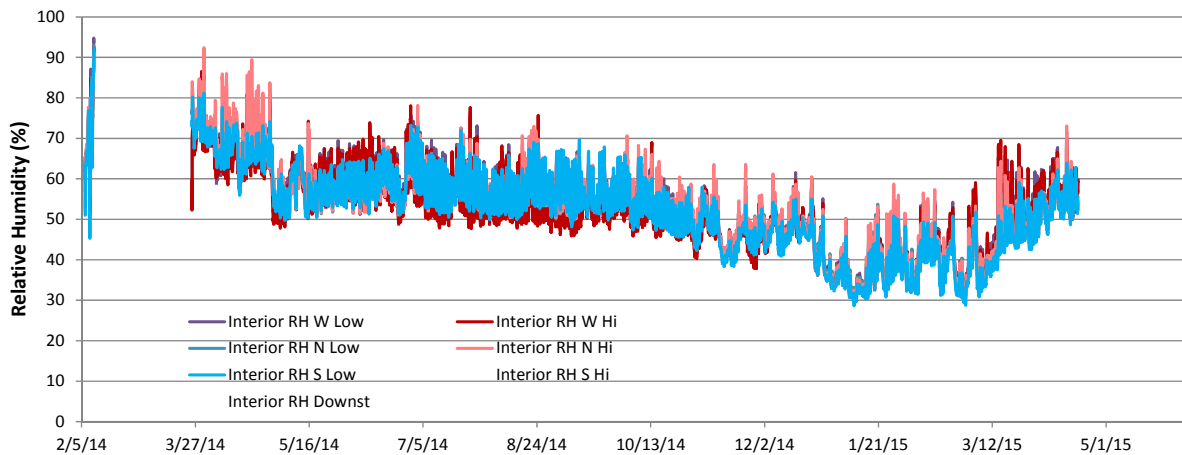


Figure 122: Houston attic and main conditioned space relative humidity

The high RH outliers in the early (March 2014) data are “south high” and “north high” attic sensors, which are consistent with previous dewpoint measurements and moisture stratification.

Space conditioning was run from May 2014 onward; the interior main space runs 45-55% RH in summer, and the attic cycling typically between 50-70%. Wintertime interior RHs are lower (30-50% RH typical), due to lower exterior dewpoint conditions, and lack of occupancy (interior moisture generation).

8.2 Unvented Roof Measurements

The following plots show roof sheathing and “wafer” sensor MCs (on the left hand axis), with peak RH (on the right hand axis). Results for the unvented (non-diffusion vent) roofs UV1 and UV2 are plotted in Figure 123 and Figure 124.

Unfortunately, a data logger failure occurred in April 2014, resulting in the loss of almost all of the RH and MC channels. The system will require a site visit for repair of the problems.

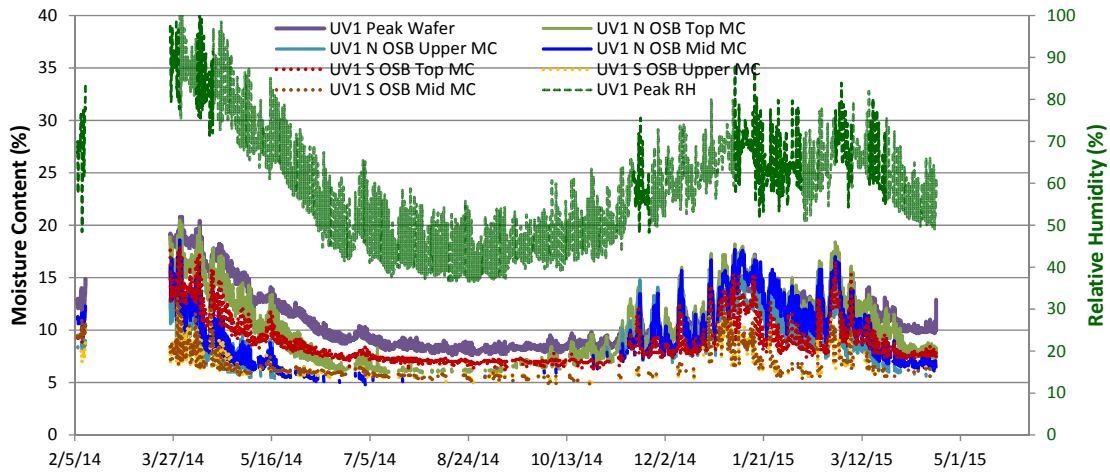


Figure 123: Unvented roof (UV1) roof MC and RH measurements

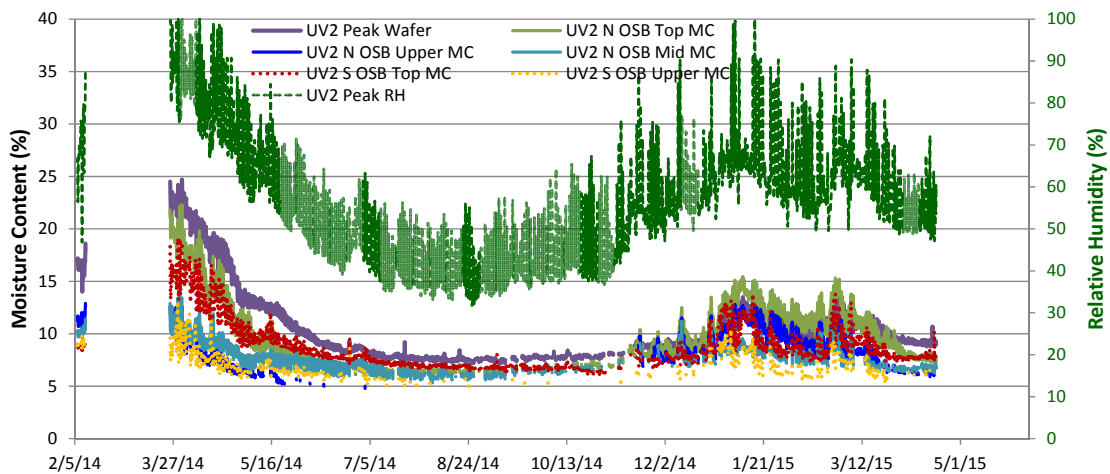


Figure 124: Unvented roof (UV2) roof MC and RH measurements

During the first winter (early 2014), the roof ridges/peaks clearly have high MCs and RHs, with RHs in the 80-100% range, and some MCs near or over 20%. Only the “falling” side of the peak MC/RH period was captured in data collection; the “rising” side occurring during the data gap from February-March). However, the trend in the gap is clear. The highest MC measurements were typically near the top of the roof assembly.

In the summer, as outdoor temperatures rose and the thermal gradient shifted inward, the RH and MCs both fell. Summertime peak RHs were in the 40-50% range. Wood MCs in the summer were consistently in the very dry/safe range (below 10%).

In the winter of 2014-2015, RH and MC measurements began to rise again, but not as high as the previous winter’s measurements. RHs had brief excursions above 80% in UV2, but they were rare. All MCs remained below 20% (below the threshold for mold growth).

8.3 Diffusion Vent Roof Measurements (Ridge)

The diffusion vent roofs were plotted in a similar manner, in Figure 125 (DV1), Figure 126 (DV2), Figure 127 (DV3), and Figure 128 (DV6). These roofs had a markedly different pattern than the unvented roofs: instead of a seasonal swing, the RH and MC measurements are relatively stable over the measurement period.

In the diffusion vent roofs, initial winter MCs and RHs are much drier (“safer”) than the unvented roof. Peak MCs remain well below 20%. However, summertime MCs are higher than in the unvented roofs. In winter 2014-2015, wood MC rose, but again well within the safe range (below 15%, typically). The highest MCs are typically towards the peak of the roof. Roof peak RH measurements cycle on a diurnal basis, with the majority of the readings in the 50-80% range. The diurnal RH cycling in the diffusion vent roofs is a greater range than that seen in the unvented roofs.

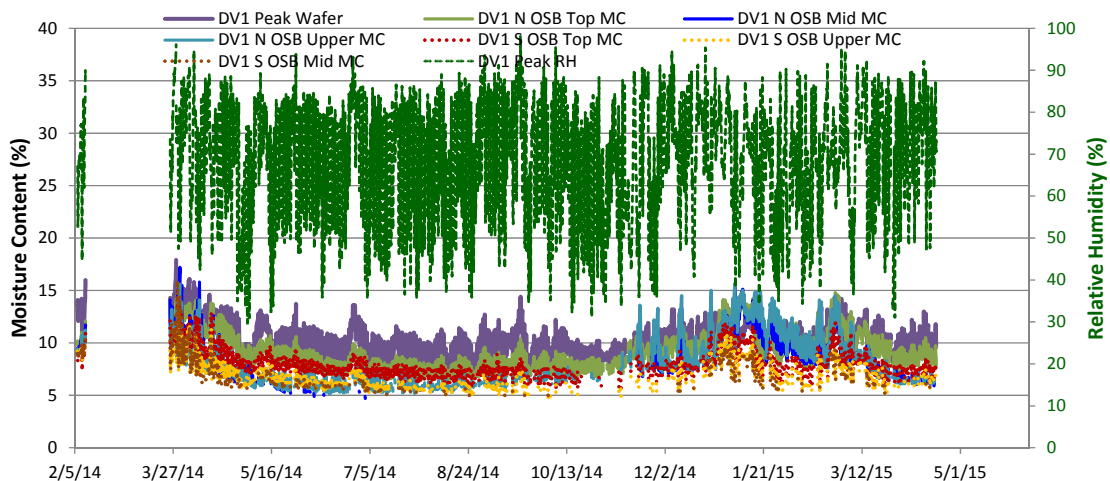


Figure 125: Diffusion vent (DV1) roof MC and RH measurements

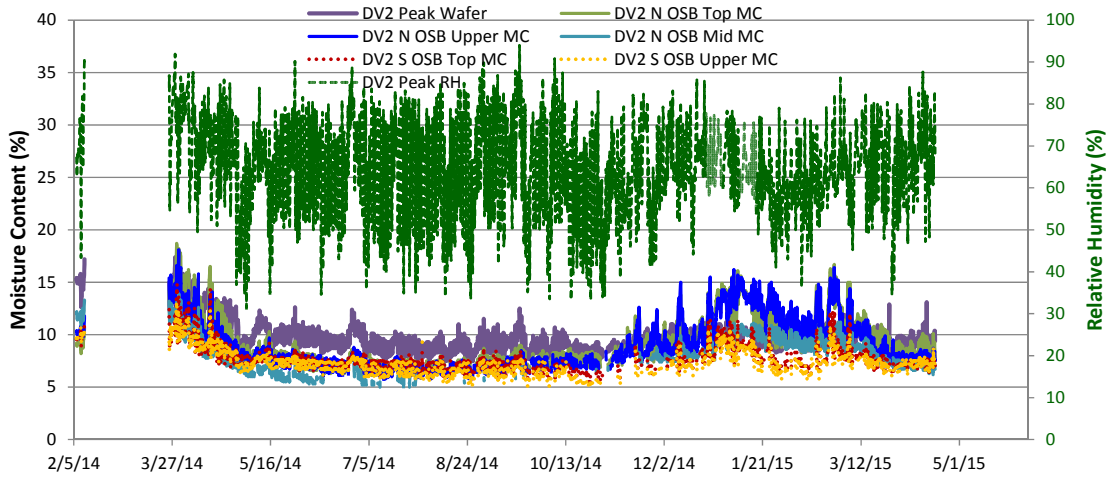


Figure 126: Diffusion vent (DV2) roof MC and RH measurements

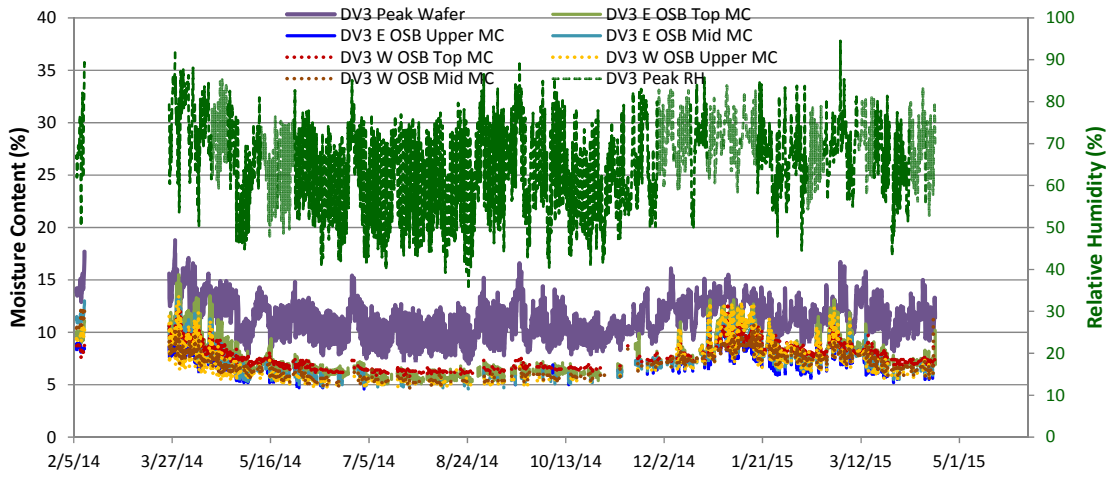


Figure 127: Diffusion vent (DV3) roof MC and RH measurements

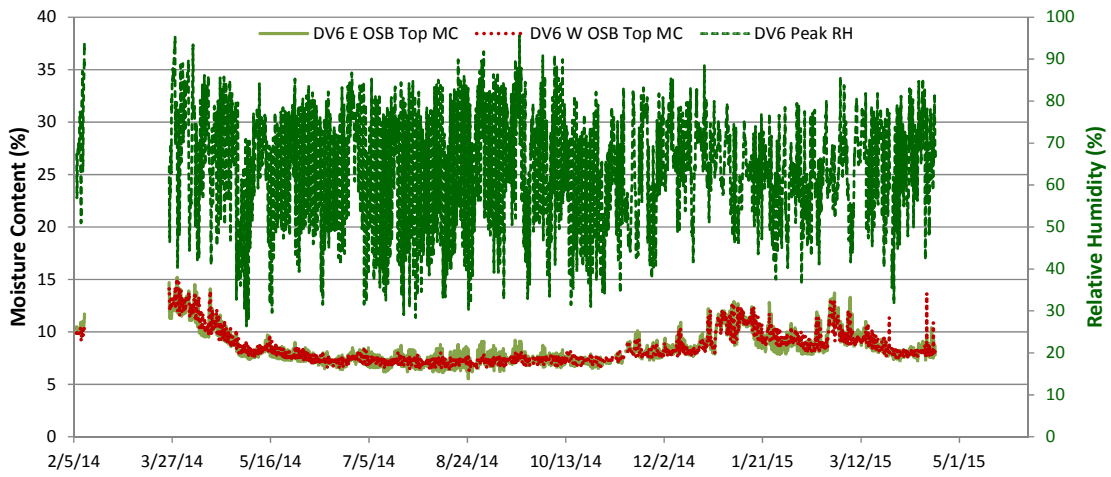


Figure 128: Diffusion vent (DV6) roof MC and RH measurements

The summertime diurnal pattern is shown in more detail in Figure 129, which plots two weeks from July 2014. The roof peak RH shows a consistent sawtooth pattern, with a slow rise, and a sharp fall on a daily basis. The drop in RH consistently occurs at 7 AM, which is consistent with morning solar warming of the roof. In the late afternoon (4-5 PM typical), RH starts to rise again, continuing to overnight until the morning.

The MCs have a similar type of sawtooth behavior, albeit over a much smaller range.

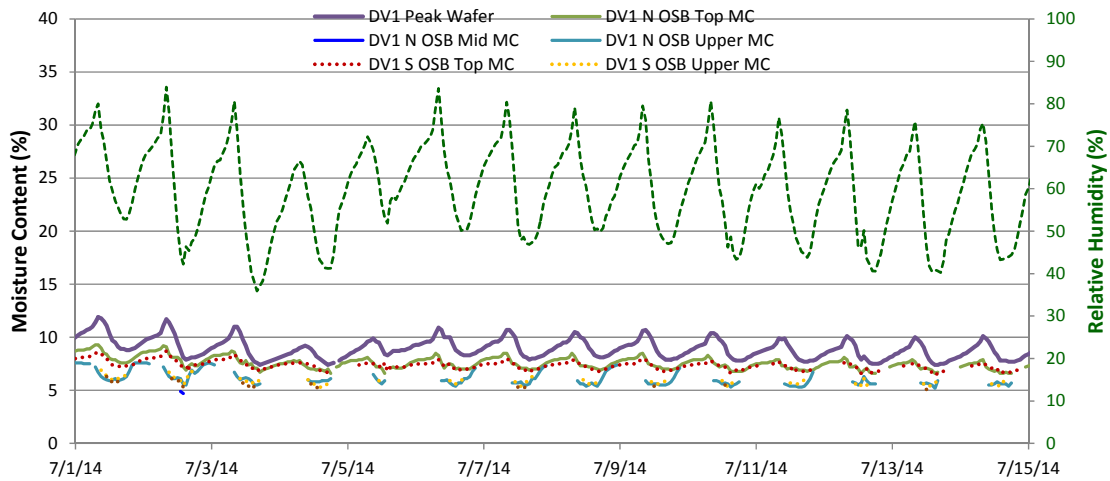


Figure 129: Diffusion vent (DV1) roof MC and RH measurements, summer (July 2014) detail

8.4 Diffusion Vent Roof Measurements (Hip)

Similar plots were generated for the diffusion vent roof detail at the hips, in Figure 130 (DV4) and Figure 131 (DV5). The hips are different from the ridge diffusion vents, due to the limited amount of diffusion vent area (2 in. diameter drilled holes near the peak).

These roofs exhibit behavior partway between the unvented and diffusion vent roofs. There is a noticeable seasonal swing in RH and MC, with the peaks in the winters. Similar to the unvented roofs, winter 2014-2015 peak RHs and MCs were much drier than the first winter.

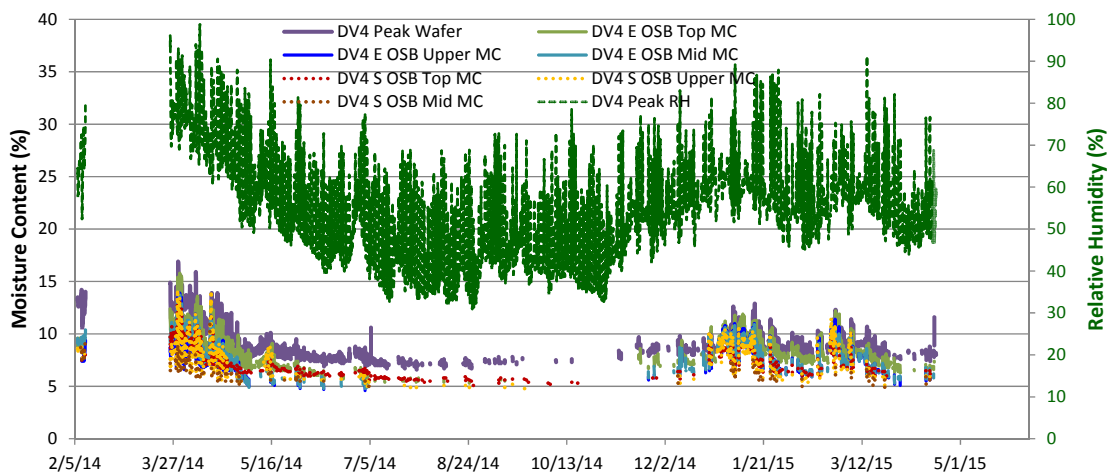


Figure 130: Diffusion vent at hip (DV4) roof MC and RH measurements

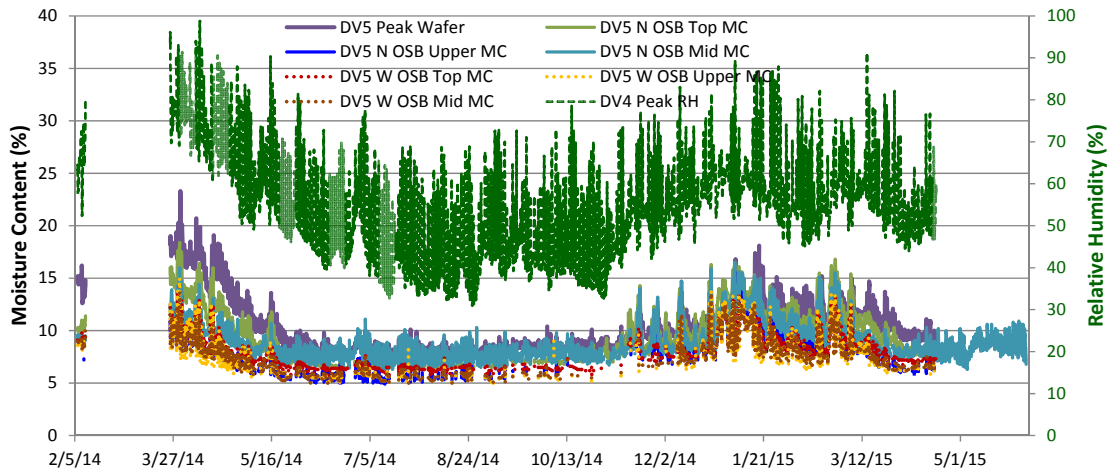


Figure 131: Diffusion vent at hip (DV5) roof MC and RH measurements

However, in the summer, RHs have a diurnal variation similar to the diffusion vent roofs, albeit a slightly lower range (40-70% RH vs. 50-80%).

Wood MCs remain mostly within the safe range, with excursions over 20% only occurring in one roof during the initial winter.

8.5 Inward Drive Experiment

The interior side RH and wafer MC for the inward drive experiment are shown in Figure 132, with exterior temperature for reference. The experiment was only put into operation in mid-April 2014, when the clear acrylic plastic cover was installed and air sealed (red dotted line), thus resulting in potential moisture accumulation. The RH and wafer MC rise after the installation of the clear plastic cover. Interior side RHs have peaks over 90% in the summer, but fall in the early winter when outdoor temperatures drop.

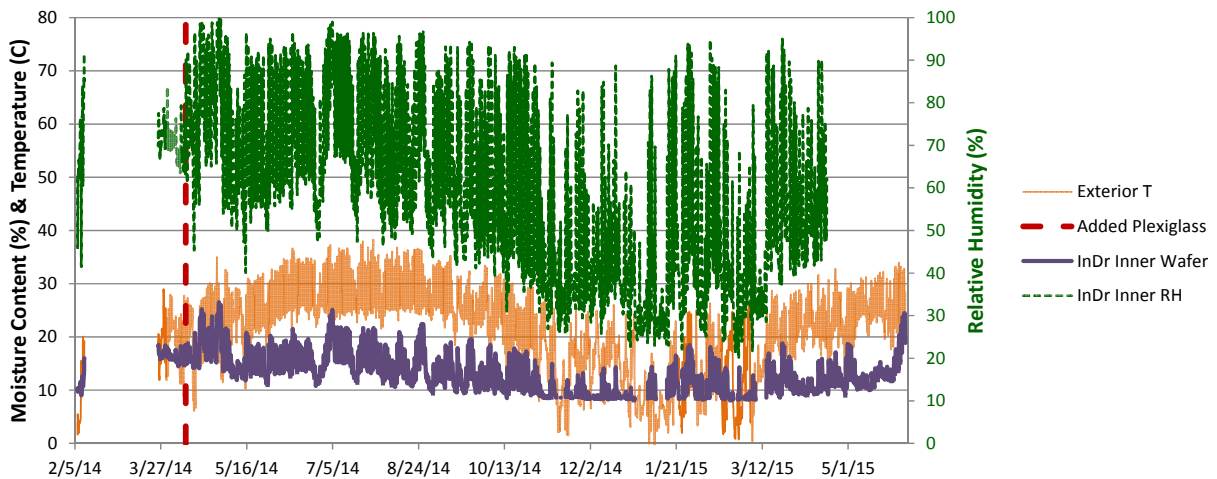


Figure 132: Inward drive interior-side RH and wafer sensor, with outdoor T

The interior side RH and wafer MC measurements move in parallel, as expected. In previous calibration (Ueno and Straube 2008), the “wafer” sensors come to equilibrium with 100% RH

conditions (air in closed container over water) at 28%–30% MC; immersing the sensors in liquid water increases MCs to the 40%–45% range. The wafer MCs remain below 28-30%, which indicates no condensation or 100% RH conditions (consistent with RH results).

The inward drive roof sheathing MC is plotted with other lower sheathing MCs (same south orientation, both unvented and diffusion vent) in Figure 133. The wafer MC and outdoor temperature are also plotted for reference. The sheathing MC in the inward drive experiment is consistent with the other sheathing MCs, which points away from accumulation of moisture within the sealed box.

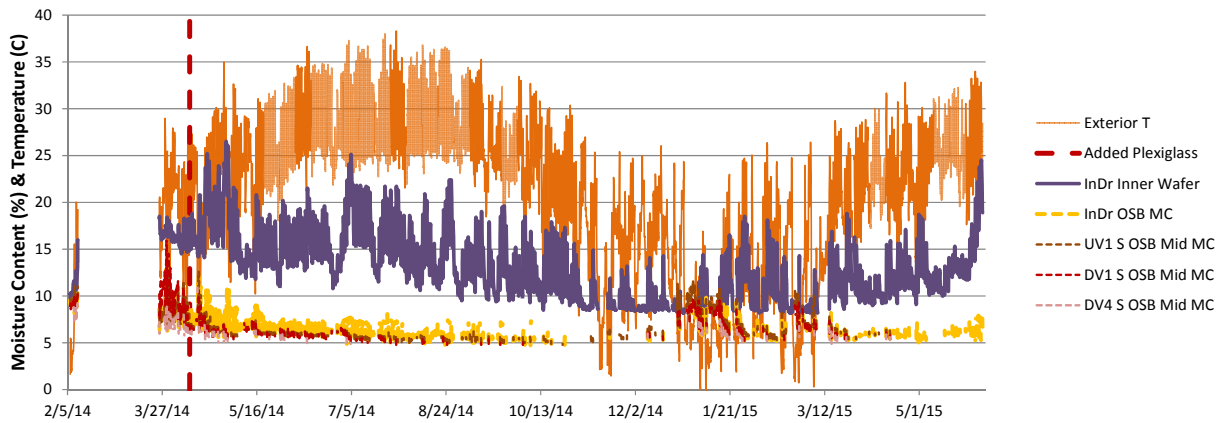


Figure 133: Inward drive wafer sensor MC and sheathing MCs, with outdoor T

The wafer MC (and RH) data were examined to see correlations could be found with exterior weather events. Comparisons with interior and exterior dewpoint showed minimal relationships. Precipitation was also plotted for correlation (Figure 134), given that wetted shingles are a suspected moisture source for inward drive. Although some wafer MC spikes correlated with precipitation, many other events were non-correlated.

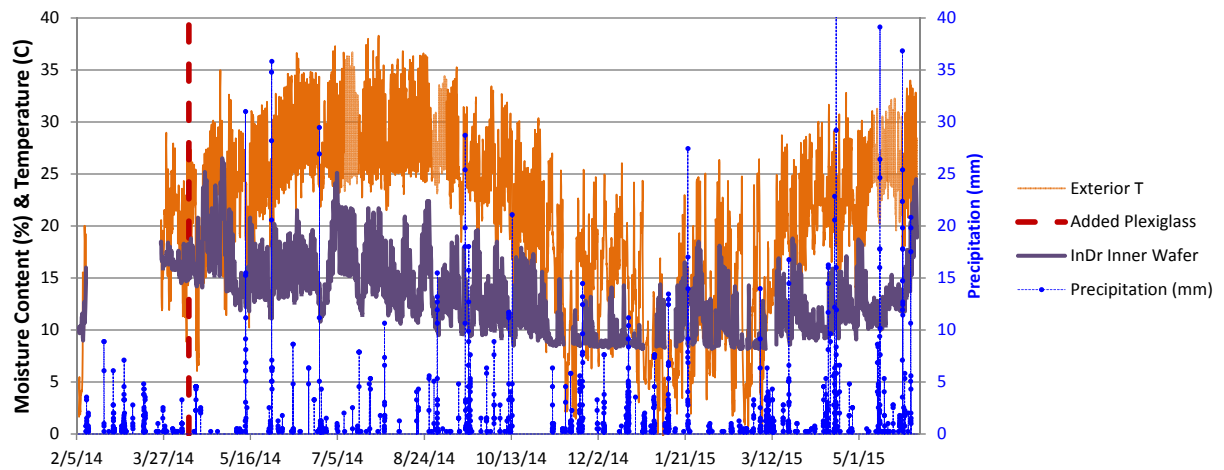


Figure 134: Inward drive wafer sensor MC and precipitation, with outdoor T

The most direct correlation to the wafer data was found by plotting the exterior sheathing temperature (24-hour rolling average), per Figure 135; this is consistent with adsorbed moisture being driven from warm/hot sheathing to the cool (interior) side of the assembly, or “ping-pong” water within the closed system. The correlation is very clear during summer conditions (May-August 2014 plotted in Figure 136).

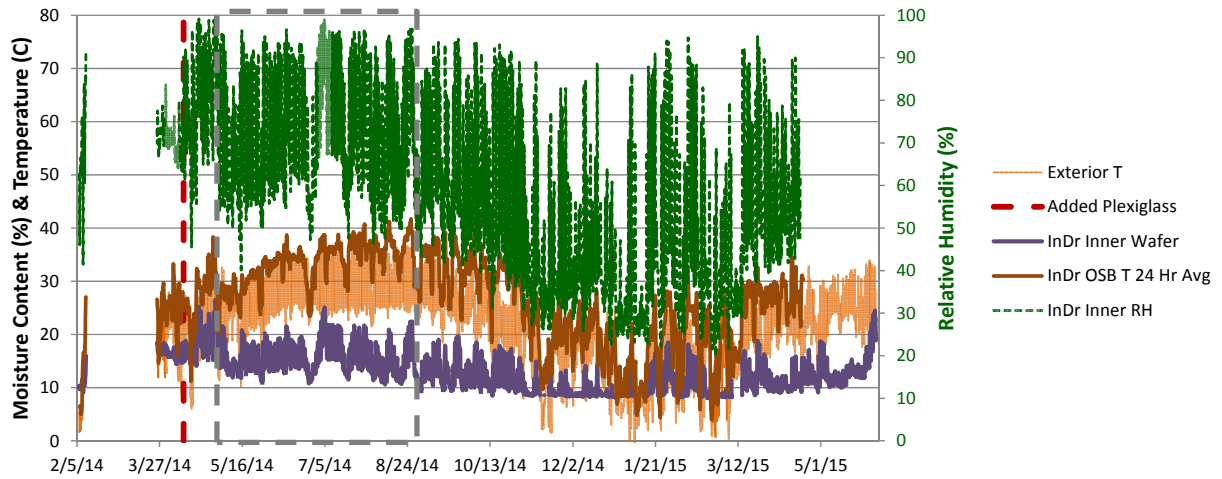


Figure 135: Inward drive interior-side RH, wafer MC and sheathing temperature 24 hour average

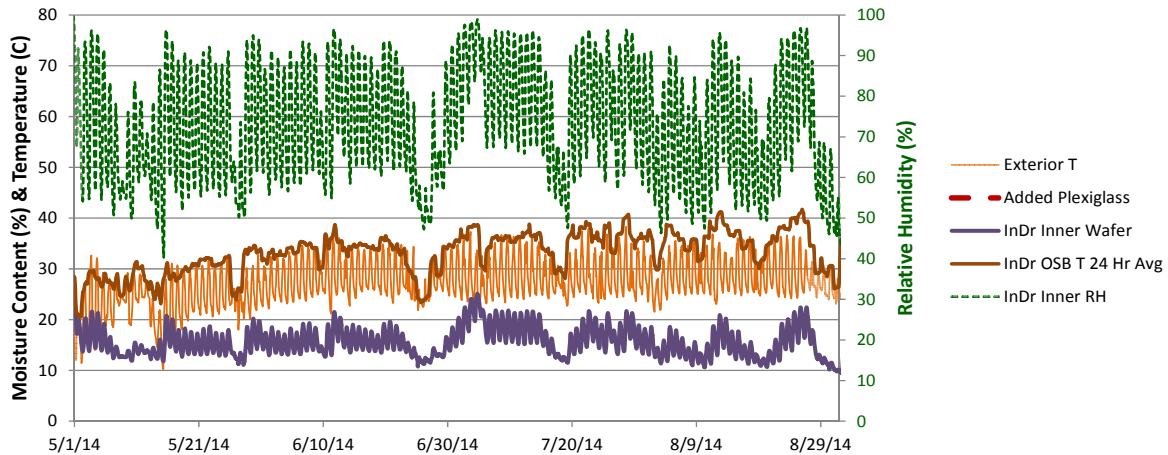


Figure 136: Inward drive interior-side RH, wafer MC and sheathing temperature 24 hour average (summertime detail)

Overall, MCs are not rising over time: this is an argument against moisture being driven through asphalt shingle layers (which would be accumulating in the “closed” assembly), with a typical roof cladding and water-resistive barrier (asphalt shingles with #15 felt).

9 Hot-Humid Climate (Houston) Analysis

9.1 Diffusion Vent and Unvented Roof Comparisons

A representative example of the relative behavior of the unvented and diffusion vent roof is shown in Figure 137, which plots roof ridge RH and wafer MC, for diffusion vent (DV1) and unvented (UV1) roofs.

The unvented roof shows the seasonal rise and fall (wetter in winter), and dry conditions in the summer. In the winter, interior moisture accumulates at the ridge under the vapor impermeable membrane. In the summer, the thermal gradient drives moisture downward, out of the assembly; the vapor impermeable membrane prevents the entry of any exterior moisture.

In comparison, the diffusion vent roof is drier in the winter, due to the vapor permeability of the diffusion vent material. In the summer, RHs are higher than the unvented roof, possibly due to connection to exterior moisture conditions, via the vapor-open ridge. This connection could also explain the diurnal cycling of RH levels.

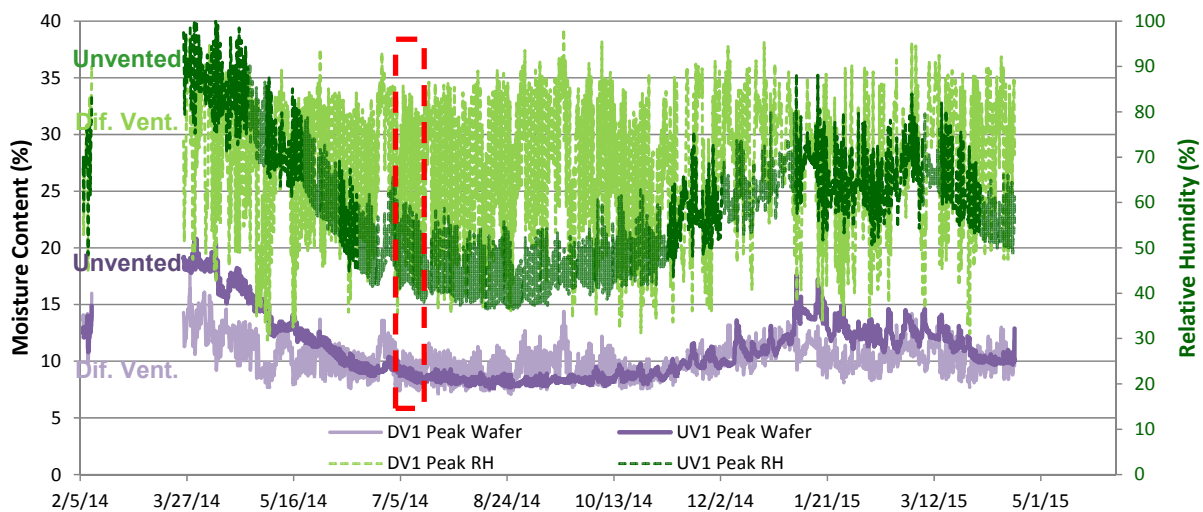


Figure 137: Diffusion vent (DV1) and unvented (UV1) comparison (ridge RH and wafer MC)

The diurnal cycling of RH levels is examined more closely for a summer period (July 2014) in Figure 138, which zooms in on the area highlighted by the red box in Figure 137. As mentioned earlier, the diffusion vent ridge RH has a sawtooth pattern, with a sharp drop in RH in the morning (6-8 AM range). In contrast, the unvented roof’s diurnal cycles are offset by several hours, with the peak/drop off occurring in the late morning (10 AM-12 noon range). These two ridge locations are on the same roofline, and should see identical exterior conditions (solar exposure).

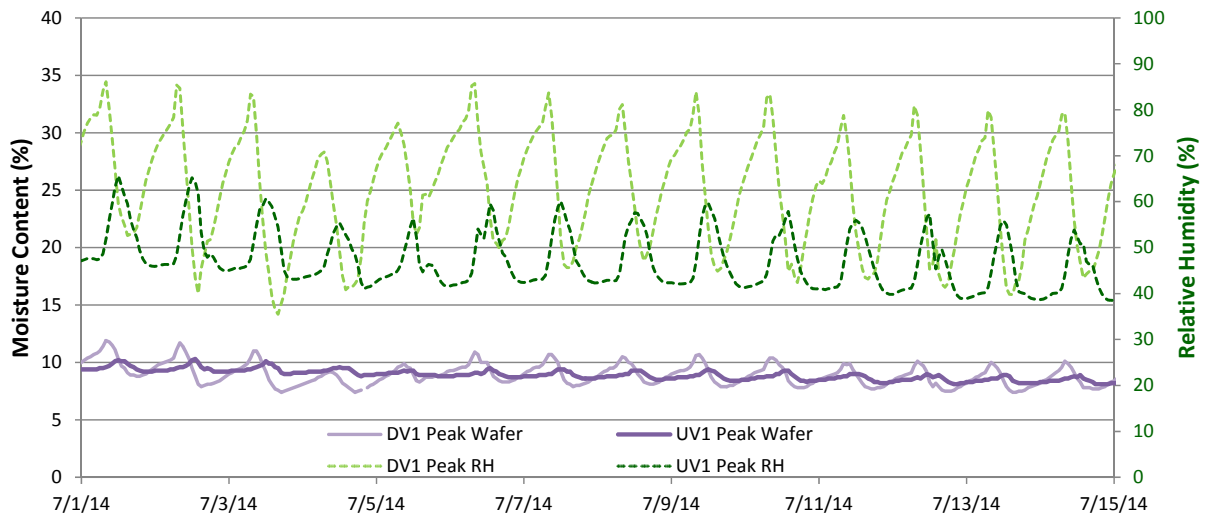


Figure 138: DV1 and UV1 comparison (ridge RH and wafer), summertime detail

Ridge RHs were plotted with ridge temperatures (Figure 139), to determine if temperature anomalies cause the “offset” behavior. Ridge temperatures track identically between the two roofs. Rising temperatures correlate with (a) a drop in DV1 RH, and (b) a rise in UV1 RH (grey lines). The diffusion vent roof has slightly lower peak temperatures than the unvented roof (typically by 5.5°F/3°C). It is plausible that the difference reflects evaporative cooling from the diffusion vent roof.

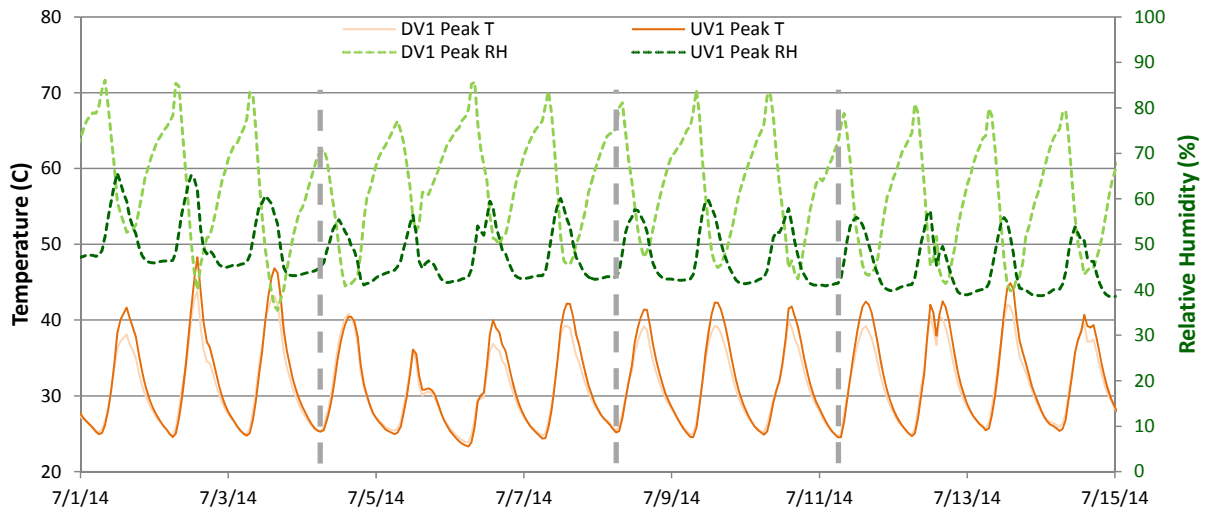


Figure 139: DV1 and UV1 comparison (ridge RH and wafer), summertime detail

As another reference, the roof T/RH sensors are plotted in terms of dewpoint temperature (absolute air moisture content), with interior (attic) and exterior dewpoints shown for reference (Figure 140). The dewpoint at the ridge rises above both attic conditions (blue lines) and exterior conditions (orange). More importantly, in terms of absolute moisture content, the unvented roof has higher (wetter) peaks than the diffusion vent roof, reversing the order seen in Figure 138.

In general, dewpoint “spikes” at the ridge is likely caused by the heating of roof sheathing, when in turn releases (desorbs) adsorbed moisture. This could easily drive dewpoints above interior conditions in the main attic space, given moisture stratification.

In the afternoons/evenings, as ridge dewpoints drop, the unvented roof drops far below ambient conditions, while the diffusion vent roof tracks closer to ambient dewpoints. This reflects the vapor-open ridge material, which couples exterior and interior moisture conditions.

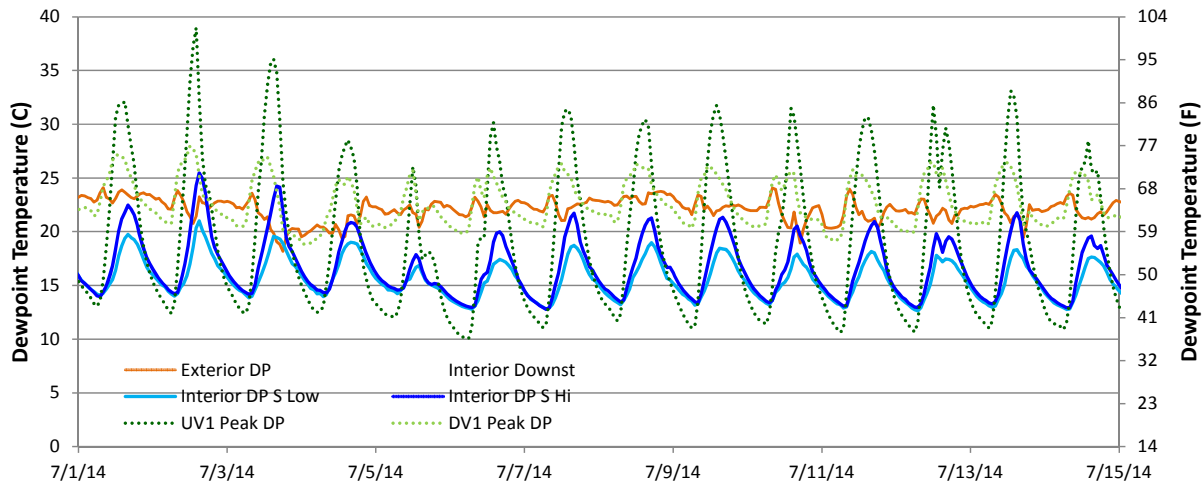


Figure 140: Summertime dewpoint comparison: interior, attic, exterior, and UV1/DV1

Overall, these monitoring results are consistent with the vapor-open diffusion vent ridge allowing drying in winter, while providing an entry point for ambient moisture in the summer.

9.2 ASHRAE 160 Analysis

ASHRAE Standard 160 (ASHRAE 2009b) provides guidance on moisture analysis for building envelope design, including the moisture performance evaluation criteria. The failure criteria (defined as the risk of mold growth) were redefined in addendum (a) (ASHRAE 2011), as follows:

6.1 Conditions Necessary to Minimize Mold Growth. *In order to minimize problems associated with mold growth on the surfaces of components of building envelope assemblies, condition shall be met: a 30-day running average surface RH < 80% when the 30-day running average surface temperature is between 5°C (41°F) and 40°C (104°F).*

Materials that are naturally resistant to mold or have been chemically treated to resist mold growth may be able to resist higher surface relative humidities and/or to resist for longer periods as specified by the manufacturer. The criteria used in Addendum a to Standard 160-2009 the evaluation shall be stated in the report.

The collected data were analyzed using ASHRAE 160 criteria; thirty-day running averages of the ridge relative humidity and temperature were calculated for each hour, and the resulting pass/fail results tabulated. It should be noted that in a strict interpretation of Standard 160, a single failing

hour would constitute an assembly failure. The number of failing hours for each assembly is shown in Table 12.

Table 12: Hours and percent of monitored period failing ASHRAE 160 criteria

Wall	# Failure Hours	% Time Failure
Unvented 1	427	5%
Unvented 2	238	3%
Diffusion Vent 1	0	0%
Diffusion Vent 2	0	0%
Diffusion Vent 3	0	0%
Diffusion Vent 4	0	0%
Diffusion Vent 5	0	0%
Diffusion Vent 6	0	0%

The only roofs that have failing ASHRAE 160 hours are the unvented assemblies; these failures occur in the first winter. This early data was missing two months due to power issues; this missing data would have added failing hours. No failing hours occurred in the unvented roofs during the second winter. However, there is no interior moisture generation in this house (unoccupied conditions/model home), which lowers wintertime condensation risks.

Although ASHRAE 160 has been commonly found to be an overly conservative standard, this analysis indicate that the diffusion vent roof has a greater margin of safety than conventional unvented designs. However, it does not answer the question whether the diffusion vent provides sufficient drying to avoid problems under typical occupancy conditions (with interior moisture generation).

10 Conclusions and Further Work

10.1 Cold Climate (Chicago)

10.1.1 *Experimental Results and Conclusions*

Seven roof assemblies were monitored in a Chicago-area test bed, including six unvented assemblies, and one control vented cathedral roof assembly. High interior moisture loading conditions were used, of 72°F/22°C and 50% RH; the roofs were monitored from October through June, capturing a winter (2013-2014) and following spring/early summer.

Under these conditions, all roofs except the vented cathedral assembly experienced wood MC and RH levels high enough to constitute failure.

- The unvented dense-pack cellulose roof experienced sheathing MCs well above 40% at the peak (risk of mold, rot, and decay). MCs lower in the roof were less severe (above 30%), but still in the high risk range. In this roof and the remaining roofs, these sheathing MCs were corroborated by rafter MC and roof peak RH. The roof peak “wafer” MC indicated that liquid water condensation was occurring at the peak of all roofs except the vented cathedral assembly.
- The diffusion vent roof had similar behavior to the unvented cellulose roof; however, in the spring (as outdoor temperatures rose), moisture levels (both MCs and RHs) fell much more rapidly in the diffusion vent roof.
- The cellulose “top vent” roofs showed similar behavior to the unvented roof, with very high MCs at the peak. The addition of the “top vent” detail showed no appreciable advantage over the unvented dense-pack cellulose assembly. The roof assembly with interior gypsum board has drier moisture levels at the lower portions of the roof than the assembly without gypsum board. This finding is consistent with the painted gypsum board providing air leakage and vapor flow control. These roofs had springtime drying rates similar to the diffusion vent roof, possibly due to upward drying into the air cavity.
- The fiberglass batt “top vent” roofs also had very high moisture levels; there was much more variation in MCs. A wintertime field visit showed significant condensation at the insulation-sheathing interface. When these roofs dried in the spring, the uppermost portions of the roof stay wettest the longest, and the lower portions of the roof dry out first.

Other general patterns from the roof monitoring were observed. They included consistent indications of moisture stratification (highest MCs in the upper portions of the roof), and drier conditions on west-side monitoring (due to solar gain), compared to the east side.

When the results were analyzed using ASHRAE Standard 160 (to determine risk of mold growth), all of the unvented roof assemblies failed for significant portions of the spring, showing that moisture levels remained high into warmer weather, allowing mold growth.

The roof was disassembled at the end of the experiment, to correlate measurements with actual assembly conditions. The unvented fiberglass batt roofs had wet sheathing and mold growth, although not structural failure. The cellulose roofs had only slight issues, such as rusted fasteners, staining and sheathing grain raise, despite the extreme moisture conditions measured. This difference was ascribed to cellulose's borate preservatives (borate salts added as a fire retardant and antifungal agent), its airflow retarding properties, and its ability to safely store moisture. The worst moisture damage in the roof assemblies was seen closer to the ridge, consistent with monitoring data. The comparison between fiberglass batt and dense-pack cellulose puts the fiberglass at a disadvantage, given the imperfections in the batt installation (voids and air gaps). A fairer comparison would have been dense-pack cellulose vs. blown-in fiberglass.

Based on the high interior moisture loading (50% RH) of this test, none of these unvented assemblies are recommended. This includes unvented cellulose roofs: although minimal actual damage was observed, all monitoring results indicated very high risk conditions for long-term durability.

10.1.2 Further Work

Although all of the unvented roofs essentially failed under these experimental conditions, further research might be warranted for more robust assemblies in a cold (Zone 5A) climate.

For instance, the use of less-open vapor control layer than latex paint on gypsum board (Class III vapor retarder) might be researched. Class II vapor retarders (0.1 to 1 perm) options should be considered, including vapor retarder paint on gypsum board, or variable-permeability vapor retarder films. The experiment also should simulate air leakage (possibly in a second winter, after establishing a baseline), to show the effect of imperfections in the air barrier, which occur commonly in construction. Use of a Class I vapor barrier (polyethylene) is not recommended.

Another option to consider is a diffusion vent roof with a higher perm rating, similar to the assembly installed in the Houston roof (200+ perm membrane vs. 50+ perm exterior gypsum board). This might be combined with the use of an interior vapor control layer.

If a top vent assembly is being considered as an experimental option, a higher permeance sheathing than OSB (i.e., plywood) should be used, per Schumacher and LePage (2012). In addition, a larger vent space should be considered.

Finally, a common geometry in retrofit insulation is a short section of sloped compact roofs/ceiling assembly, which connects two smaller attics (a.k.a. "story and a half" geometry; Figure 141). Retrofit dense-packing of the short section of the rafter bay is a very cost-effective method to insulate and reduce air leakage, but it is nominally an unvented roof that does not meet code. On the other hand, the top of the assembly is typically vapor-open, offering diffusion drying (and limited air leakage drying) at the termination/transition.

Experiments could be devised to test these types of assemblies, to determine whether moisture risks are controlled in this assembly. Hopefully, this research could provide guidance on specifics such as acceptable materials, required densities, or maximum rafter bay lengths.



Figure 141: Story and a half compact roof example (with insulation and ventilation chute)

10.2 Hot-Humid Climate (Houston)

10.2.1 Experimental Results and Conclusions

A house with a conditioned/unvented roof was built in the Houston area and monitored; it is an unoccupied model. The roof is insulated with blown/adhered fiberglass insulation, directly on the underside of the roof sheathing. The majority of the roof has a “diffusion vent” detail at the ridge and hips (high-permeance membrane over openings), with some sections of conventional unvented roof (self-adhered bituminous membrane) as a control comparison.

The roof has been monitored February 2014 through June 2015 (16 months); attic conditions are not directly controlled, but are indirectly conditioned by duct leakage and air leakage from the interior. As expected, attic temperatures and dewpoint temperatures (absolute air moisture content) are between interior and exterior conditions, but generally closer to interior conditions. The dewpoints show a diurnal cycle that is consistent with moisture adsorption/desorption from the roof sheathing.

In the control unvented roofs, roof peak RHs reached high levels (90%+) in the first winter; as exterior conditions warmed, RHs quickly fell to 40-50% in the summer, due to the inward thermal gradient (“pushes” moisture out of the roof sheathing/inward). MC measurements were consistent with RH measurements: initial winter conditions were higher than levels recommended for durability, but fell to safe levels in the summer. In the second winter (2014-2015), peak RHs rose again (60-80% typical), but not to the same levels as the first winter.

In contrast, the diffusion vent roofs had drier conditions at the roof peak in wintertime, but during the summer, RHs and MCs were higher than the unvented roof. However, these moisture levels were well within the safe range. The diffusion vent roof also showed strong diurnal variations of RH levels. Both of these behaviors are consistent with the roof rafter bay having a hygric/moisture connection to outside air, due to the vapor-open diffusion vent. The hip roofs treated with a diffusion vent showed behavior halfway between the unvented and diffusion vent roofs. This was attributed to the limited diffusion vent area (2 in. diameter drilled holes, rather than 3 in. strip) available in the hip geometry.

The first and second winters had different interior conditions. The first winter had high RHs (due to drying of construction moisture), while the second winter had low RHs (no occupancy/moisture generation).

Overall, these results indicate that the diffusion vent roof has a greater amount of drying (and less wintertime moisture accumulation) than the unvented roof. However, the unvented roof did not have moisture contents high enough to truly constitute “failure.”

An experiment was also devised to examine the effect of inward vapor drives in unvented roof assemblies, for instance, due to moisture in shingle laps being driven inward. A section of rafter bay was isolated with vapor impermeable materials and an airtight acrylic plastic interior cover. The monitoring data did not show a growing or “ratcheting” moisture content. These results are consistent with moisture adsorbing and desorbing from the sheathing (a.k.a. “ping-pong moisture”), rather than moisture being driven through the shingles.

The air leakage measurements of the unvented attic showed leakage at roof-wall connections. This shows a potential challenge of substituting air-permeable insulation for air-impermeable spray foam: greater attention will be required to ensure good air barrier detailing at connections.

10.2.2 Further Work

Results are still being collected and analyzed at the experimental roof in Houston; an instrumentation failure from April 2015 is slated to be repaired. As discussed above, the unvented roof assembly was not driven to failure; the failures seen in previous work in Houston and Jacksonville were not replicated.

One issue was the lack of interior moisture generation in the unoccupied model house, which results in lower wintertime RH levels. Higher interior RH levels would increase moisture conditions in the attic, and increase condensation risks.

To understand the effect of operating the house in unoccupied conditions (no interior moisture generation), the interior conditions were compared to those collected circa 2001-2002 by Rudd and Henderson (2007). Their data covered new construction Houston-area houses with added energy efficiency features (good airtightness, unvented attics, low solar gain windows) built under the Building America program. Some houses also had dehumidification systems installed (standalone dehumidifier, or two-stage cooling equipment). Data were recorded in both the main space and the unvented attic space. All of these houses were occupied.

Results are presented as whisker/box plots, showing the range and distribution of measured moisture contents. The whisker/box plots show median (center of box), lower and upper quartile of data (extent of box), and maximum/minimum (lines extending from box). Results are shown for interior temperature (Figure 142), relative humidity (Figure 143), and dewpoint (Figure 144). Data were selected for the winter periods (December-February) in all houses.

Figure 142 shows that the diffusion vent roof test house was operated at a higher temperature than the circa 2001 Building America houses, and with a smaller setpoint variation range.

Figure 143 shows that wintertime RH levels were lower in the diffusion vent roof house. When results are plotted as dewpoint (Figure 144), interior conditions are closer to (albeit still lower than) the circa 2001 Building America houses.

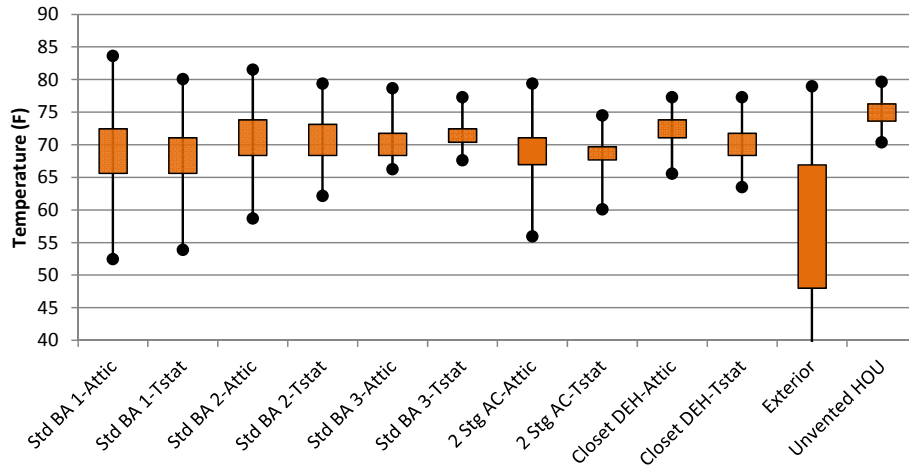


Figure 142: Rudd and Henderson (2007) interior temperature data and Houston unvented data

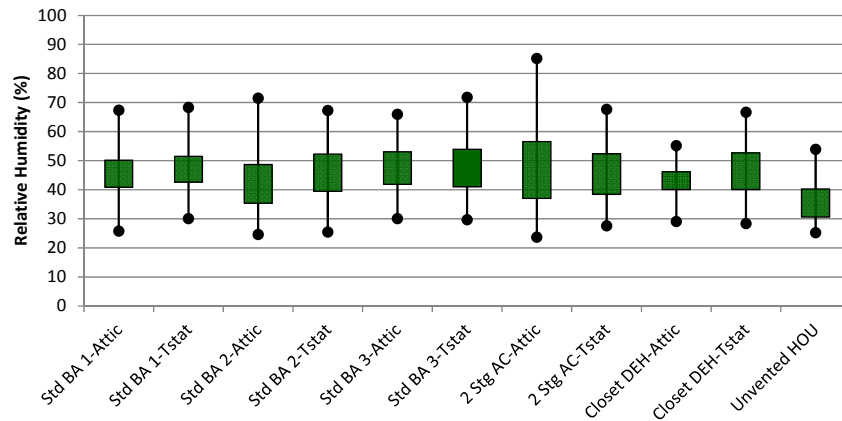


Figure 143: Rudd and Henderson (2007) interior RH data and Houston unvented data

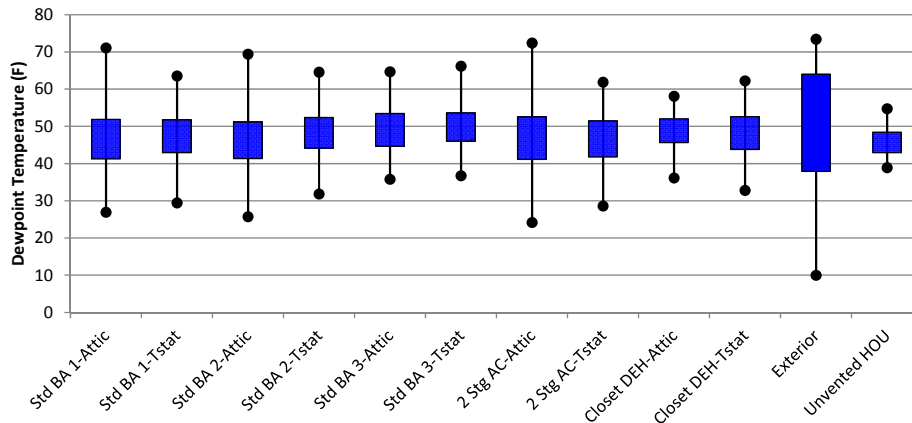


Figure 144: Rudd and Henderson (2007) interior dewpoint data and Houston unvented data

Adding humidification during the fall/winter of 2015-2016 could demonstrate the difference in diffusion vent and unvented roof behavior, under conditions simulating high occupancy. Interior RH conditions in the 40-50% range will be used.

References

- Arena, L.; P. Mantha, A. Karagiozis. (2010). “Monitoring of Internal Moisture Loads in Residential Buildings.” Report for U.S. Department of Housing and Urban Development Washington, DC, December 2010.
- Arena, L.; Owens, D., Mantha, P. (2013). “Measured Performance of an R-40 Double-Stud Wall in Climate Zone 5A” *Buildings XII Conference Proceedings*. Atlanta, GA: American Society of Heating, Refrigerating and Air-Conditioning Engineers, Inc.
- Arena, L. (2014). “ASHRAE 160: Modeling and Measured Data.” Building America Expert Meeting 2014: Guidance on Modeling Enclosure Design in Above Grade Walls.
<http://www.buildingscience.com/documents/bareports/ba-1403-guidance-modeling-enclosure-design-above-grade-walls-expert-meeting/view>
- [ASHRAE] American Society of Heating, Refrigerating and Air-Conditioning Engineers, Inc. (2009a). *2009 ASHRAE Handbook—Fundamentals*. Atlanta, GA: American Society of Heating, Refrigerating and Air-Conditioning Engineers, Inc.
- [ASHRAE] American Society of Heating, Refrigerating and Air-Conditioning Engineers, Inc. (2009b). *ANSI/ASHRAE Standard 160-2009: Criteria for Moisture-Control Design Analysis in Buildings*. Atlanta, GA: American Society of Heating, Refrigerating and Air-Conditioning Engineers, Inc.
- [ASHRAE] American Society of Heating, Refrigerating and Air-Conditioning Engineers, Inc. (2011). *ANSI/ASHRAE Standard 160-2009: Criteria for Moisture-Control Design Analysis in Buildings: Addendum a*. Atlanta, GA: American Society of Heating, Refrigerating and Air-Conditioning Engineers, Inc.
- Bohac, D. (2002). “Zone Pressure Diagnostics: A new protocol shows how to make a valuable diagnostic test even more useful.” *Home Energy Magazine*, May/June 2002, Berkeley, CA: Home Energy Magazine.
- Boudreaux, P., S. Pallin, R. Jackson. (2013) “Moisture Performance of Sealed Attics in the Mixed-Humid Climate” ORNL/TM-2013/525 Oak Ridge, TN: Oak Ridge National Laboratory, Energy and Transportation Science Division.
- Derome, D. (2005). “Moisture Accumulation in Cellulose Insulation Caused by Air Leakage in Flat Wood Frame Roofs.” *Journal of Building Physics*, January 2005 vol. 28 no. 3 269-287.
- Fitzgerald, J. (2010). Personal communication.
- [FPL] Forest Products Laboratory. (2010). *Wood Handbook—Wood As an Engineering Material*. General Technical Report FPL-GTR-190. Madison, WI: U.S. Department of Agriculture, Forest Service, Forest Products Laboratory.

Glass, S.V. (2013). “Hygrothermal Analysis of Wood-Frame Wall Assemblies in a Mixed-Humid Climate.”. Research Paper FPL-RP-675. Madison, WI: U.S. Department of Agriculture, Forest Service, Forest Products Laboratory. 25 p.

Holladay, M. (2013) “Musings of an Energy Nerd: Return to the Backyard Tape Test.” *Green Building Advisor*, <http://www.greenbuildingadvisor.com/blogs/dept/musings/return-backyard-tape-test>, Accessed December 2013.

ICC. (2009). *International Residential Code*. Country Club Hills, IL: International Code Council.

James, W.L., (1963, rev. 1988), “Electric moisture meters for wood.” Gen. Tech. Report FPL-GTR-6. Madison, WI: U.S. Dept. of Agriculture, Forest Service, Forest Products Laboratory, 1988.

Lstiburek, J. (2006) “Understanding Attic Ventilation,” *ASHRAE Journal*, April 2006, Vol. 48, No. 4, pp. 36-38, 40, 42-45, Atlanta, GA: American Society of Heating, Refrigeration, and Air-Conditioning Engineers, Inc. <http://www.buildingscience.com/documents/digests/bsd-102-understanding-attic-ventilation/>

Lstiburek, J. (2010a) “Building Sciences: Mind the Gap, Eh?” *ASHRAE Journal*, January 2010, pp. 57-63, Atlanta, GA: American Society of Heating, Refrigeration, and Air-Conditioning Engineers, Inc. <http://www.buildingscience.com/documents/insights/bsi-038-mind-the-gap-eh/>

Lstiburek, J. (2010b) “Building Sciences: Don’t be Dense with Insulation,” *ASHRAE Journal*, August 2010, pp. 54-57, Atlanta, GA: American Society of Heating, Refrigeration, and Air-Conditioning Engineers, Inc. <http://www.buildingscience.com/documents/insights/bsi-043-dont-be-dense/>

Lstiburek, J. (2011) “A Crash Course in Roof Venting.” *Fine Homebuilding Magazine*, August/September 2011, pp. 68-72. Newtown, CT: Taunton Press. (<http://www.buildingscience.com/documents/published-articles/pa-crash-course-in-roof-venting/view>)

Lstiburek, J. (2014) “Building Sciences: Cool Hand Luke Meets Attics,” *ASHRAE Journal*, April 2014, pp. 52-57, Atlanta, GA: American Society of Heating, Refrigeration, and Air-Conditioning Engineers, Inc. <http://www.buildingscience.com/documents/insights/bsi-077-cool-hand-luke-meets-attics>

[NREL] National Renewable Energy Laboratory. (2013a). FY 2014 Residential Energy System Research Needs. Golden, Colorado: NREL, 25 pp.

[NREL] National Renewable Energy Laboratory. (2013b). “Building America Technical Innovations Leading to 50% Savings – A Critical Path”. Golden, Colorado: NREL, 48 pp.

Rose, W. and D. McCaa. (1998). “Temperature and moisture performance of wall assemblies with fiberglass and cellulose insulation.” (pp. 133-144). *Proceedings: Thermal Performance of*

the Exterior Envelopes of Buildings VII. (ISBN 1-883413-70-2). Atlanta, GA: American Society of Heating, Refrigerating and Air-Conditioning Engineers, Inc.

Rudd, A.F., J.W. Lstiburek, and N.A. Moyer (1997). “Measurement of Attic Temperatures and Cooling Energy Use In Vented and Sealed Attics in Las Vegas, Nevada”, *EEBA Conference*, Minneapolis, MN, March 1997.

Rudd, A.F. and J.W. Lstiburek. (1998) “Vented and Sealed Attics in Hot Climates” *ASHRAE Transactions*, TO-98-20-3, June 1998.

Rudd, A.F. and H. Henderson. (2007) “Monitored Indoor Moisture and Temperature Conditions in Humid-Climate US Residences.” *ASHRAE Transactions*, Volume 113, Part 1, DA-07-046.

Salonvaara, M.; A. Karagiozis; A. Desjarlais. (2013) “Moisture Performance of Sealed Attics in Climate Zones 1 to 4.” *Proceedings: Thermal Performance of the Exterior Envelopes of Buildings XII.* Atlanta, GA: American Society of Heating, Refrigerating and Air-Conditioning Engineers, Inc.

Schumacher, C.J. (2011). BA-1109: “Building America High Impact Task: Support of Standards Development—Dense-pack Airflow Resistance Final Research Report.”
<http://www.buildingscience.com/documents/bareports/ba-1109-high-impact-project-densepack-airflow-resistance/>

Schumacher, C.J. and R. LePage. (2012). BA-1308: “Moisture Control for Dense-Packed Roof Assemblies in Cold Climates: Final Measure Guideline.” <http://www.buildingscience.com/documents/bareports/ba-1308-moisture-control-dense-packed-roof-assemblies-cold-climates/view>

Smegal, J. and J. Straube. (2014) “Ventilation and Vapour Control for SPF-insulated Cathedral Ceilings.” Report for the Canadian Urethane Foam Contractors Association Inc. Waterloo, ON: Building Science Consulting Inc.

Straube, J., D. Onysko, and C. Schumacher. (2002). Methodology and Design of Field Experiments for Monitoring the Hygrothermal Performance of Wood Frame Enclosures. *Journal of Thermal Env. & Bldg. Sci.*, Vol.26, No.2—October 2002.

Straube, J., E. Burnett (2005) *Building Science for Building Enclosures*, Building Science Press, Westford, MA.

Straube, J., R. Smith, G. Finch. (2009). “Spray Polyurethane Foam: The Need for Vapour Retarders in Above-Grade Residential Walls.” Report for Canadian Urethane Foam Contractors Association (CUFCA), March 2009.

Ueno, K., and Straube J. (2008) “Laboratory Calibration and Field Results of Wood Resistance Humidity Sensors”, *Proceedings of BEST I Conference*, Minneapolis, June 10-12, 2008.

Ueno, K., and J.W. Lstiburek. (2015) “Field Monitoring of Cold Climate Double Stud Walls with Cellulose and Low-Density Foam Insulation,” *Proceedings of BEST 4 Conference*, Kansas City, April 2015.

Van Straaten, R. (2003). “Measurement of Ventilation and Drying of Vinyl Siding and Brick Clad Wall Assemblies.” Master of Applied Science in Civil Engineering Thesis, University of Waterloo, Waterloo, ON.

Wilkinson, J. K. Ueno, D. De Rose, J.F. Straube, D. Fugler. (2007) “Understanding Vapour Permeance and Condensation in Wall Assemblies.” *11th Canadian Conference on Building Science and Technology*, Banff, Alberta, 2007

Appendix A: Monitoring Equipment

The testing and monitoring equipment required to perform the field monitoring of the two unvented roofs is as follows:

Table 13: Testing and monitoring equipment specifications

Measurement	Equipment Needed
Temperature	NTC (negative temperature coefficient) thermistor, $\pm 0.2^{\circ}\text{F}/0.1^{\circ}\text{C}$
Relative humidity	Thermoset polymer capacitive relative humidity sensor, $\pm 3.5\%$ RH
Wood moisture content	Electric resistance-based moisture content pin sensors
Data acquisition and collection	Campbell Scientific CR1000 measurement and control system with Campbell Scientific AM16/32B Multiplexers
Outdoor temperature/ relative humidity	Campbell Scientific HMP60-L -40°F to 140°F (-40°C to $+60^{\circ}\text{C}$) range; $\pm 1.1^{\circ}\text{F}$ (0.6°C) accuracy; RH accuracy at 0° to $+40^{\circ}\text{C}$: $\pm 3\%$ RH (0 to 90% RH); $\pm 5\%$ RH (90 to 100% RH) RH Accuracy at -40° to 0°C and $+40^{\circ}$ to $+60^{\circ}\text{C}$: $\pm 5\%$ RH (0 to 90% RH); $\pm 7\%$ RH (90 to 100% RH)
Telecommunications	Raven XTG GPRS/EDGE Sierra Wireless Cellular Modem

Appendix B: Chicago Attic Roof Ventilation Dewpoints

Temperature and relative humidity sensors were installed in the airstream of the ventilated roof assemblies (1 through 5), in order to provide some indication of whether moisture removal was occurring. To measure absolute air moisture content, dewpoints were calculated for the T/RH data, and compared with interior (test attic) and exterior dewpoint data.

10.2.3 Roof 1 (Vented)

The intake (soffit/eave), exhaust (ridge), interior, and exterior dewpoint for the vented roof (1) are plotted in Figure 145. The general trend is that the ventilation space dewpoints mostly match exterior conditions. However, there is one period (highlighted in the grey rectangle) when the exhaust dewpoint is noticeably higher; this data is expanded in Figure 146.

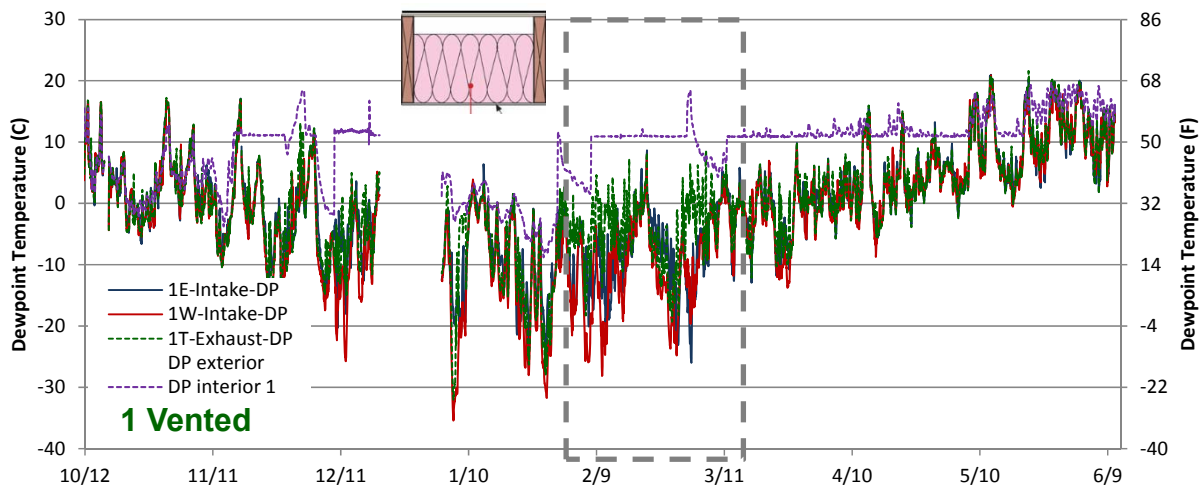


Figure 145: Intake and exhaust dewpoints, w. interior & exterior (Roof 1-Vented)

This expanded period appears to match when the humidification system was running during colder weather. This might indicate some level of moisture removal at low exterior dewpoints.

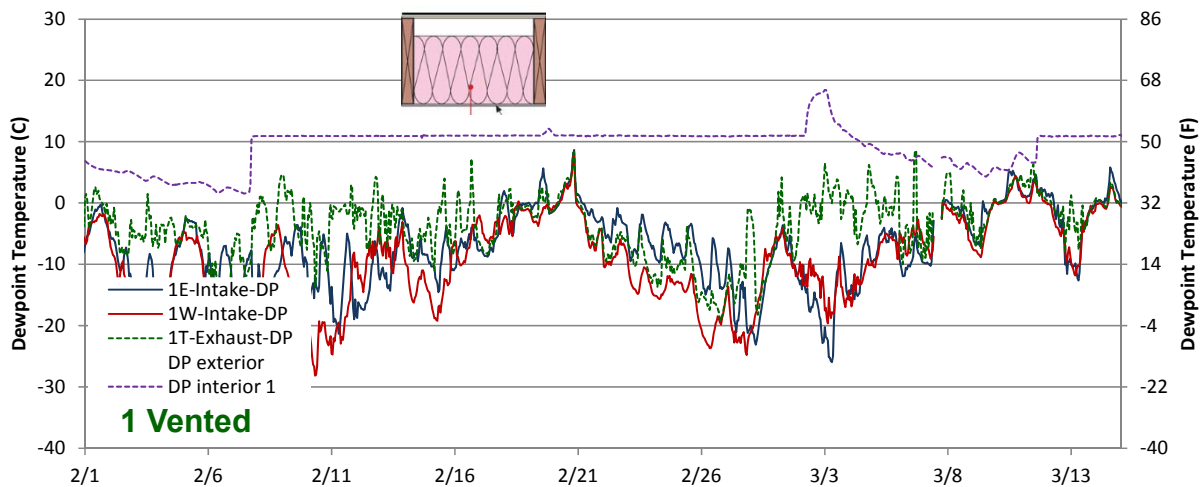


Figure 146: Intake and exhaust dewpoints, w. interior & exterior (Roof 1-Vented)-Detail

10.2.4 Roofs 2 and 3 (Top Vent Cellulose)

The T/RH sensors for the top vent (mesh space under shingle) roofs are shown in Figure 147; the intake is behind the mesh at the soffit, and the exhaust is inserted into the housewrap ridge covering (shown before cutting the ventilation holes).



Figure 147: Intake (L) and exhaust (R) T/RH sensors for “top vent” roofs

The data for the top vent cellulose roof with gypsum board (2) is shown in Figure 148; the highlighted period from Roof 1 is shown here, but in this roof, the dewpoints are all close to exterior conditions. A close up of that period (Figure 149) seems to indicate that the exhaust dewpoint is slightly higher during this period, but not by the same degree as the vented assembly. This would indicate that more moisture is removed from the vented roof than the top vent roof.

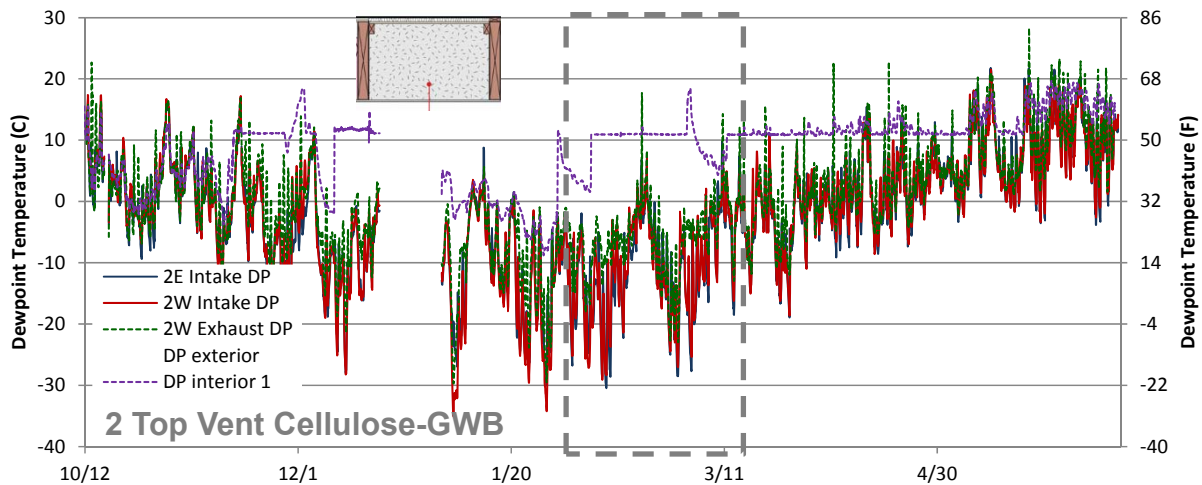


Figure 148: Intake and exhaust dewpoints, w. interior & exterior (Roof 2-Top Vent Cell.-GWB)

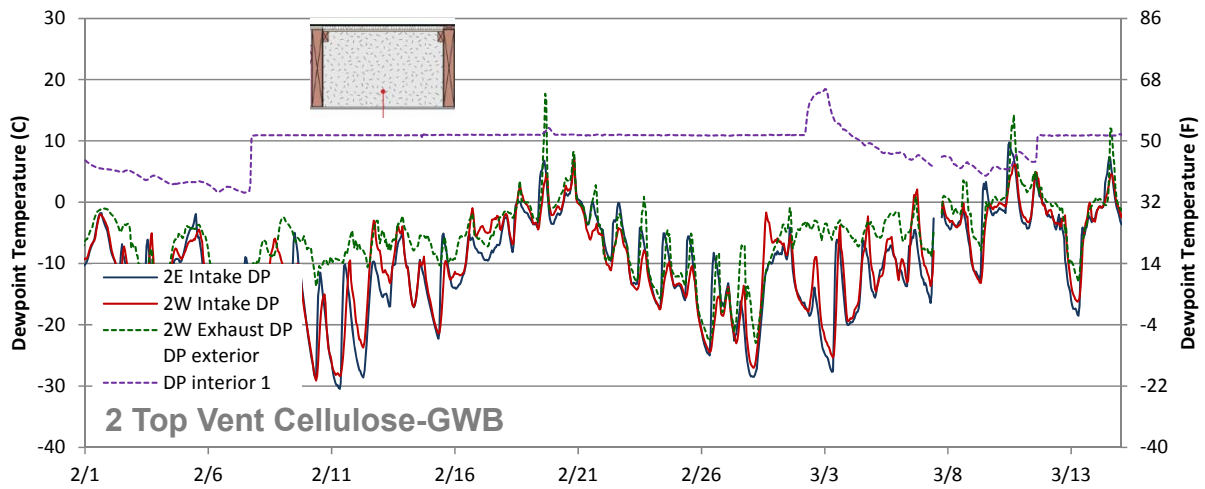


Figure 149: Intake and exhaust dewpoints, w. interior & exterior (Roof 2-Top Vent Cell.-GWB), detail

Similar plots are shown for the top vent cellulose roof, no gypsum board (3), in Figure 150 and Figure 151, with mostly similar patterns.

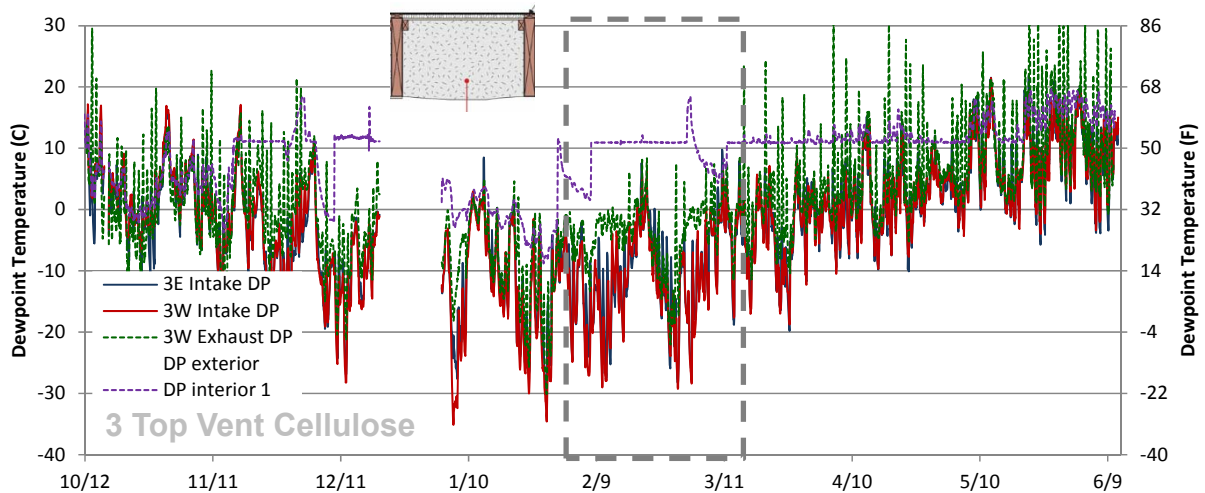


Figure 150: Intake and exhaust dewpoints, w. interior & exterior (Roof 3-Top Vent Cell.)

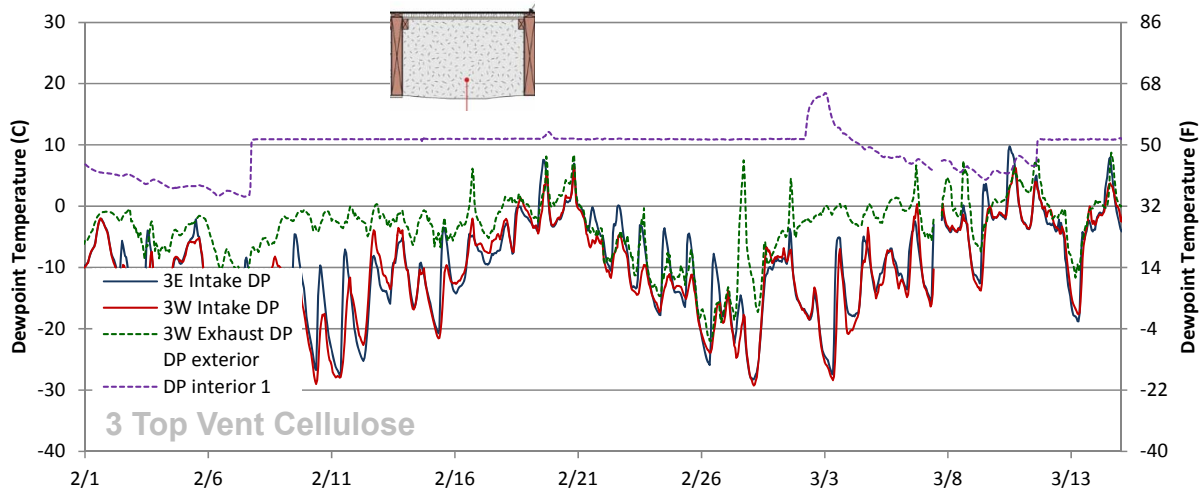


Figure 151: Intake and exhaust dewpoints, w. interior & exterior (Roof 3-Top Vent Cell.), detail

10.2.5 Roofs 4 and 5 (Top Vent Fiberglass)

Dewpoints are plotted for the top vent fiberglass roofs with gypsum board (5) and without gypsum board (4) in Figure 152 and Figure 153, respectively. Roof 5 shows elevated exhaust dewpoints (compared to exterior/intake), while Roof 4 shows smaller differences, but greater variations.

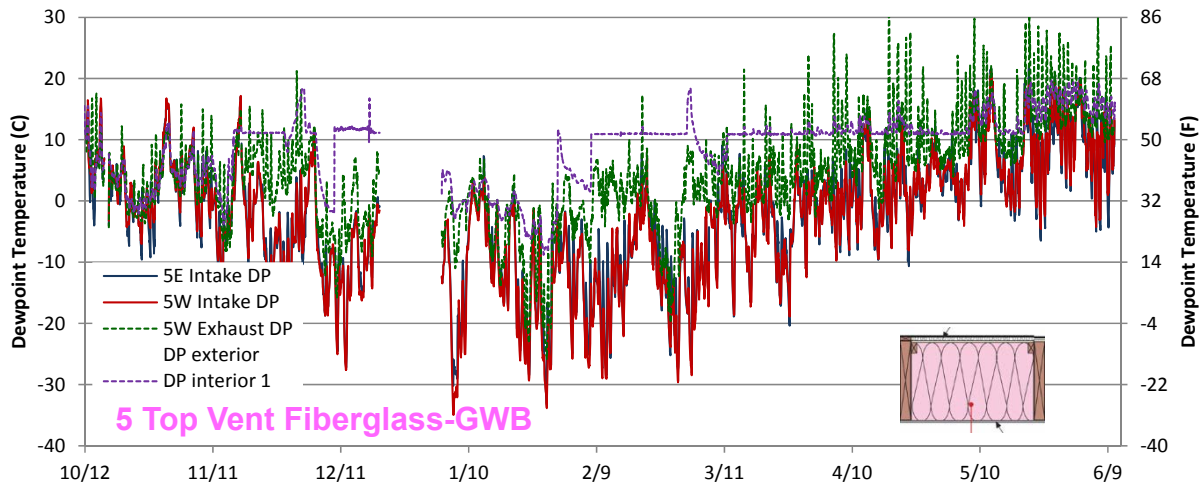


Figure 152: Intake and exhaust dewpoints, w. interior & exterior (Roof 5-Top Vent FG-GWB)

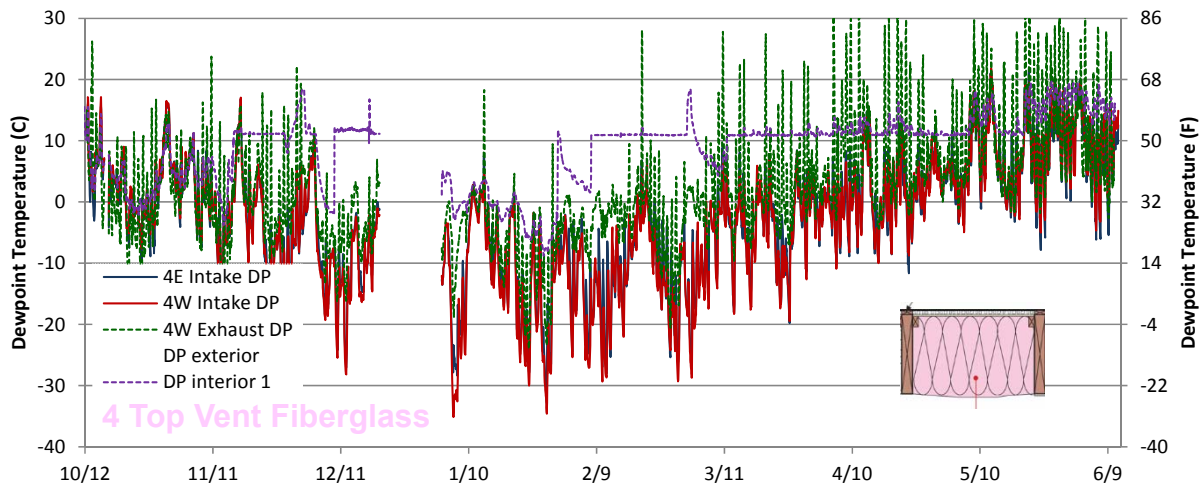


Figure 153: Intake and exhaust dewpoints, w. interior & exterior (Roof 4-Top Vent FG)

10.2.6 Ventilation Space Conclusions

Unfortunately, not many conclusions can be drawn from the ventilation space measurements. Although higher dewpoints at the exhaust may indicate removal of moisture, they might also simply indicate static accumulation (and stratification) of moisture, if there is minimal airflow. To truly measure moisture removal, both intake/exhaust air moisture content and airflow would need to be measured. Given the limited (~½ in.) mesh airspace under the shingles, it seems plausible that the airflow might be relatively low. Measurement of the low velocity airflows occurring in ventilation cavities, however, is difficult and instrumentation-intensive to monitor in-situ (Van Straaten 2003).

Appendix C: Chicago Sheathing T and Ventilation Space

Examination of dewpoint temperatures of the ventilation spaces (in the top vent roofs) gave inconclusive results: the difference in dewpoint might reflect moisture removal, or simply moisture accumulation (see Section 0). Another way of gauging whether effective ventilation is occurring through the “top vent” mesh is to examine the sheathing temperatures. Ventilation air movement up the roof might carry some heat with it, possibly cooling the lower roof surfaces (or the entire roof surface), relative to the analogous unvented roof.

Sheathing temperatures were plotted for top vent cellulose (2) and unvented (7) roofs; they are basically identical except for the presence/absence of the mesh spacer under the asphalt shingles.

Temperatures plots from two weeks in winter are shown in Figure 154 and Figure 155. As a general behavior, both roofs show temperatures peaks for east side several hours before the west side, which is consistent with the sun path and geometry.

One significant difference was seen on 1/21; the top vent (2) cellulose west-facing sensors spike higher than the unvented cellulose (7) roofs. However, the presence or absence of snow on the roof (Figure 156) is likely causing this difference rather than ventilation effects. The snow melt pattern might be influenced by heat loss through the roof assemblies, but it is probably mostly caused by wind-blown snow deposition and other geometry effects.

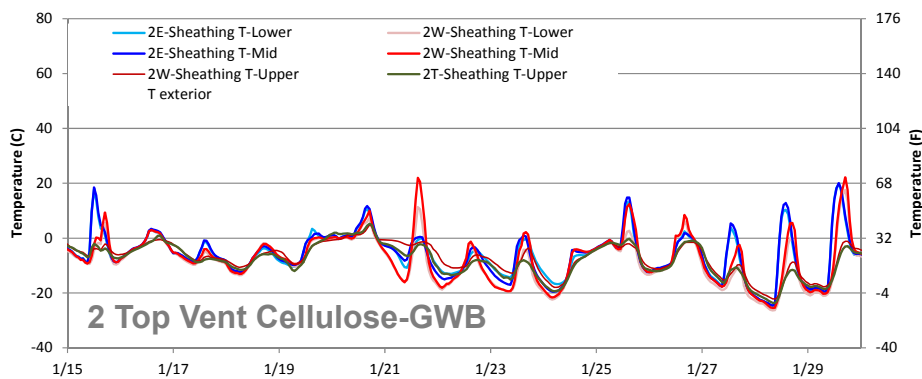


Figure 154: Wintertime sheathing temperatures for Roof 2 (top vent cellulose with gypsum board)

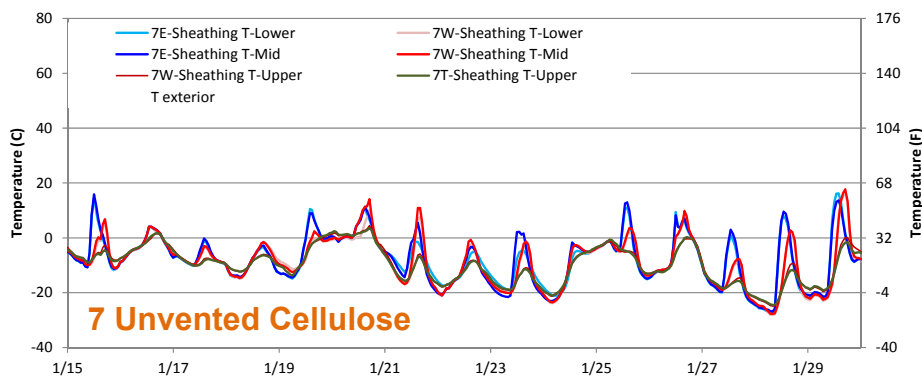


Figure 155: Wintertime sheathing temperatures for Roof 7 (unvented cellulose)



Figure 156: Snow deposits and melting at front (west) orientation of test roof

Similar plots for summertime (May) conditions are shown in Figure 157 and Figure 158. The roof sheathing temperatures are close enough to be basically indistinguishable, between the two roofs. The east-west peaking patterns are similar to wintertime behavior.

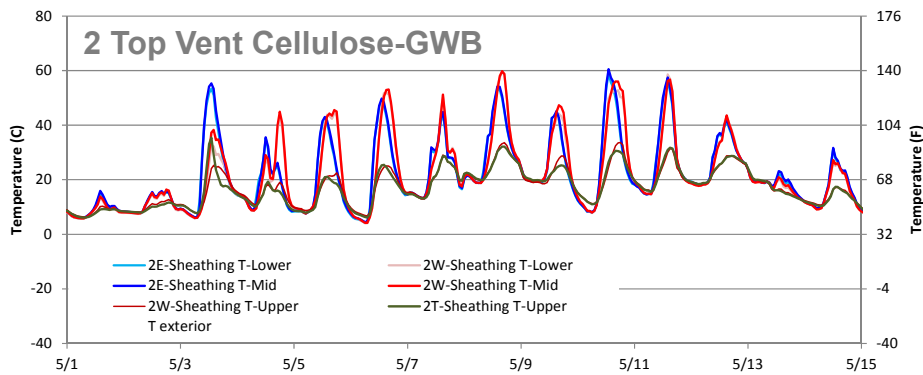


Figure 157: Summertime sheathing temperatures for Roof 2 (top vent cellulose with gypsum board)

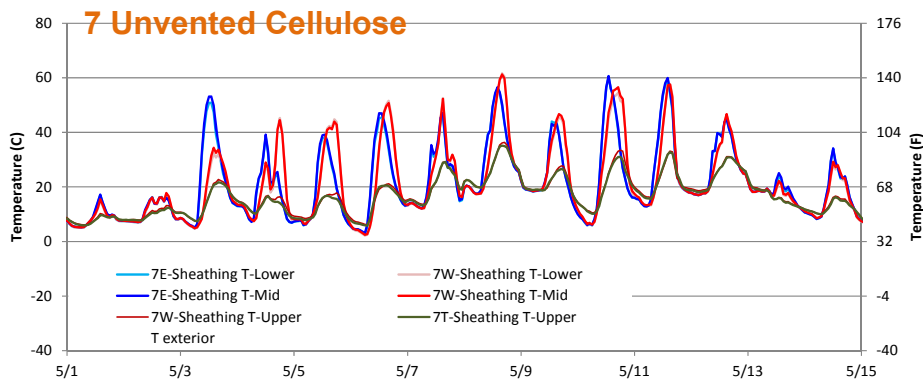


Figure 158: Summertime sheathing temperatures for Roof 7 (unvented cellulose)

The one striking pattern is the lower temperatures seen at the “upper” sheathing areas; it is seen on both orientations in both roofs. The reason is likely the shading effect of the “doghouse”

detail; the upper/top sheathing temperatures are shaded/shielded from direct solar gain by this ventilated roof area (Figure 159). Overall, the temperature measurements show little indication of the “top vent” detail having an effect on sheathing temperatures.

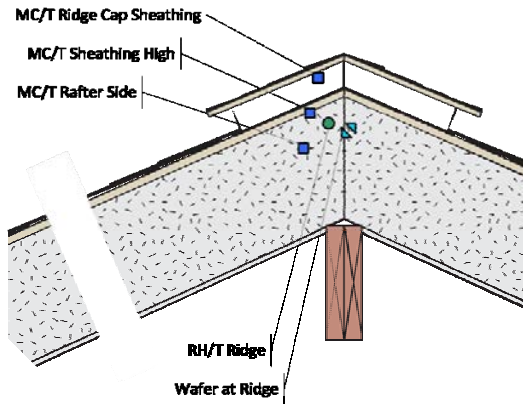


Figure 159: Ridge and “doghouse” monitoring detail, unvented cellulose roof

As another comparison, sheathing temperatures for the vented fiberglass roof (1) are plotted in Figure 160, given that it is known to have good ventilation, with its open geometry (~4 in. air space between sheathing and fiberglass batt). The summertime roof sheathing temperatures in the vented fiberglass (1) roof are noticeably lower than the top vent (2) cellulose and unvented cellulose (7) roofs.

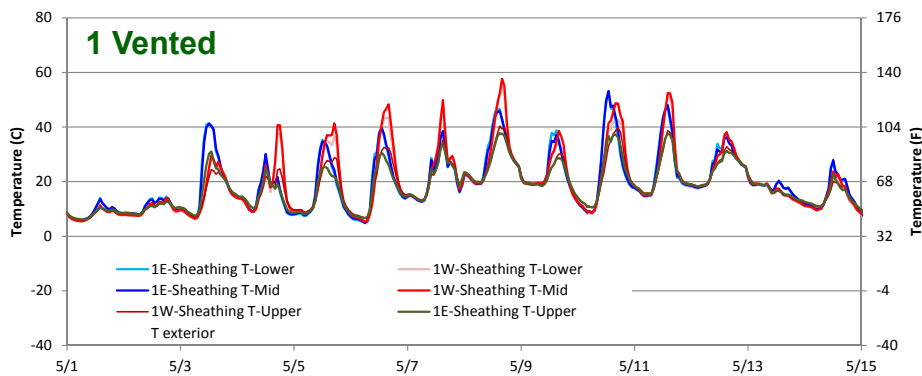


Figure 160: Summertime sheathing temperatures for Roof 1 (vented fiberglass)

As a general point, small airflows can have a substantial effect on effective vapor permeance of claddings (e.g., asphalt shingles). However, given the limited heat capacity of air, these small airflows would have almost insignificant effects on temperature and energy flows (Straube and Burnett 2005).

buildingamerica.gov

U.S. DEPARTMENT OF
ENERGY | Energy Efficiency &
Renewable Energy

DOE/GO-000000-0000 ▪ Month Year

About this Report

This report was prepared with the cooperation of the U.S. Department of Energy's Building America Program.

About the Authors

Kohta Ueno is a senior associate with Building Science Corporation whose responsibilities include forensic field investigations of building failures, consulting work with construction teams, project management, and public speaking/education. His consulting experiences have included design charrettes, meetings, and field verification; this work has been done with builders, architects, owners, and developers. He has conducted extensive research and field work on topics as varied as the hygrothermal behavior of basement wall insulation, double stud wall durability, interior insulation retrofits of mass masonry buildings, multifamily ventilation systems, and simplified space conditioning systems. He also has long-term experience in computer modeling (WUFI, THERM, HEAT3), field testing and verification, HVAC design, and residential energy analysis and simulations.

Joseph Lstiburek, Ph.D., P.Eng., ASHRAE Fellow, is a principal of Building Science Corporation. Dr. Lstiburek has been a licensed Professional Engineer in the Province of Ontario since 1982 and is an ASHRAE Fellow. He is also an Adjunct Professor of Building Science at the University of Toronto. He has over thirty years of experience in design, construction, investigation, and building science research. Through the Department of Energy's Building America program, Dr. Lstiburek has forged partnerships with designers, builders, developers, materials suppliers and equipment manufacturers to build higher performance buildings across the U.S.

Direct all correspondence to: Building Science Corporation, 30 Forest Street, Somerville, MA 02143.

Limits of Liability and Disclaimer of Warranty:

Building Science documents are intended for professionals. The author and the publisher of this article have used their best efforts to provide accurate and authoritative information in regard to the subject matter covered. The author and publisher make no warranty of any kind, expressed or implied, with regard to the information contained in this article.

The information presented in this article must be used with care by professionals who understand the implications of what they are doing. If professional advice or other expert assistance is required, the services of a competent professional shall be sought. The author and publisher shall not be liable in the event of incidental or consequential damages in connection with, or arising from, the use of the information contained within this Building Science document.